Cyanobacteria from Coastal Environments of Cabo Verde: A Study of Biodiversity and Biotechnological Potential, with Emphasis on Antioxidants

Aimone Jussiene Cardoso Duarte
Master in Applications in Biotechnology and Synthetic Biology
Department of Biology
Faculty of Sciences of the University of Porto
2025

Cyanobacteria from Coastal Environments of Cabo Verde: A Study of Biodiversity and Biotechnological Potential, with Emphasis on Antioxidants

Aimone Jussiene Cardoso Duarte
Master in Applications in Biotechnology and Synthetic Biology
Department of Biology
2025

Supervisor
Doctor Graciliana Lopes
Assistant Researcher
Interdisciplinary Centre of Marine and Environmental Research (CIIMAR)

Co-supervisors
Doctor Guilherme Scotta Hentschke
Researcher
Interdisciplinary Centre of Marine and Environmental Research (CIIMAR)

Professor Vitor Vasconcelos
Full Professor
Faculty of Sciences, University of Porto (FCUP)
Interdisciplinary Centre of Marine and Environmental Research (CIIMAR)

Acknowledgements

Firstly, I am deeply grateful to my supervisor, Doctor Graciliana Lopes, who has been essential throughout this dissertation journey, for her exceptional guidance, constant availability and steady support, as well as for the encouragement that made the process lighter and opened opportunities to learn beyond the dissertation. Her expertise, professionalism and kind personality were fundamental in shaping this study.

I also thank Professor Vitor Vasconcelos for the opportunity to carry out an internship at CIIMAR and for co-supervising this work. Among the master's courses, Blue Biotechnology at the Faculty of Sciences stood out and helped me choose this area. Coming from the Cabo Verde archipelago, with an Exclusive Economic Zone of nearly 800,000 km², the ocean has always fascinated me, giving this work special meaning.

I am thankful to my co-supervisor, Doctor Guilherme Scotta Hentschke, for his guidance and support. At CIIMAR, I extend my appreciation to the BBEH group, especially Flavio Oliveira, for constructive feedback, thoughtful suggestions and constant help, to Priscila, my colleague at CIIMAR, for working together and the moments we shared, and Teresa, who welcomed me at the beginning, helped me settle in and made the lab feel more welcoming.

My heartfelt thanks go to my master's classmates for the moments we shared, which made the city and this intense year more welcoming, especially Filipa, Beatriz, and Pedro.

I would like to extend my gratitude to the Faculty of Sciences of the University of Porto (FCUP) and the master's coordinators, Professors Paula Gomes and Paula Tamagnini.

Last but not least, my deepest gratitude goes to my family and friends, whose love sustained me across the distance and through health challenges. I am especially grateful to my mother, Bernardina Cardoso Varela, my father, António Duarte, and my little brother, Diego, for their constant love and support. My heartfelt thanks also go to Paulo Morais, my partner and my family away from home, always by my side with love and patience. To my dear friends, thank you for the laughs, partnership and warmth, with a special mention to Aline and Ruth, my oldest and dearest friends who have been part of my life for as long as I can remember.

As a Cabo Verdean, I could not close without saying, "*Si ka badu, ka ta biradu*".– Eugénio Tavares

Resumo

As cianobactérias são produtoras prolíficas de metabolitos especializados, de interesse crescente para a biotecnologia azul nas áreas da cosmética, dos alimentos e do diagnóstico. Neste trabalho, cianobactérias marinhas de Cabo Verde foram caracterizadas sistematicamente para estabelecer a sua colocação taxonómica, quantificar pigmentos e avaliar a bioatividade *in vitro*. Recorreu-se a um fluxo de trabalho polifásico que combinou filogenia rRNA 16S/ITS, morfologia e microscopia eletrónica de varrimento (MEV) para estabelecer a colocação taxonómica de seis isolados filamentosos. Uma linhagem, provisoriamente designada *Salileptolyngbya* sp. LEGE 181209, apresentou uma característica ultraestrutural distintiva (pseudovacúolos bem visíveis) e divergência ITS 16S–23S consistente com separação ao nível de espécie. Os ensaios de PCR dirigidos a genes de biossíntese de toxinas (mcyA, anaC) não produziram amplificação em nenhuma estirpe, sustentando um perfil de segurança favorável para utilizações subsequentes. Uma extração sequencial com solventes de diferente polaridade (acetona e água) originou frações com perfis de pigmentos complementares, caracterizadas por HPLC-PDA e espectrofotometria. Nos extratos acetónicos, os carotenoides totais atingiram o valor máximo em *Salileptolyngbya* sp. LEGE 181219 (≈81 μg mg^{-1} de extrato seco), com zeaxantina até ≈17 μg mg^{-1}; as clorofilas totais foram mais elevadas em *Leptothoe* sp. LEGE 181201 (≈127 μg mg^{-1}) e a luteína atingiu ≈3.2 μg mg^{-1} na mesma estirpe. Nos extratos aquosos, a ficocianina atingiu ≈248 μg mg^{-1} em LEGE 181219, enquanto a ficoeritrina atingiu ≈121 μg mg^{-1} em LEGE 181201. Ensaios celulares em queratinócitos HaCAT evidenciaram citotoxicidade baixa a ausente entre 12.5–200 μg mL^{-1} (24–48 h). Nos ensaios de sequestro do radical óxido nítrico ($^{\bullet}NO$), os extratos acetónicos foram, em geral, mais eficazes: *Leptothoe* LEGE 181201 atingiu IC_{50} ≈ 550 μg mL^{-1}; entre as frações aquosas, a melhor resposta foi observada para *Salileptolyngbya* LEGE 181219 (IC_{25} ≈ 1260 μg mL^{-1}). As análises quimiométricas (PCA/HCA) distinguiram as estirpes pela composição em pigmentos e apoiaram a seleção de produtoras de elevado desempenho.

Em conjunto, estes resultados identificam as cianobactérias de Cabo Verde como fontes acessíveis de corantes naturais de elevado valor, com potencial antioxidante compatível com diversas aplicações. Considerando a produtividade em pigmentos, o desempenho antioxidante e a segurança, a estirpe *Salileptolyngbya* LEGE 181219 destaca-se como produtora rica em ficocianina, enquanto a estirpe *Leptothoe* LEGE 181201 sobressai pela ficoeritrina e clorofila-*a*. Para além dos pigmentos, o conjunto mais amplo de

metabolitos destes extratos de cianobactérias permanece uma via promissora para futuras descobertas e aplicações.

Palavras-chave: Ficobiliproteínas; Carotenoides; Clorofilas; Óxido nítrico; Antioxidantes; *Salileptolyngbya* sp. LEGE 181209.

Abstract

Cyanobacteria are prolific producers of specialized metabolites of growing interest for blue biotechnology across cosmetics, foods, and diagnostics. Here, marine cyanobacteria from Cabo Verde were systematically characterized to resolve their taxonomy, quantify pigments, and assess *in vitro* bioactivity. A polyphasic workflow combining 16S rRNA/ITS phylogenetics, morphology, and scanning electron microscopy (SEM) was used to establish the taxonomic placement of six filamentous isolates. One lineage, provisionally designated *Salileptolyngbya* sp. LEGE 181209, exhibited a diagnostic ultrastructural feature (conspicuous pseudovacuoles) and 16S–23S ITS divergence consistent with species-level separation. PCR assays targeting toxin biosynthetic genes (mcyA, anaC) yielded no amplification in any strain, supporting a safety-forward profile for downstream use. A sequential extraction with solvents of different polarity (acetone and water) yielded complementary pigment fractions profiled by HPLC-PDA and spectrophotometry. In acetone extracts, total carotenoids peaked in *Salileptolyngbya* sp. LEGE 181219 (≈81 μg mg^{-1} dry extract), with zeaxanthin up to ≈17 μg mg^{-1}; total chlorophylls were highest in *Leptothoe* sp. LEGE 181201 (≈127 μg mg^{-1}), and lutein reached ≈3.2 μg mg^{-1} in the same strain. In aqueous extracts, phycocyanin reached ≈248 μg mg^{-1} in LEGE 181219, whereas phycoerythrin peaked at ≈121 μg mg^{-1} in LEGE 181201. Cell-based assays in HaCAT keratinocytes showed low to absent cytotoxicity across 12.5–200 μg mL^{-1} (24–48 h). In nitric oxide (NO) scavenging assays, acetone extracts were generally more effective: *Leptothoe* LEGE 181201 reached IC_{50} ≈ 550 μg mL^{-1}; among aqueous fractions, the best response was observed for *Salileptolyngbya* LEGE 181219 (IC_{25} ≈ 1260 μg mL^{-1}). Chemometric analyses (PCA/HCA) differentiated strains by pigment composition and supported the selection of high-performing producers.

Altogether, these results identify Cabo Verde cyanobacteria as accessible sources of high-value natural colorants with antioxidant readouts supporting diverse applications. Considering pigment productivity, antioxidant performance, and safety, *Salileptolyngbya* LEGE 181219 emerges as a phycocyanin-rich lead producer, while *Leptothoe* LEGE 181201 stands out for phycoerythrin and chlorophyll-*a*. Beyond pigments, the broader metabolite space of these cyanobacterial extracts remains a promising avenue for future discovery and application.

Keywords: Phycobiliproteins; Carotenoids; Chlorophylls; Nitric oxide; Antioxidants; *Salileptolyngbya* sp. LEGE 181209.

Table of Contents

List of Tables viii

List of Figures ix

List of Abbreviations xii

1. Introduction 1

1.1. Cyanobacteria biodiversity 1

1.2. Importance of Taxonomic studies for the description of new species 3

1.3. Cyanobacteria as source of specialized metabolites 4

1.3.1. Cyanobacteria Pigments 5

Carotenoids 5

Phycobiliproteins 7

1.3.1.1. Blue Biotechnology – cyanobacteria pigments as promising molecules in different fields 9

1.4. Oxidative stress and Reactive Species 10

1.4.1. Nitric Oxide 11

1.4.2. Antioxidants 12

2. Objectives 15

3. Materials and Methods 16

3.1. Isolation of Cyanobacteria strains 16

3.2. DNA extraction, PCR amplification and sequencing 17

3.3. Phylogenetic analysis 18

3.4. Scanning Electron Microscopy (SEM) 18

3.5. Cultures scale-up and collection of biomass 19

3.6. Preparation of extracts 20

Acetone extract 20

Water extract 21

3.7. Cytotoxicity to human keratinocytes (HaCAT) 21

3.7.1. Cells culturing 21

3.7.2. Cytotoxicity assessment by the MTT assay 22
3.8. Chemical Analysis 22
3.8.1. Carotenoids profiling by HPLC-PDA 22
3.8.2. Phycobiliproteins and Chlorophylls profiling by spectrophotometry 23
3.8.3. Determination of Total Phenolics Content (TPC) by Folin-Ciocalteu Method 24
3.8.4. Determination of Total Sugars by the Phenol-Sulfuric Method 25
3.9. Nitric Oxide Scavenging 26
3.10. Statistical Analysis 26
4. Results and Discussion 28
4.1. Diversity of Cabo Verde isolates 28
Toxin analysis 34
4.2. Cytotoxicity of Cyanobacteria extracts 35
4.3. Chemical profile 37
4.3.1. Acetonic extracts 37
Carotenoids and Chlorophylls profiling by HPLC-PDA 37
4.3.2. Aqueous extracts 41
Phycobiliproteins and Chlorophylls 41
Total Phenols 44
Total Sugars 46
4.3.3. Chemotaxonomy and chemical characterization 47
4.3.4. Nitric Oxide Scavenging 52
5. Conclusions 54
6. Future Perspectives 55
References 56

List of Tables

Table 1. Examples of commonly occurring carotenoids in cyanobacteria.[1] 7
Table 2. Calibration curves of authentic standards used for quantification of different carotenoids and chlorophylls. 23
Table 3. Morphological and molecular summary of the six cyanobacterial strains isolated from Cabo Verde. 31
Table 4. Morphological comparisons of *Salileptolyngbya* species. 33

List of Figures

Figure 1. Cyanobacteria: (A) Plecctonema, (B) Synechocystis, (C) Microcystis, (D) Planktothrix, (E) Anabaena, (F) Merismopedia. Adapted from [11]..... 2
Figure 2. Representative Cabo Verde coastal habitat. 3
Figure 3. Chemical structures of different carotenoids present in cyanobacteria, including β-carotene (A), zeaxanthin (B), echinenone (C) and lutein (D). 6
Figure 4. Chemical structures of phycobilins in phycobiliproteins found in cyanobacteria. A, B, C, and D tag the tetrapyrrole rings. Adapted from [46]..... 8
Figure 5. The nitric oxide synthase reactions. Adapted from [71]. 11
Figure 6. (a) Cabo Verde Islands location. The dotted circle marks the Cabo Verde islands. (b) Map of Cabo Verde Islands. (c,d) Location of the sampling sites at Santo Antão and São Vicente Islands. The map was created using the geom_sf() function from the ggplot2 package in R. First, the geographic data were loaded and prepared using the sf package. The ggplot() function initiated the plot, and geom_sf() was used to add the spatial data layer to the map. 16
Figure 7. Cultivation of cyanobacterial strains in 40 mL flasks at the bioterium of aquatic organisms (BOGA, CIIMAR). 19
Figure 8. Cultivation of cyanobacterial strains in 4 L photobioreactors at the bioterium of aquatic organisms (CIIMAR). 20
Figure 9. Calibration curve of gallic acid used for the quantification of total phenolic content (TPC) by the Folin–Ciocalteu method. 25
Figure 10. Calibration curve for glucose using the phenol-sulfuric acid method..... 26
Figure 11. Maximum-Likelihood phylogenetic tree based on 16S rRNA gene sequences of the Cabo Verde isolates and related cyanobacterial taxa. The dark-grey strip indicates the order Nodosilineales. Strains obtained in this study are marked with red dots. 29
Figure 12. Morphological features of the six cyanobacterial strains isolated from Cabo Verde: (A) Leptolyngbyaceae cyanobacterium LEGE 181156, (B) *Leptothoe* sp. LEGE 181201, (C) *Salileptolyngbya* sp. LEGE 181209, (D) Geminocystaceae cyanobacterium LEGE 181210, (E) *Salileptolyngbya* sp. LEGE 181216 and (F) *Salileptolyngbya* sp. LEGE 181219. Images were captured using a Leica DMLB light microscope equipped with a digital camera. 30
Figure 13. Light and scanning electron micrographs of *Salileptolyngbya* sp. LEGE 181209. (A) Light microscopy showing a dense aggregate of entangled filaments in liquid culture (10 µm). (B) Slide preparation with China ink, showing individual dispersed filaments (10 µm). (C,D) Light-microscopy details of trichomes displaying clear cross-

wall constrictions and homogeneous cell content (10 µm). (E,F) Scanning electron micrographs of trichomes with firm sheaths; bright spherical inclusions (white spheres) correspond to internal pseudovacuoles (4 µm). (G) Scanning electron micrograph of trichomes without visible pseudovacuoles (4 µm). 32
Figure 14. Predicted secondary structures of the 16S–23S ITS regions (D1–D1′, Box B and V3 domains) of (A) *Salileptolyngbya* sp. LEGE 181209 compared with (B) *S. diazotrophicum*, showing clear structural differences supporting species-level separation. 34
Figure 15. PCR gels showing absence of mcyA (A) and anaC (B) amplification. Positive control (+); *Leptothoe* sp. LEGE 181201; *Salileptolyngbya* sp. LEGE 181209; Geminocystaceae cyanobacterium LEGE 181210; *Salileptolyngbya* sp. LEGE 181216; *Salileptolyngbya* sp. LEGE 181219; Leptolyngbyaceae cyanobacterium LEGE 181156. 35
Figure 16. Viability of keratinocytes (HaCAT) after 24 h and 48 h of incubation with cyanobacteria acetonic extracts at concentrations ranging from 12.5-200 µg mL^{-1}. Results are expressed as % of MTT reduction relative to the untreated control. DMSO (20%) was used as the positive control for cytotoxicity. Results are presented as mean ± SD of at least three independent experiments, performed in quadruplicate. Statistical differences are indicated at *p<0.05 (non-parametric bootstrap resampling, 1000 iterations). 36
Figure 17. Viability of keratinocytes (HaCAT) after 24 h and 48 h of incubation with cyanobacteria aqueous extracts at concentrations ranging from 12.5-200 µg mL^{-1}. Results are expressed as % of MTT reduction relative to the untreated control. DMSO (20%) was used as the positive control for cytotoxicity. Results are presented as mean ± SD of at least three independent experiments, performed in quadruplicate. Statistical differences are indicated at *p<0.05 (non-parametric bootstrap resampling, 1000 iterations). 36
Figure 18. Carotenoid and chlorophylls profiles of the acetonic extracts of the cyanobacteria *Leptolyngbyaceae* cyanobacterium LEGE 181156, *Leptothoe* sp. LEGE 181201, *Salileptolyngbya* sp. LEGE 181209, *Salileptolyngbya* sp. LEGE 181216, *Salileptolyngbya* sp. LEGE 181219 and *Geminocystaceae* cyanobacterium LEGE 181210. HPLC-PDA recorded at 450 nm. Identified pigments: lutein (1), oxygenated derivative of β-carotene (2), chlorophyll-*a* (3), zeaxanthin (4), chlorophyll-*a* derivative (5), myxoxanthophyll (6), oxygenated derivative of β-carotene (7), β-cryptoxanthin (8), β-carotene derivative (9), β-carotene (10), and β-carotene derivative (11). 39

Figure 19. Carotenoid and chlorophylls content (µg mg^{-1} dry extract) in acetonic extracts, quantified by HPLC-PDA. Different superscript letters denote statistical differences at $p < 0.05$ (non-parametric bootstrap resampling, 1000 iterations). 40
Figure 20. Phycobiliproteins (A–C) and chlorophylls (D–E) in aqueous extracts (µg mg^{-1} dry extract). Different superscript letters indicate significant statistical differences at $p<0.05$ (non-parametric bootstrap test). APC, allophycocyanin; PC, phycocyanin; PE, phycoerythrin; TChls, total chlorophylls; Chl-*a*, chlorophyll-*a*. 42
Figure 21. Total phenolics-A (µg gallic acid equivalents (GAE) mg^{-1} dry extract) and total sugars-B (µg glucose equivalents mg^{-1} dry extract) contents in cyanobacteria aqueous extracts. Different superscript letters indicate significant statistical differences at $p<0.05$ (non-parametric bootstrap test). 45
Figure 22. Principal component analysis (PCA) biplot of carotenoids and chlorophylls detected in acetonic extracts. The first two principal components explained 78.9% of the total variance (PC1: 57.6%; PC2: 21.3%). Arrows indicate pigment loadings, and strain codes correspond to cyanobacterial isolates from Cabo Verde. 48
Figure 23. Dendrogram obtained by hierarchical cluster analysis (HCA) based on carotenoid and chlorophylls profile of acetonic extracts from cyanobacterial strains. .. 48
Figure 24. Principal component analysis (PCA) biplot of aqueous pigments (phycobiliproteins and total chlorophylls). The first two principal components explained 89.3% of the total variance (PC1: 71.3%; PC2: 18.0%). 49
Figure 25. Dendrogram obtained by hierarchical cluster analysis (HCA) based on aqueous pigment composition (phycobiliproteins and total chlorophylls) of cyanobacterial strains. 50
Figure 26. Principal component analysis (PCA) biplot of phenolic compounds and sugars. The first two principal components explained 100% of the variance (PC1: 74.6%; PC2: 25.4%). 51
Figure 27. Dendrogram obtained by hierarchical cluster analysis (HCA) based on phenolic and sugar contents of cyanobacterial strains. 51
Figure 28. Nitric oxide ($^{\bullet}NO$) scavenging activity of cyanobacterial extracts. Dose–response curves for the acetonic extract of *Leptothoe* sp. LEGE 181201 (red) and the aqueous extract of *Salileptolyngbya* sp. LEGE 181219 (blue). Results are expressed as mean ± SD of three independent experiments performed in duplicate. 52

List of Abbreviations

anaC – Anatoxin synthetase gene C

ATCC – American Type Culture Collection

CAT – Catalase

CIIMAR – Interdisciplinary Centre of Marine and Environmental Research

DNA – Deoxyribonucleic acid

DMEM Glutamax – Glutamax Dulbecco's Modified Eagle Medium

DMSO – Dimethyl sulfoxide

EPS – Exopolysaccharides

GPX – Glutathione peroxidase

GR – Glutathione reductase

HaCAT – Immortalized human adult keratinocyte cell line

HPLC – High Performance Liquid Chromatography

HPLC-PDA – High Performance Liquid Chromatography with Photodiode Array Detector

IC_{25} – Concentration required to achieve 25% inhibition

IC_{50} – Concentration required to achieve 50% inhibition

ITS – Internal Transcribed Spacer

iTOL – Interactive Tree of Life (phylogenetic tree tool)

LEGE CC – Blue Biotechnology and Ecotoxicology Culture Collection of CIIMAR

LOX – Lipoxygenase

LPS – Lipopolysaccharide

mcyA – Microcystin synthetase gene A

MTT – 3-(4,5-dimethylthiazol-2-yl)-2,5-diphenyltetrazolium bromide

$^{\bullet}NO$ – Nitric Oxide radical

NO_2^- – Nitrite

$O_2^{\bullet -}$ – Superoxide anion radical

PCA – Principal Component Analysis

PCR – Polymerase Chain Reaction

PDA – Photodiode Array

PE – Phycoerythrin

PHE – Phycoerythrobilin

PPC – Photosynthetic pigment content

ROS – Reactive Oxygen Species

rRNA – Ribosomal Ribonucleic Acid

SEM – Scanning Electron Microscopy

SOD – Superoxide dismutase

1. Introduction

1.1. Cyanobacteria biodiversity

Cyanobacteria are ancient architects of life on Earth, having played a pivotal role in shaping the planet's atmosphere and sustaining early ecosystems [1]. These photosynthetic prokaryotes, belonging to the domain *Bacteria*, are Gram-negative due to their characteristic cell wall structure and are the only known prokaryotes capable of performing oxygenic photosynthesis — a turning point in Earth's history [2].

They are characterized by the presence of chlorophyll-*a* and accessory pigments such as carotenoids and phycobiliproteins, organized within thylakoid membranes that assemble into phycobilisomes [3], [4]. Unlike most bacteria, cyanobacteria possess this extensive internal membrane system supporting oxygenic photosynthesis, distinguishing them within the prokaryotic domain [5]. Although lacking membrane-bound organelles and a true nucleus, typical of prokaryotes, their cellular organization is notably complex, enabling efficient photosynthetic function [6]. Many filamentous species fix atmospheric nitrogen by differentiating specialized cells called heterocysts, which provide a microoxic environment necessary for nitrogenase activity [7]. Furthermore, cyanobacteria exhibit unique growth and reproductive strategies uncommon in other bacteria, including true and false filament branching, formation of motile filaments (hormogonia), and multiple or asymmetrical cell fission, that contribute to their ecological success [8].

This functional and structural complexity translates into broad morphological and ecological diversity. Forms range from unicellular (coccoid) to colonial and complex filamentous types (**Figure 1**), occurring across marine and freshwater systems, soils, deserts, and extreme habitats such as hot springs and polar regions [9], [10]. In some species, filaments are embedded in a gelatinous matrix, forming cohesive colonies. Filamentous cyanobacteria are particularly prevalent, conferring advantages such as improved nutrient acquisition and resilience under fluctuating conditions [11].

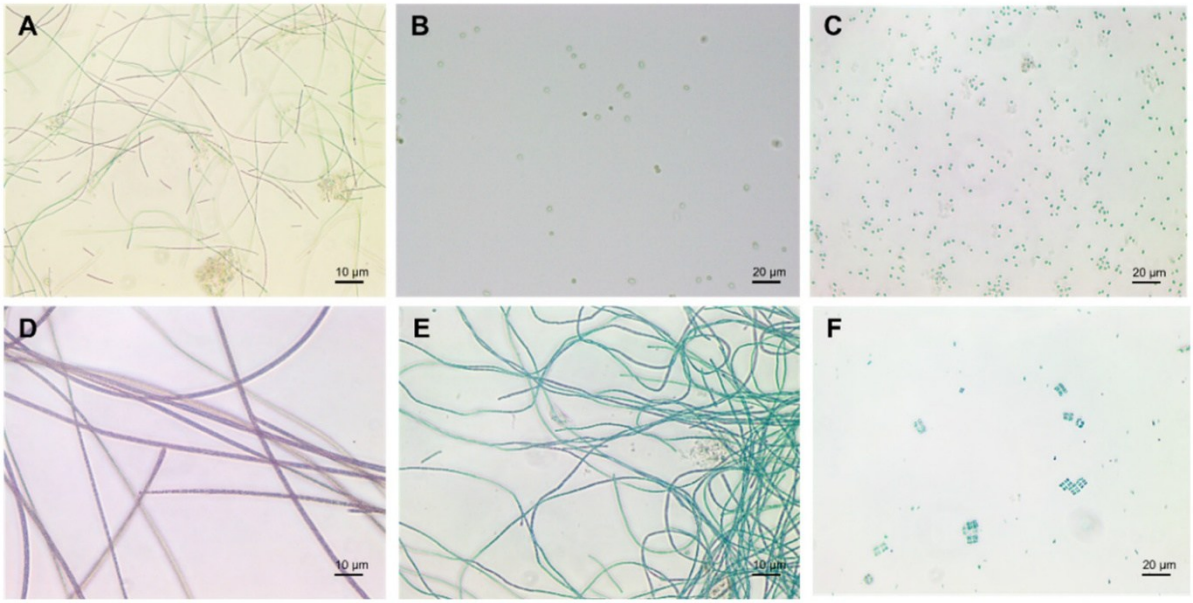


Figure 1. Cyanobacteria: (A) Plecctonema, (B) Synechocystis, (C) Microcystis, (D) Planktothrix, (E) Anabaena, (F) Merismopedia. Adapted from [11].

Cyanobacteria biodiversity remains underexplored despite clear ecological relevance and potential applications. Over the last years, there has been a growing interest in investigating underexplored habitats, aiming to discover new species and bioactive compounds [12]. Although cyanobacteria are widespread, many species remain undescribed, particularly those inhabiting isolated or unique ecosystems. In this context, the Cabo Verde archipelago has recently emerged as a promising environment for the description of new species of cyanobacteria, due to its particular combination of marine and terrestrial habitats (**Figure 2**).

Cabo Verde is an African island country in the central Atlantic Ocean, comprising ten volcanic islands grouped into two main groups: the Barlavento (windward) and Sotavento (leeward) islands. With nearly 800,000 km² of Exclusive Economic Zone [13] and a tropical dry climate, the archipelago hosts diverse ecological niches and is strategically positioned in the emerging blue economy [14]. While tourism and fisheries are central to the national economy, there is growing focus on exploring and conserving marine biodiversity to foster innovation and resilience. Within this context, microbial communities, particularly cyanobacteria, have attracted increasing scientific interest for their ecological significance and applied potential.

Several cyanobacterial strains isolated from the marine environments of Cabo Verde have been assigned to genera such as *Salileptolyngby* sp., *Leptothoe* sp., *Baaleninema* sp., *Neolyngbya* sp., and *Nodosilinea* sp., *Cyanobium* sp., as reported by Morone et al.

[15], [16]. Their phylogenetic distinctiveness and capacity to produce bioactive metabolites, including anti-inflammatory and antioxidant compounds, highlight the unexplored biotechnological value of the region's cyanobacterial diversity. In addition, *Gibliniella gelatinosa* sp. nov., was recently described from Cabo Verde's marine environments by Morais et al. [17], reinforcing the ecological uniqueness and scientific relevance of these islands. Ongoing exploration therefore offers opportunities to uncover microbial resources of ecological and applied importance.



Figure 2. Representative Cabo Verde coastal habitat.

1.2. Importance of Taxonomic studies for the description of new species

Cyanobacterial taxonomy has evolved significantly over the past decades transitioning from morphology-based classification systems to integrative polyphasic approaches that combine morphological, molecular, chemical, and ecological data [18]. Traditional classifications relied heavily on visible traits, including cell shape, colony architecture, pigmentation, and specialized cells (heterocytes and akinetes). However, these features are often influenced by environmental conditions and exhibit considerable phenotypic plasticity or convergent evolution, leading to misidentifications and unstable classifications.

The incorporation of molecular techniques, particularly 16S rRNA gene sequencing, have provided a more robust phylogenetic framework, enabling the resolution of many

taxonomic ambiguities. Nevertheless, some groups remain polyphyletic, and ongoing taxonomic revisions continue to refine evolutionary relationships. For higher resolution at the species/strain level, additional genetic markers, such as the internal transcribed spacer (ITS) region, rbcL, and cpcBA-IGS, as well as whole genome sequencing are increasingly employed [19]. When integrated with ecological and biochemical profiles, these datasets underpin the modern polyphasic concept.

Accurate identification is essential to understand diversity, distribution, and evolution, but also for bioprospecting species with biotechnological potential [20]. In underexplored regions such as Cabo Verde, polyphasic approaches are likely to reveal novel taxa and clarify ecological roles. Such discoveries can be pivotal for identifying strains that produce specialized metabolites with relevance to health, industry, and environmental applications, thereby linking taxonomy, biodiversity conservation, and biotechnology [21].

1.3. Cyanobacteria as source of specialized metabolites

Cyanobacteria inhabit environments from oceans and lakes to deserts, hot springs, and polar regions, either as free-living forms or in symbioses. This ecological versatility is closely linked to their ability to biosynthesize a wide array of structurally diverse specialized metabolites, also known as secondary metabolites, which frequently act as adaptive responses to environmental stressors such as ultraviolet (UV) radiation, salinity, oxidative pressure, and nutrient limitation [22]. These specialized metabolites span peptides, alkaloids, polyketides, phenolics, terpenes, and polyunsaturated fatty acids (PUFAs) [23]. Notably, several of these molecules display potent biological activities, such as antimicrobial, antiviral, antifungal, antitumoral, anti-inflammatory, antioxidant, and cytotoxic effects [24], [25]. Consequently, cyanobacterial metabolites are being explored across multiple sectors: in medicine, they offer potential leads for drug development; in cosmetics, they contribute to the formulation of UV-protective and anti-aging products; in the nutraceutical field, they provide protein and PUFA-rich extracts; and in the environmental sector, they serve as natural pesticides or agents for bioremediation [26]. Due to their photoautotrophic nature, cyanobacteria are constantly exposed to sunlight and UV radiation. To mitigate the damaging effects of such exposure, many species have evolved the ability to produce photoprotective and antioxidant compounds of biotechnological interest. For example, scytonemin is a lipid-soluble, UV-screening pigment with demonstrated value in cosmetics and medicine [27], while mycosporine-like amino acids (MAAs) are small, water-soluble molecules with UV-absorbing and antioxidant functions [28]. These exemplify dual ecological and

therapeutic functions, making them promising candidates for incorporation into sunscreens, anti-aging formulations, and pharmaceutical products [16].

Cyanobacterial growth rates and modest nutrient requirements favor scalable cultivation, while genome mining, metabolic engineering, and synthetic biology expand opportunities to optimize yields. Among bioactive classes, pigments stand out for their multifunctionality: beyond roles in photosynthesis and photoprotection, carotenoids and phycobiliproteins exhibit antioxidant capacity and broad biotechnological potential [29].

1.3.1. Cyanobacteria Pigments

Most cyanobacteria are fundamentally photoautotrophic, relying primarily on photosynthesis to acquire the energy and nutrients needed for growth. This process begins with light absorption by pigments that capture specific wavelengths of the visible spectrum and convert them into chemical energy to support metabolism [30]. These pigments are arranged across two photosystems and a phycobilisome attached to thylakoid membranes, ensuring efficient light capture and energy transfer. They are generally classified into three main groups: chlorophylls, carotenoids, and phycobiliproteins, each contributing uniquely to the photosynthetic process.

Carotenoids

Carotenoids are hydrophobic terpenoids distributed across cyanobacteria, algae, and plants, and in some bacteria and fungi. They contribute to light harvesting and protect the photosynthetic apparatus from photo-oxidative stress caused by reactive oxygen species (ROS). In cyanobacteria, carotenoids stabilize photosystems and support non-photochemical quenching mechanisms, safeguarding cells under fluctuating light [31]. Structurally, carotenoids are tetraterpenoids composed of 40 carbon atoms, arranged in a backbone of eight isoprene units. They are divided into two main classes: carotenes, which are purely hydrocarbons and therefore highly hydrophobic (e.g., β-carotene), and xanthophylls, which are oxygenated derivatives of carotenes and more hydrophilic due to the presence of functional groups like hydroxyl (e.g., Zeaxanthin) or keto groups (e.g., Echinenone). These structural differences affect their polarity and influence interaction within pigment–protein complexes biological functions (**Figure 3**) [32], [33].

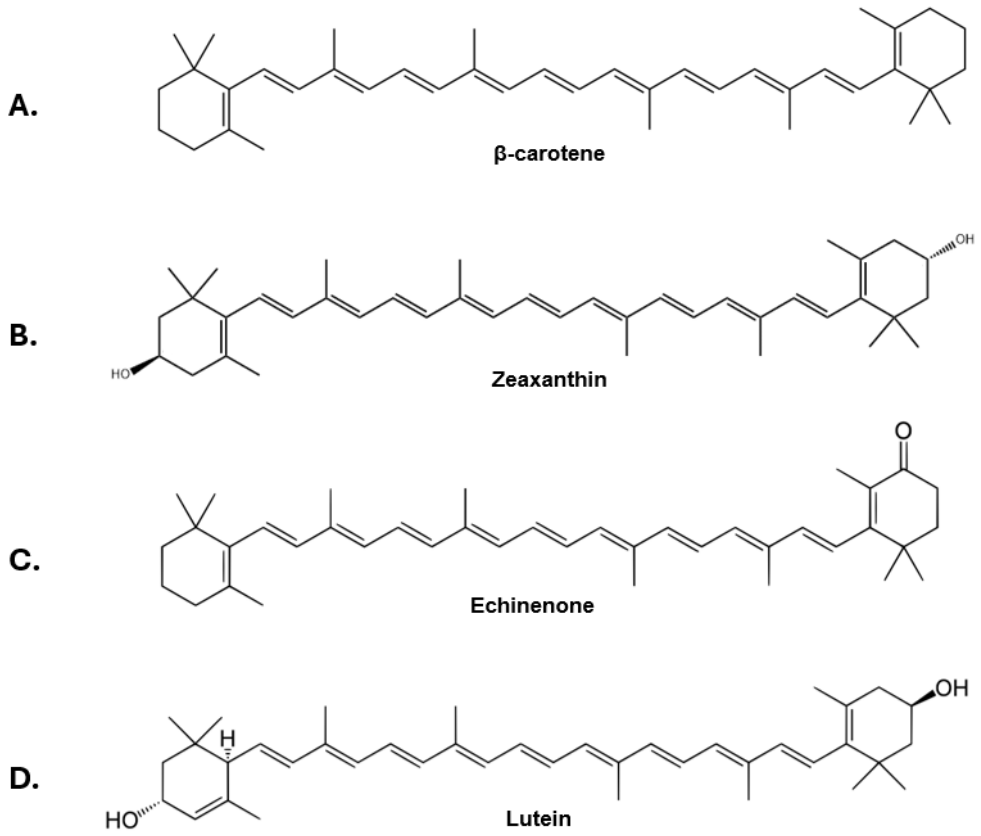


Figure 3. Chemical structures of different carotenoids present in cyanobacteria, including β-carotene (A), zeaxanthin (B), echinenone (C) and lutein (D).

In cyanobacteria, carotenoids are synthesized via the DOXP/MEP (non-mevalonate) pathway. 1-Deoxy-D-xylulose 5-phosphate (DOXP) is converted to 2-C-methyl-D-erythritol 4-phosphate (MEP) [34], [35], leading to isopentenyl pyrophosphate (IPP) and dimethylallyl pyrophosphate (DMAPP), the building blocks of geranylgeranyl pyrophosphate (GGPP) [36]. Phytoene, formed by phytoene synthase (CrtB), undergoes desaturation (CrtP, CrtQ) to lycopene, which then cyclizes to β-carotene. Subsequent hydroxylations and ketolations yield xanthophylls such as zeaxanthin, echinenone, and lutein [37].

Beyond physiology, carotenoids are valued for antioxidant and anti-inflammatory properties [15], [38]. Astaxanthin, a ketocarotenoid with potent bioactivity, shows promise in neuroprotection, skin health, and functional foods [39]. Based on the literature review for this thesis, the most frequently reported carotenoids in cyanobacteria include β-carotene, zeaxanthin, echinenone, lutein, canthaxanthin, and myxoxanthophyll. Although, some genera also produce rarer compounds such as nostoxanthin or

caloxanthin. The table below presents some examples of the carotenoids most commonly associated with specific cyanobacterial species:

Table 1. Examples of commonly occurring carotenoids in cyanobacteria.[1]

Cyanobacteria Species	β-carotene	Zeaxanthin	Myxoxanthophyll	Lutein	Echinenone	References
Salileptolyngbya sp. LEGE 181184	44.45 ± 0.46	42.89 ± 0.4	9.20 ± 0.14	2.07 ± 0.01	–	[15]
Leptothoe sp. LEGE 181153	22.42 ± 1.78	49.93 ± 4.29	1.71 ± 0.08	3.88 ± 0.25	–	[15]
Leptothoe sp. LEGE 11479	39.79 ± 8.12	192.91 ± 3.20	–	1.38 ± 0.10	–	[40]
Scytonema sp. LEGE 221230	30.09 ± 0.48	–	–	0.71 ± 0.09	11.43 ± 0.11	[41]
Drouetiella sp. LEGE 221231	63.67 ± 1.23	–	–	1.65 ± 0.11	3.18 ± 0.05	[41]
Baaleninemaa sp. LEGE 181148	34.56 ± 1.16	58.17 ± 2.48	11.31 ± 0.27	2.71 ± 0.11	1.00 ± 0.04	[15]
Salileptolyngbya sp. LEGE 181187	48.85 ± 2.54	58.25 ± 2.45	13.44 ± 2.87	6.33 ± 0.22	–	[15]
Neolyngbya sp. LEGE 181188	19.70 ± ≤ 0.01	25.19 ± ≤ 0.01	13.04 ± 0.08	1.43 ± 0.03	–	[15]
Nodosilinea sp. LEGE 181189	76.39 ± 6.52	59.58 ± 2.95	15.52 ± 0.25	5.11 ± 0.24	–	[15]
Leptolyngbya boryana LEGE 15486	20.41 ± 3.20; 159.39 ± 5.0	52.68 ± 0.40	–	0.38 ± 0.02	1.70 ± 0.08	[40]; [42]
Cyanobium gracile LEGE 12431	23.96 ± 0.18	0.03 ± 0.001; 6.30 ± 0.025	–	–	7.31 ± 0.15	[32]
Nodosilinea nodulosa LEGE 06102	0.04 ± ≤ 0.001	0.039 ±≤ 0.001	–	0.05 ±≤ 0.001	0.046 ±≤ 0.001	[43]
Cephalothrix lacustris LEGE 15493	18.39 ± 0.25; 137.50 ± 2.8	99.55 ± 0.515	–	0.58 ± 0.03	1.79 ± 0.01	[40]; [42]

[1]Data are reported as mean ± SD (where available) in μg/mg; not-determined values are denoted by "–".

Phycobiliproteins

Phycobiliproteins are vividly colored, water-soluble light-harvesting proteins assembled into the phycobilisome at the thylakoid surface. They absorb in spectral regions less efficiently captured by chlorophylls, particularly in the 450–670 nm range [22]. These

pigments are composed of two main components: a protein backbone (apoprotein) and linear open-chain tetrapyrrole chromophores known as phycobilins, which are covalently attached to specific cysteine residues on the protein via thioether bonds [44], [45]. The type of phycobilin present determines the color and spectral properties of each phycobiliprotein. The different phycobilins are phycocyanobilin (blue color), phycoerythrobilin (red color), phycourobilin (orange color), and phycoviolobilin (purple color), each composed of four pyrrole rings (A, B, C and D) linked by a one carbon bridge. The pyrrole rings A and D contain one oxygen atom, and rings B and C are associated with propionic acid residues as illustrated in **Figure 4** [22].

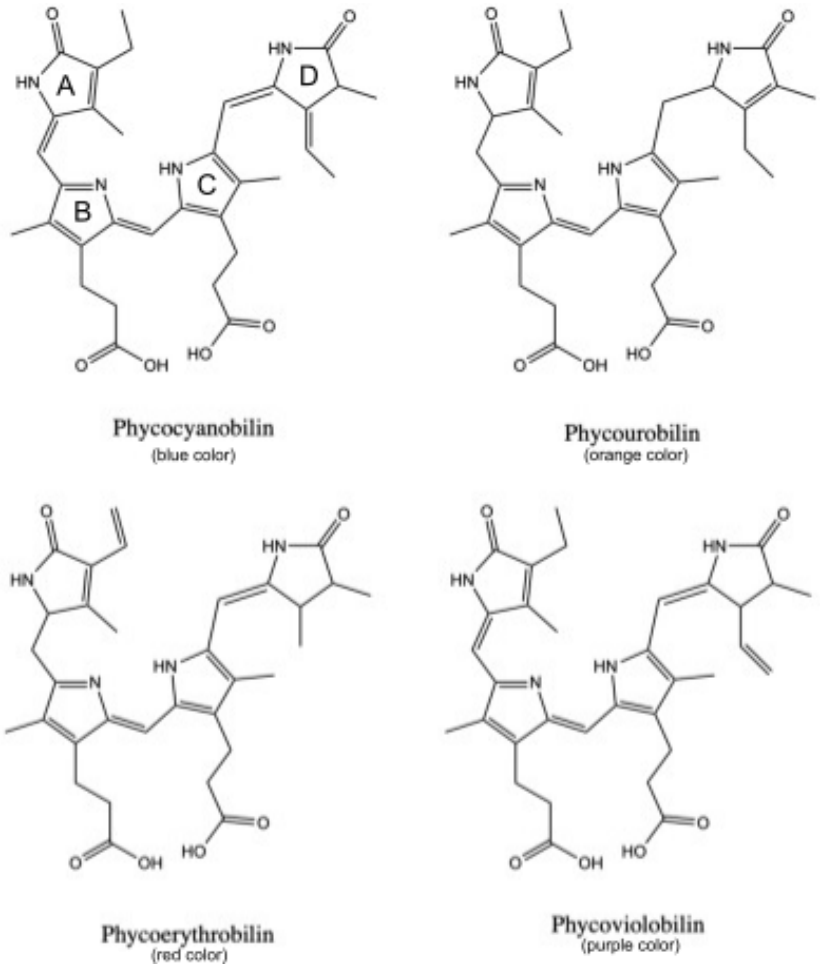


Figure 4. Chemical structures of phycobilins in phycobiliproteins found in cyanobacteria. A, B, C, and D tag the tetrapyrrole rings. Adapted from [46].

Cyanobacteria possess four major types of phycobiliproteins, distinguished by their color and specific light absorption properties. Allophycocyanin (APC) is a bluish-green pigment that absorbs light mainly at 650–660 nm and is typically found at the core of the phycobilisome. Phycocyanin (PC), with its characteristic blue color, absorbs maximally

between 610–625 nm and is one of the most abundant pigments in cyanobacteria. Phycoerythrin (PE), a red pigment, captures light in the range of 490–570 nm, allowing the organism to efficiently capture green light. Lastly, Phycoerythrocyanin (PEC) is a less common phycobiliprotein that absorbs between 560–600 nm and it occurs in specific cyanobacterial groups adapted to specific light environments. Together they funnel energy to photosystem reaction centers with high efficiency, enabling growth in low-light or spectrally shifted environments (e.g., turbid/deep waters). Photoprotection is mediated in part by the Orange Carotenoid Protein (OCP), which reduces phycobilisome fluorescence under high light [47]. Some cyanobacteria also exhibit chromatic acclimation, altering phycobiliprotein composition in response to light quality [48].

Due to their intense fluorescence, biocompatibility, and stability, they have attracted considerable attention in fluorescent labelling, diagnostics, and as natural food colorants. For example, R-phycoerythrin is commonly used as a fluorescent marker in flow cytometry and immunoassays [49], while C-phycocyanin is employed as a natural blue dye in food products such as yoghurts, ice creams, and beverages [50]. Additionally, studies have demonstrated anti-inflammatory activity of C-phycocyanin in cell models, supporting its potential in therapeutic formulations [51].

1.3.1.1. Blue Biotechnology – cyanobacteria pigments as promising molecules in different fields

Demand for natural compounds with health benefits and fewer side effects has risen steadily, attracting pharmaceutical, nutraceutical, and cosmetic industries. Among the many bioactive molecules of natural origin, cyanobacterial pigments, particularly carotenoids and phycobiliproteins, have emerged as versatile candidates with broad biological activities and biotechnological potential [12], [52].

Carotenoids are valued for their potent antioxidant, anti-inflammatory, anti-tumour, antimicrobial properties and photoprotective properties. Their ability to scavenge free radicals and prevent lipid peroxidation is particularly relevant to diseases associated with oxidative stress, such as cardiovascular disorders, neurodegenerative diseases, and certain cancers [53], [54]. β-carotene and β-cryptoxanthin, act as provitamin A compounds and support immune regulation and epithelial maintenance [55]. Lutein and zeaxanthin have contributed to ocular protection, including age-related macular degeneration and cataracts [56]. In cosmetics, astaxanthin and lutein are incorporated to enhance skin hydration, prevent photoaging, and provide UV protection. Their intrinsic

antioxidant activity can also stabilize cosmetic products, reducing the need for synthetic preservatives [53], [54].

Phycobiliproteins have likewise gained industrial relevance as high-quantum-yield fluorescent markers (e.g., PE, APC) in biomedical assays [58]. As natural colorants, they align with demand for sustainable ingredients [59]. Their antioxidant, anti-inflammatory, immunomodulatory, and anticancer properties support use as functional ingredients [60], and they have been explored as biodegradable textile dyes [61].

A promising avenue is the multifunctional use of pigments as both bioactive and natural stabilizers that limit oxidative degradation, extending shelf life in cosmetic, pharmaceutical, and food products [62]. As research advances and consumer awareness continues to rise, these pigments are poised to play an increasingly important role in the future of blue biotechnology [52].

1.4. Oxidative stress and Reactive Species

Redox homeostasis is a tightly regulated physiological state that maintains a balance between oxidant production and antioxidant defense, enabling normal cellular function. This equilibrium can be perturbed under certain physiological or pathological conditions, such as intense physical activity, inflammation, radiation, pollutants, or infection. When reactive species exceed antioxidant capacity, oxidative stress ensues, leading to damage in essential biomolecules like lipids, proteins and DNA [63].

Reactive species include reactive oxygen species (ROS), reactive nitrogen species (RNS), and others. At controlled levels, they act as signalling molecules regulating gene expression, immune responses, and apoptosis; in excess, they are deleterious [64]. ROS are generated as natural by-products of aerobic metabolism, particularly during mitochondrial oxidative phosphorylation, and include radical and non-radical species: including superoxide anion radical ($O_2^{\bullet -}$), hydroxyl radical (•OH), peroxyl radical ($RO_2^{\bullet}$), hydrogen peroxide (H_2O_2), singlet oxygen ($^1O_2$), and hypochlorous acid (HOCl) [65]. Superoxide anion radical, considered the "primary" ROS, can initiate the formation of secondary species through enzymatic or non-enzymatic reactions. Its major source is the mitochondrial electron transport chain, specifically complexes I (NADH dehydrogenase) and III (ubiquinone-cytochrome c reductase), with additional sources such as NADPH oxidases, xanthine oxidase, and peroxisomal β-oxidation [66]. To counterbalance ROS production, cells rely on an intricate antioxidant defense system. Key enzymatic antioxidants include superoxide dismutase (SOD), catalase (CAT), and glutathione peroxidase (GPx), which act sequentially to convert ROS into less harmful

compounds. For instance, SOD catalyses the dismutation of $O_2^{\bullet -}$ into H_2O_2 and O_2, while CAT and GPx reduce H_2O_2 to water, thereby preventing the formation of the highly reactive •OH [67].

Reactive nitrogen species, including nitric oxide (•NO) and derivatives (NO^-, NO^+, $ONOO^-$), also shape redox homeostasis. •NO rapidly reacts with $O_2^{\bullet -}$ to form peroxynitrite ($ONOO^-$) [66]. Physiologically, RNS regulate vascular tone, neurotransmission, and immunity, but in excess, they trigger nitrosative stress analogous to oxidative stress.

1.4.1. Nitric Oxide

Nitric oxide is a small, highly diffusible, and short-lived free radical with dual physiological and pathological roles in both prokaryotic and eukaryotic systems. It was first identified as an endogenous signalling molecule in mammals, but its presence and functions extend to plants, algae, and cyanobacteria, where it participates in a variety of metabolic and stress-response pathways [68], [69]. In biological systems, •NO is synthesized enzymatically from L-arginine and molecular oxygen via nitric oxide synthases (NOS), producing L-citrulline as a co-product [68]. NOS enzymes are complex, modular oxidoreductases that require multiple cofactors for proper activity, including flavin adenine dinucleotide (FAD), flavin mononucleotide (FMN), (6R)-5,6,7,8-tetrahydrobiopterin (BH_4), heme, and reduced nicotinamide adenine dinucleotide phosphate (NADPH) as an electron donor [70]. Electrons flow from NADPH through FAD and FMN in the reductase domain to the heme group in the oxygenase domain, where L-arginine is oxidized to produce •NO. Calcium/calmodulin binding is required for the activation of constitutive NOS isoforms, while inducible NOS (iNOS) remains active independently of calcium once expressed [70], [71] (**Figure 5**).

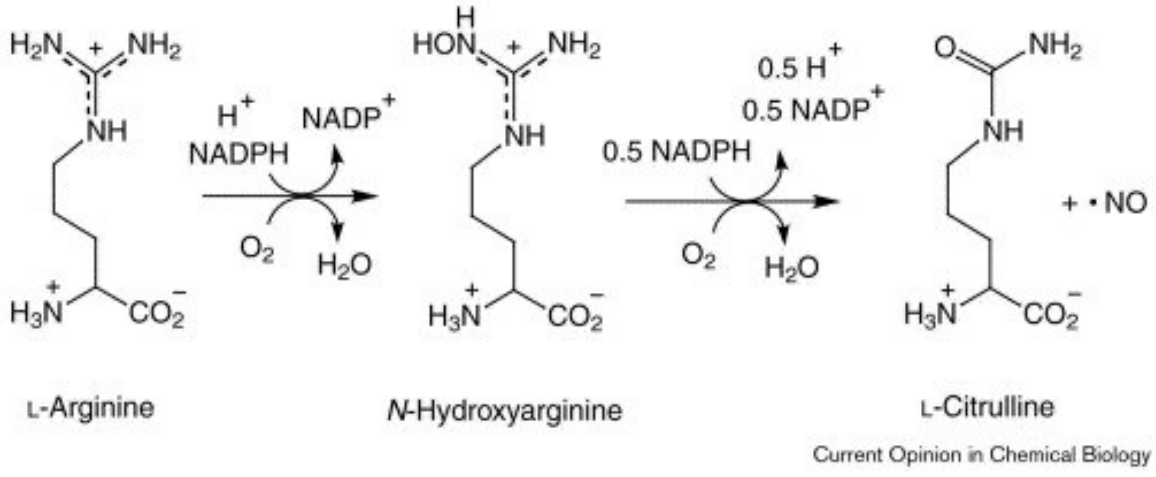


Figure 5. The nitric oxide synthase reactions. Adapted from [71].

Three main NOS isoforms are found in mammals: neuronal NOS (nNOS), endothelial NOS (eNOS), and inducible NOS (iNOS). The constitutive isoforms (nNOS and eNOS) generate low, transient •NO levels in response to physiological stimuli, serving as precise signalling molecules. In contrast, iNOS produces higher and sustained •NO amounts upon induction by pro-inflammatory cytokines or microbial products [71]. This distinction underlies the dual nature of •NO: at controlled concentrations, it regulates vasodilation, neurotransmission, immune defense, and platelet aggregation [72], but in excess, it contributes to cytotoxic and inflammatory processes. The reactivity of •NO stems from its unpaired electron, enabling rapid interactions with O_2, $O_2^{\bullet-}$, transition metals, and thiols. Reaction with $O_2^{\bullet-}$ forms $ONOO^-$, a potent oxidant and nitrating agent capable of inducing protein tyrosine nitration, lipid peroxidation, and DNA strand breaks [73]. This nitrosative stress parallels oxidative stress and is implicated in the pathology of cardiovascular diseases, neurodegeneration, chronic inflammation, and cancer [74].

In photosynthetic microorganisms such as cyanobacteria, •NO plays signalling roles that include regulation of photosynthetic efficiency, nitrogen assimilation, and defense responses to environmental stressors [69]. •NO can modulate gene expression and enzyme activities, often through post-translational modifications like S-nitrosylation and tyrosine nitration. Its production in cyanobacteria may occur via oxidative routes similar to NOS-like activity or through reductive pathways using nitrite as a substrate under anoxic conditions [71]. The interplay between •NO, ROS, and antioxidant defenses in cyanobacteria is critical for maintaining redox balance, particularly under high light, nutrient stress, or pollutant exposure.

Given its multifaceted nature, •NO is both a signalling mediator essential for homeostasis and a potential driver of cellular damage when produced excessively or inappropriately. Understanding the fine regulation of •NO production, its interaction with other reactive species, and its modulation by antioxidant systems is therefore fundamental not only in biomedical contexts but also in exploring the stress physiology and biotechnological potential of cyanobacteria.

1.4.2. Antioxidants

To counteract the potentially deleterious effects of reactive species, living organisms have evolved a sophisticated network of antioxidant defense systems that maintain redox homeostasis. Antioxidants can be broadly defined as molecules that, at low concentrations, can delay or inhibit the oxidation of biomolecules such as proteins, lipids, carbohydrates, and nucleic acids. They act by preventing the formation of reactive species or by neutralizing them through electron or hydrogen donation [75]. Antioxidant

systems are usually divided into enzymatic and non-enzymatic components, with repair and adaptive mechanisms forming the third and fourth lines of defense.

Enzymatic antioxidants act as the first line of defense, rapidly converting reactive species into less harmful molecules. Key enzymes include SOD, which transforms $O_2^{\bullet-}$ into hydrogen peroxide and oxygen; CAT, which breaks down hydrogen peroxide into water and oxygen; and GPx and glutathione reductase (GR), which reduce hydrogen peroxide and lipid hydroperoxides while maintaining the pool of reduced glutathione (GSH) [76], [77]. These enzymes act together: for example, SOD generates H_2O_2, which is then removed by CAT or GPx, preventing the formation of highly reactive hydroxyl radicals through the Fenton reaction.

Non-enzymatic antioxidants form the second line of defense and include small molecules such as GSH, vitamins C and E, carotenoids, flavonoids, phenolic acids, and other secondary metabolites. They neutralize free radicals, stop chain reactions, and protect cell structures from oxidative damage [78]. Once oxidized, many of these antioxidants can be regenerated by other molecules, showing how interconnected these systems are.

Third-line defenses repair oxidative damage after it occurs. They include DNA repair enzymes (polymerases, glycosylases, nucleases) and proteolytic systems (proteases, peptidases) that remove damaged proteins. Fourth-line defenses are adaptive responses in which oxidative stress triggers genes that increase antioxidant enzymes and protective proteins, strengthening the cell's resistance [79].

Cyanobacteria are increasingly recognized as valuable sources of natural antioxidants. They produce bioactive compounds such as carotenoids, phycobiliproteins, phenolic compounds, mycosporine-like amino acids (MAAs), and certain fatty acids [80]. For example, *Arthrospira* (*Spirulina*) species are rich in C-phycocyanin, β-carotene, and polyunsaturated fatty acids, all with strong antioxidant activity demonstrated in both *in vitro* and *in vivo* models [81], [82]. Similar findings were reported by Wang et al. [83], who demonstrated that *Spirulina platensis* extracts obtained by supercritical CO_2 extraction exhibited high radical scavenging and reducing power, largely due to their phycocyanin and carotenoid content. Likewise, El-Baky et al. [84] showed that methanolic extracts of *Spirulina maxima* had strong antioxidant activity in DPPH and ABTS assays, correlating with high phenolic and carotenoid levels. The antioxidant potential of cyanobacterial extracts often results from the combined action of several compounds. Extraction efficiency and composition vary with the solvent used. Polar solvents such as methanol tend to yield higher phenolic content and greater radical

scavenging activity, while acetone can produce fractions with stronger antibacterial activity [85]. In one comparative study, methanol and acetone extracts from several cyanobacterial strains had the highest phenolic content and antioxidant capacity, while water extracts were less active [86].

Overall, the diverse antioxidant systems in cyanobacteria, encompassing both enzymatic and non-enzymatic mechanisms, support their survival in oxidative environments and highlight their potential as sustainable sources of bioactive compounds. By protecting against oxidative damage through multiple mechanisms, cyanobacteria offer a promising platform for new antioxidant applications in biotechnology, health, and environmental management. This dual ecological and industrial relevance strengthens the case for further exploration of cyanobacterial diversity and metabolism, particularly regarding oxidative stress modulation.

Following the biochemical insights into antioxidant mechanisms, it is also essential to evaluate how the extracts interact with human cells. For this reason, cytotoxicity assays in HaCaT keratinocytes are commonly performed to predict their safety and potential downstream applications. HaCAT cells, an immortalized human keratinocyte line, are highly relevant models for predicting compatibility with the skin barrier, particularly for ingredients intended for direct contact with human skin, such as cosmetic, dermatological, or topical pharmaceutical formulations. The evaluation of cytotoxicity is a crucial step in the characterization of natural extracts, as it ensures the absence of harmful compounds that could compromise future applications in health-related fields. These assays provide insight into cells viability, membrane integrity, and metabolic function, allowing the detection of dose- and time-dependent toxicity while identifying early cellular stress responses. Furthermore, using human keratinocyte models supports sustainable research practices by reducing the need for animal testing and offering reproducible and physiologically relevant data [87], [88]. Overall, evaluating cytotoxicity in HaCAT cells is crucial for validating the putative safety of bioactive molecules and for strengthening their potential incorporation into future pharmaceutical, cosmetic, or nutraceutical formulations.

2. Objectives

The global need for new therapeutics and safe, sustainable bioactive compounds continues to drive the screening of renewable biological resources. Cyanobacteria are especially promising because they produce a wide array of specialized metabolites with documented antioxidant, anti-inflammatory, antimicrobial, and photoprotective activities and increasing industrial relevance. Exploring poorly studied habitats increases the chances of discovering novel lineages and chemical diversity. Within this context, the Cabo Verde archipelago offers a distinctive Atlantic setting where taxonomic novelty can co-occur with bioactive metabolite profiles of interest for blue biotechnology.

To achieve this, the study pursued the following specific objectives:

i. Isolation, maintenance and scale-up of filamentous marine cyanobacteria selected from the LEGE-CC under controlled conditions;
ii. Establishment of the taxonomic placement of each strain by combining DNA sequencing with morphology and SEM;
iii. Preparation of lipophilic and hydrophilic extract fractions using a sequential extraction scheme;
iv. Evaluation of the cytotoxic effects of the extracts on HaCAT keratinocytes;
v. Chemical characterization of the extracts, with emphasis on pigments and other metabolite classes;
vi. Assessment of antioxidant potential by the *in vitro* Griess reaction ($^{\bullet}$NO scavenging assay).

3. Materials and Methods

3.1. Isolation of Cyanobacteria strains

Biological samples were originally collected from marine coastal ecosystems of Cabo Verde, specifically from the islands of Santo Antão and São Vicente, as represented in the sampling location map (**Figure 6**) [17]. Samples were placed in falcon tubes containing Z8 medium enriched with 10 µg L^{-1} of vitamin B12, and supplemented with 25 g L^{-1} of synthetic sea salts (Tropic marine, Berlin, Germany) ($Z8_{25}$) [89], and transported to the Blue Biotechnology Environment and Health (BBEH) group at the Interdisciplinary Centre of Marine and Environmental Research (CIIMAR/CIMAR LA) for strains isolation.

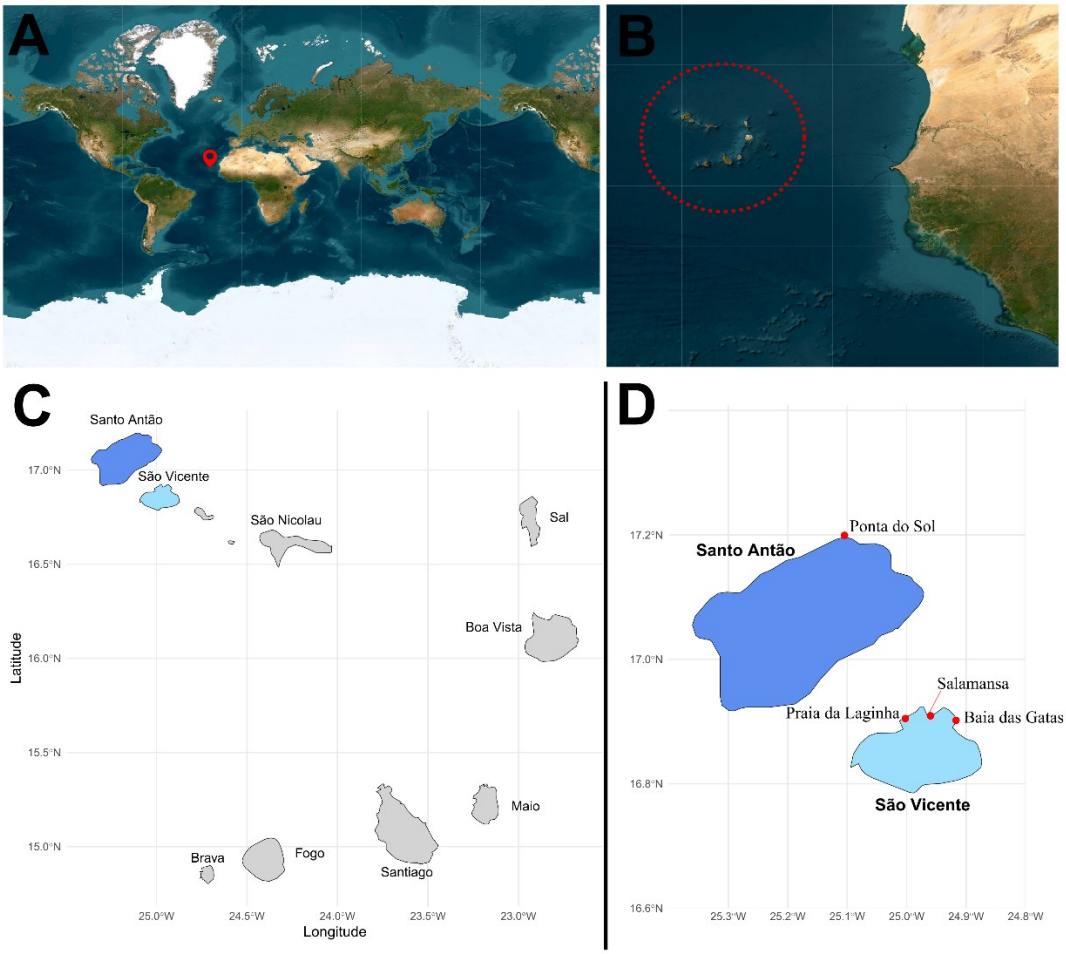


Figure 6. (a) Cabo Verde Islands location. The dotted circle marks the Cabo Verde islands. (b) Map of Cabo Verde Islands. (c,d) Location of the sampling sites at Santo Antão and São Vicente Islands. The map was created using the geom_sf() function from the ggplot2 package in R. First, the geographic data were loaded and prepared using the sf package. The ggplot() function initiated the plot, and geom_sf() was used to add the spatial data layer to the map.

Environmental samples were transferred to sterile 40 mL flasks with fresh $Z8_{25}$ medium under aseptic conditions to promote the growth and visualization of microbial diversity. After incubation, cyanobacterial diversity was initially examined using a Leica DMLB light microscope (Leica Microsystems, Germany), allowing identification of distinct morphotypes. Cyanobacterial strains were then isolated by micromanipulation of individual trichomes [90], under aseptic conditions and transferred into 24-well plates containing $Z8_{25}$ medium [91].

Cultures were maintained for approximately 2–3 weeks at 19 °C, under a 12:12 h light:dark cycle and a light intensity of 25 µmol photons m^{-2} s^{-1}. Cultures were regularly monitored to ensure the absence of visible contamination. Once morphological homogeneity and absence of contaminants were confirmed, six successfully isolated strains were transferred to sterile 40 mL culture flasks with fresh medium and maintained under the same conditions. These strains were subsequently deposited in the Blue Biotechnology and Ecotoxicology Culture Collection (LEGE-CC) at CIIMAR for further morphological analyses during exponential growth phase. Microphotographs of each isolate were taken using a Leica DMLB microscope equipped with a camera and LEICA LAS version 4.12.0 image analysis software.

3.2. DNA extraction, PCR amplification and sequencing

Cells from freshly grown cultures were harvested and washed by centrifugation using fresh culture medium. Genomic DNA was extracted from the six strains using the PureLink Genomic DNA Kit (Invitrogen, Waltham, MA, USA), following the manufacturer's protocol for Gram-negative bacteria.

The 16S rRNA gene was amplified via polymerase chain reactions (PCR) using cyanobacteria-specific primers 27SF [92] and 23SR [93]. Additionally, independent PCR reactions were performed to assess the presence of toxin-synthesis-related genes encoding microcystin (mcyA) and anatoxin (anaC), using specific primer sets and PCR programs as previously described [94]. The PCR reactions were carried out in a final volume of 20 µL containing 5.9 µL of molecular biology-grade water, 4 µL of Green GoTaq Flexi Buffer, 2 µL of magnesium chloride ($MgCl_2$), 2 µL of each forward and reverse primer, 1.5 µL of deoxynucleotide triphosphate (dNTPs), 0.5 µL of bovine serum albumin (BSA), 0.1 µL of GoTaq Flexi DNA Polymerase (Promega, USA), and 2 µL of genomic DNA [95]. Reactions were conducted in a Veriti Thermal Cycler (Applied Biosystems, Thermo Fisher Scientific, Singapore). PCR cycling conditions included an initial denaturation at 94 °C for 5 minutes, followed by 10 cycles of denaturation at 94 °C

for 45 seconds, annealing at 57 °C for 45 seconds, and extension at 72 °C for 2 minutes. PCR products were analysed by electrophoresis on 1.5% (*w/v*) agarose gels stained with SYBR Safe DNA gel stain (Invitrogen by Thermo Fisher Scientific, USA). DNA fragments of the expected size were excised and purified using the NZYGelPure kit (NZYTech, Portugal), according to the manufacturer's instructions. Purified amplicons were subsequently sent for sequencing using multiple internal primers to ensure full coverage of the 16S rRNA gene, as described by Oliveira et al. [96].

3.3. Phylogenetic analysis

The phylogenetic analysis aimed to position the Cabo Verde strains among the cyanobacterial genera. For that, we aligned the 16S rRNA gene sequences of the studied isolates with sequences of cyanobacterial reference strains and additional sequences retrieved from GenBank (NCBI) by BLAST. The alignment was performed using MAFFT [97], with the full-length of the 16S rRNA gene sequences. The outgroup used was *Gloeobacter violaceus* PCC 8105 (AF132791). This alignment contained 453 sequences. The phylogenetic reconstruction was performed using the FastTree method [98], with the bootstrap value set to the default of 1000 as per the manual. The resulting tree was edited using iTOL [99].

The 16S rRNA gene and 16S-23S ITS p-distances were calculated using MEGA11. The 16S-23S ITS secondary structures of D1-D1´, Box B and V3 helices were folded using MFold [100], according to Lukesova et al. [101].

3.4. Scanning Electron Microscopy (SEM)

SEM analysis was used to examine cell surface morphology [102], following the protocol described by Brito et al. [103]. Cells were harvested by centrifugation and fixed overnight (12 h) at 4 °C in a final solution of 2% glutaraldehyde (for electron microscopy, VWR–BHD Chemicals, Czech Republic) prepared in 50mM sodium cacodylate buffer, pH 7.4 (Electron Microscopy Sciences, Pennsylvania, USA). After postfixed overnight, cells were washed once in double-strength sodium cacodylate buffer. Dehydration was performed through a graded ethanol series in deionized water (*v/v*) of 25%, 50%, 75%, and 100%, with each step lasting 5 minutes (Ethanol Absolute, Molecular Biology Grade, Fisher BioReagents, UK). Between steps, cells were collected by centrifugation at 11000 × g for 1 minute at room temperature (Micro Star 17R, VWR, Radnor, PA, USA). In the final step, 500 µL of 100% ethanol was added to fully submerge the sample. The critical-point drying was used (CPD 7501, Polaron Range) to preserve the sample's ultrastructure. Samples were coated with a gold/palladium (Au/Pd) thin film in adhesive

carbon tape, by sputtering, using the SPI Module Sputter Coater equipment for 80 seconds and a 15 mA current. SEM/EDS analysis was performed using a high resolution (Schottky) Environmental Scanning Electron Microscope with X-Ray Microanalysis and Electron Backscattered Diffraction analysis: FEI Quanta 400 FEG ESEM / EDAX Genesis X4M. Images were taken with the SEM software version 4.1.10.2127 at an acceleration voltage of 15kV with the Everhart-Thornley detector (ETD) for secondary electrons (SE) and Backscattered Electron Detector (BSED) for backscattered electrons (BSE).

3.5. Cultures scale-up and collection of biomass

Six cyanobacterial strains from LEGE-CC were selected to represent different taxonomic orders for preliminary cytotoxicity and antioxidant screening: *Leptothoe* sp. LEGE 181201, *Salileptolyngbya* sp. LEGE 181209, Geminocystaceae cyanobacterium LEGE 181210, *Salileptolyngbya* sp. LEGE 181216, *Salileptolyngbya* sp. LEGE 181219, and Leptolyngbyaceae cyanobacterium LEGE 181156.

Biomass was transferred under aseptic conditions in a laminar-flow cabinet. Cultures were grown sequentially from 4 mL to 400 mL (**Figure 7**). At this stage, concentrated were then pooled to reach 4 L total volume. The 4 L cultures were maintained in photobioreactors equipped with aeration systems providing continuous air flow, including both inlet and outlet streams, to ensure optimal conditions for cyanobacterial growth.



Figure 7. Cultivation of cyanobacterial strains in 40 mL flasks at the bioterium of aquatic organisms (BOGA, CIIMAR).

All strains were cultivated in $Z8_{25}$ medium [89] and the cultures were maintained in the bioterium of aquatic organisms (BOGA) at CIIMAR at a constant temperature (25 °C), under continuous aeration, with light intensity of 10–30 µmol photons m^{-2} s^{-1} and a photoperiod of 14 h light/10 h dark (**Figure 8**).



Figure 8. Cultivation of cyanobacterial strains in 4 L photobioreactors at the bioterium of aquatic organisms (CIIMAR).

Fresh biomass was harvested by filtration using nylon mesh filters (Kunststoff-Analysensieb, DIN 4197) with 11 µm or 20 µm pore sizes, selected according to the strain morphology. Filtered biomass was immediately frozen, freeze-dried (Telstar LyoQuest), and stored at −20 °C until extraction.

3.6. Preparation of extracts

Sequential acetone and aqueous extracts were prepared from dry, pulverized biomass to recover compounds across polarities. Biomass was finely pulverized to increase surface area and improve solvent penetration.

Acetone extract

Acetone extraction was performed using 0.5 g of dry biomass, which was immersed in 40 mL acetone and subjected to ultrasound-assisted extraction with an MS-72 probe (Bandelin Sonoplus, Berlin, Germany) for 5 min. Samples were kept on ice throughout the procedure to prevent temperature increases caused by sonication, thereby preserving thermolabile compounds and minimizing potential oxidative degradation.

Subsequently, centrifugation was employed to remove cellular debris at 5000 Gs for 5 minutes at 4 °C using a Thermo Scientific™ HERAUS Megafuge™ 16R centrifuge

(Waltham, MA, USA). Supernatants were filtered through 0.22 µm sterile syringe filters (FilterBio). The biomass underwent four additional extraction cycles. Combined filtrates were concentrated and evaporated under reduced pressure using a BUCHI R-210 Rotary Evaporator (Cambridge, MA, USA) set at 200 mbar, with the water bath at 30 °C and the condenser at −8 °C, to gently remove the solvent without degrading the extracted compounds. Residues were weighed for yield and stored at −20 °C until chemical and biological analyses.

Water extract

Following acetone extraction, residual biomass was left in a fume hood overnight to evaporate any remaining solvent. The dry pellet was then extracted with 40 mL ultrapure water following the same procedure, repeated four additional times.

After extraction, aqueous supernatants were directly collected into a clean container and frozen for subsequent lyophilization. Dried extracts were weighed (yield) and stored at room temperature until analysis.

3.7. Cytotoxicity to human keratinocytes (HaCAT)

To evaluate the safety profile of the acetone and aqueous cyanobacterial extracts, a preliminary *in vitro* cytotoxicity screening was conducted with human keratinocytes (HaCAT, ATCC) before further chemical and biological analyses.

3.7.1. Cells culturing

The HaCAT line (ATCC) was thawed and maintained for at least one week prior to assays to allow recovery. During this period, only medium replacement was performed. Cells were cultured in high-glucose Dulbecco's Modified Eagle Medium (DMEM, Gibco) supplemented with 10% fetal bovine serum (FBS, Gibco), 1% penicillin-streptomycin (100 IU $mL^{-1}$and 10 mg mL^{-1}, respectively; Gibco), and 0.1% amphotericin B (Gibco). Cultures were kept at 37 °C in a humidified atmosphere with 5% CO_2, and culture medium was renewed every two days.

At 80–90% confluency, adherent cells were detached by removing the medium, washing with phosphate-buffered saline (PBS, Gibco), and incubated with TrypLE Express Enzyme (Gibco) for 2–5 minutes to detach the adherent cells. The enzymatic reaction was neutralized with an equal volume of DMEM. Cells were centrifuged (Eppendorf 5430), resuspended in 1 mL DMEM, and seeded into new flasks for maintenance or used in cytotoxicity assay. All procedures were performed under sterile conditions in a Thermo

Scientific™ Safe 2020 laminar flow chamber (Thermo Fisher Scientific, Waltham, MA, USA).

3.7.2. Cytotoxicity assessment by the MTT assay

Cells viability was assessed by the reduction of 3-(4,5-dimethylthiazol-2-yl)-2,5-diphenyltetrazolium bromide (MTT, 98%; Thermo Scientific), as previously described in the literature [42], [104]. After detachment, 10 µL of the cell suspension was mixed with 10 µL trypan blue solution (Corning) and counted in a Neubauer chamber under an inverted microscope (Olympus CKX41).

Cells were seeded in 96-well plates at a density of 2.5×10^4 cells mL^{-1} for both 24 and 48h assays. After 24 h adhesion period, medium was removed and cells were exposed for 24 and 48 h to five serial concentrations of each cyanobacterial extract (12.5 to 200 µg mL^{-1}). Acetone extracts were solubilized in dimethyl sulfoxide (DMSO, Gibco) and diluted in DMEM to ensure a final DMSO concentration below 1%. Aqueous extracts were resuspended in PBS and diluted in DMEM. All extracts serial dilutions were prepared from a 20 mg mL^{-1} stock. Solvent controls included 1% DMSO (acetone-extract control) and DMEM (aqueous-extract control). A 20% DMSO solution in DMEM was used as a positive control for cell death.

After the exposure, 20 µL MTT solution was added per well and plates incubated 3 h. Medium was removed, 100 µL DMSO was added to solubilize the purple-colored formazan crystals, plates were gently agitated, and absorbance read at 550 nm on a Synergy HT multi-detection microplate reader (BioTek, Bad Friedrichshall, Germany) with Gen5™ software. Assays were conducted in quadruplicate and results were expressed as mean ± standard deviation. Cytotoxicity was expressed as percentage (%) of cell viability relative to solvent control.

3.8. Chemical Analysis

3.8.1. Carotenoids profiling by HPLC-PDA

Dried extracts were dissolved in HPLC-grade acetone to 5 or 10 mg mL^{-1} depending on chromatographic resolution. Pigments profile were determined in the acetone extract using a Waters Alliance 2695 high-performance liquid chromatography (HPLC) system equipped with a photo diode-array (PDA) detector (USA), following a previously described method reported by Morone et al. [43]. Separation used a YMC Carotenoid C30 (250 × 4.6 mm, 5 µm) column, at 25 °C using a column heater (Waters Corporation, Milford, CT, USA). The mobile phase consisted of methanol (A) and methyl tert-butyl ether (B) (VWR Prolabo), applying the following gradient elution: starting with 5% B,

followed by 10% B at 5 min, 18% B at 20 min, 30% B at 28 min, 50% B from 31 to 37 min, 80% B from 38 to 47 min, and returning to 5% B from 48 to 50 min. The flow rate was 0.9 mL min^{-1}, with an injection volume of 5 µL. Chromatographic data were processed in Empower2® software (Waters Corporation, Milford, MA, USA). Spectra were collected between 250 and 750 nm. Compounds were identified by retention times and UV-Vis spectra with those of authentic standards. Carotenoids were quantified by peak absorbance at 450 nm and compared with calibration curves of the respective external standards.

The following standards were used: lutein, β-carotene, chlorophyll-*a*, zeaxanthin and β-cryptoxanthin (Extrasynthese, Genay, France; Sigma-Aldrich, St. Louis, MO, USA; DHI, Hørsholm, Denmark). Unidentified carotenoids were quantified as β-carotene, the most representative carotene; β-carotene derivatives as β-carotene; chlorophyll derivative as chlorophyll-*a*, the major cyanobacteria chlorophyll; and mixoxanthophyll as zeaxanthin, the most representative xanthophyll in this study. Calibration curves were performed with five different concentrations of standards, selected as representative of the range of compounds concentration expected in the samples. Calibration plots, R^2, LOD and LOQ values are shown in **Table 2**.

Table 2. Calibration curves of authentic standards used for quantification of different carotenoids and chlorophylls.

Standards	Calibration Curve	r^2	LOD [a]	LOQ [b]
Lutein	y = 52314156.52x - 197720.04	0.9900	0.00565702	0.01714249
β-carotene	y = 34727408.00x - 96390.00	1.0000	0.00369039	0.01118299
Chlorophyll-*a*	y = 5242773.3333x + 26570.00	0.9981	0.00890869	0.02699603
Zeaxanthin	y = 66258082.7826x + 130225.43	0.9997	0.00125300	0.00379696
β-cryptoxanthin	y = 17708546.7826x + 68409.87	0.9977	0.00640751	0.01941671

[a] limit of detection (mg mL^{-1}); [b] limit of quantification (mg mL^{-1}).

3.8.2. Phycobiliproteins and Chlorophylls profiling by spectrophotometry

Pigments in aqueous extracts were quantified spectrophotometrically. Aqueous extracts were resuspended in ultrapure water (for phycobiliproteins) or acetone (for chlorophylls), adjusted to 0.5 mg mL^{-1}, and analyzed in duplicate. Results were expressed in µg of pigment per mg of dry extract [105]. Because PBPs are water-soluble proteins, their

determination was performed using water as solvent. Absorbance was read at 562, 615, and 652 nm, and concentrations were calculated using standard equations as previously described [106]:

$$Phycocyanin\ (PC) = \frac{(A_{615nm} - 0.474 \times A_{652nm})}{5.34}$$

$$Allophycocyanin\ (APC) = \frac{(A_{652nm} - 0.208 \times A_{615nm})}{5.09}$$

$$Phycoerythrin\ (PE) = \frac{(A_{562nm} - 2.41 \times PC - 0.849 \times APC)}{9.62}$$

Chlorophylls were resuspended in acetone due to their hydrophobic nature and absorbance of the resulting solution was read at 630, 647, 664, and 691 nm. Concentrations were calculated according to the following equations [106]:

$$Chl\ a = -0.3319\ (A_{630nm}) - 1.7485\ (A_{647nm}) + 11.9442\ (A_{664nm}) - 1.4306(A_{691nm})$$

$$Total\ Chl = 21.3877\ (A_{630nm}) + 10.3739\ (A_{647nm}) + 5.3805\ (A_{664nm}) + 5.5309\ (A_{691nm})$$

3.8.3. Determination of Total Phenolics Content (TPC) by Folin-Ciocalteu Method

Total phenolics content of aqueous extracts was quantified by the colorimetric Folin–Ciocalteu method, as previously described [107], with slight modifications. Under alkaline conditions, phenolics reduce the reagent, forming a blue-colored complex whose intensity is proportional to total phenolics [108], [109].

Aqueous extracts were resuspended in 80% ethanol to a final concentration of 10 mg/mL. For each sample, 25 µL of extract was mixed with 500 µL deionized water, 100 µL sodium carbonate solution (Na_2CO_3, 75 g L^{-1}), and 25 µL Folin–Ciocalteu reagent (Sigma-Aldrich). Blanks contained 25 µL of 80% ethanol instead of reagent. Mixtures were incubated 60 min at room temperature in the dark. Then 200 µL from each reaction

mixture was transferred to a 96-well plate and absorbance read at 725 nm. Gallic acid was used to build a calibration curve (**Figure 9**). Results are expressed as mg gallic acid equivalents (GAE) per mg of dry extract. Results are presented as mean ± standard deviation of two independent experiments.

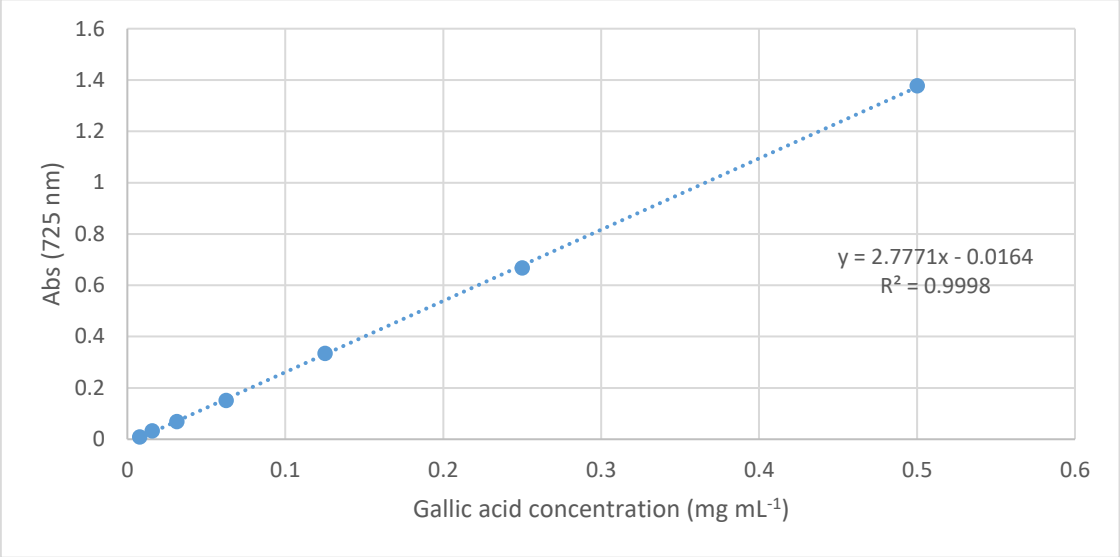


Figure 9. Calibration curve of gallic acid used for the quantification of total phenolic content (TPC) by the Folin–Ciocalteu method.

3.8.4. Determination of Total Sugars by the Phenol-Sulfuric Method

Total sugars were quantified by the phenol–sulfuric acid method [110], with slight modifications. Carbohydrates form stable yellow–orange chromophores upon treatment with phenol and concentrated sulfuric acid (H_2SO_4), and absorbance correlates with sugar content [111].

Extracts were diluted in 80% ethanol; a 20% phenol solution and a 1000 mg·L^{-1} glucose monohydrate solution were prepared. Standard solutions ranging from 50 to 1000 mg·L^{-1} were used to construct the glucose calibration curve (**Figure 10**). In microtubes, 100 µL of standard, sample, blank or sample blank were added, followed by 500 µL of H_2SO_4 and 100 µL of phenol. Then, 200 µL from each microtube was transferred to a 96-well plate. After 30 min incubation in the dark, absorbance was read at 490 nm. Analyses were performed in triplicate and expressed as glucose equivalents (mg GE per mg of dry extract).

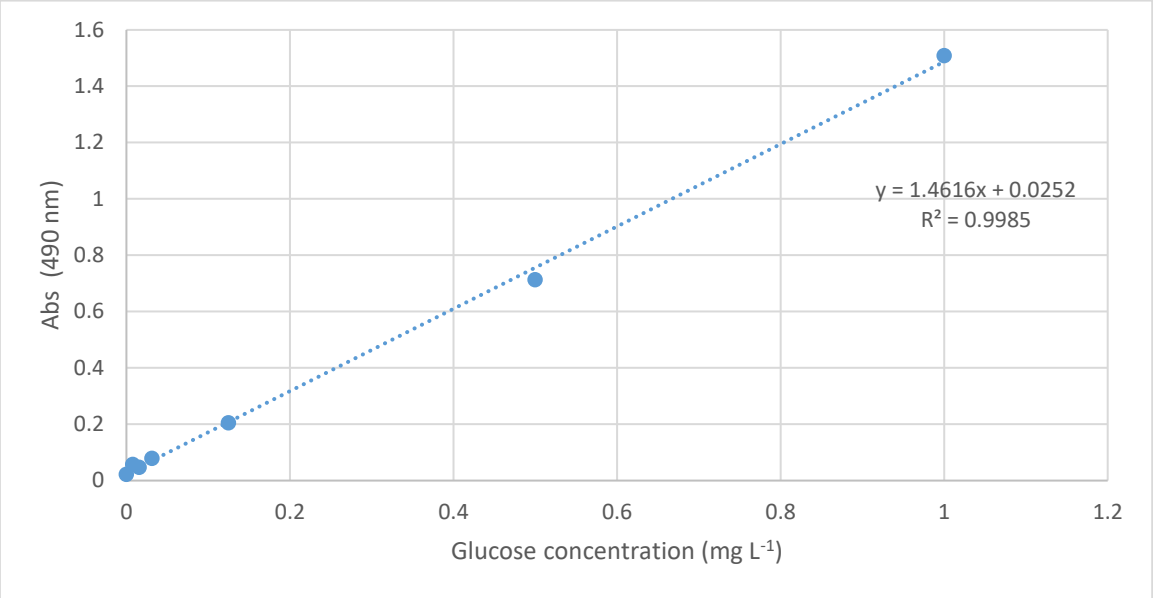


Figure 10. Calibration curve for glucose using the phenol-sulfuric acid method.

3.9. Nitric Oxide Scavenging

Nitric oxide scavenging was evaluated using the Griess reaction [112], [113] as described in [15]. Aqueous extracts were resuspended in phosphate buffer (KH_2PO_4, pH= 7.0), and acetone extracts in DMSO. Serial dilutions were prepared from a stock at a final concentration of 20 mg mL^{-1}. For the assay, 75 µL of each extract at different concentrations was incubated with 75 µL sodium nitroprusside (SNP, 2.5 mg mL^{-1}) in phosphate buffer under light for 1 h. Then, 75 µL Griess reagent (1 % sulfanilamide and 0.1 % N-(1-napthyl) ethylenediamine in 2 % H_3PO_4) was added. After 10 min in the dark at room temperature, absorbance was read at 562 nm.

•NO scavenging capacity was expressed as % relative to control. Three independent experiments were performed in duplicate, and quercetin served as a positive control. The IC values and the corresponding dose–response curves were calculated as previously described.

3.10. Statistical Analysis

For analysis, various R packages were employed to ensure robust and accurate data interpretation. Data were first checked for normality using the Shapiro–Wilk test, implemented through the ‘shapiro.test()’ function from the ‘stats’ package. Homogeneity of variances was assessed using Levene’s test, which was conducted using the ‘leveneTest()’ function from the ‘car’ package. Since the data did not follow a normal distribution, group comparisons were performed using a non-parametric bootstrap

approach with 1,000 iterations. This method resampled the original data with replacement to estimate the sampling distribution of the mean differences between groups. The empirical p-value was calculated as the proportion of resampled mean differences greater than or equal to the observed difference. This approach is particularly suitable for small sample sizes (<30) or when the assumption of normality is violated. Data visualization and the generation of summary statistics were performed using the ggplot2 and base R packages, which facilitated the creation of barplots, boxplots, and other graphical representations to illustrate the distribution and significance of the data. PCA was performed with the PCA() function from the FactoMineR package. The map was created using the geom_sf() function from the ggplot2 package in R. First, the geographic data were loaded and prepared using the sf package. The ggplot() function initiated the plot, and geom_sf() was used to add the spatial data layer to the map [114].

4. Results and Discussion

Cyanobacteria are increasingly recognized not only as essential contributors to marine ecosystems but also as prolific sources of specialized metabolites with multifunctional potential. Their remarkable ability to adapt to diverse environmental conditions translates into the biosynthesis of compounds with antioxidant, antimicrobial, and broader biotechnological relevance. In particular, strains from Cabo Verde have revealed notable capacities for metabolite production, reinforcing their value as models for chemical and biotechnological exploration [12], [15]. In this context, strains isolated from the Cabo Verde archipelago were chemically characterized, with emphasis on pigments, phenolics, carbohydrates, and radical scavenging activities, in order to evaluate their contribution to blue biotechnology and their potential for innovative applications.

4.1. Diversity of Cabo Verde isolates

The phylogenetic analysis of 16S rRNA sequences revealed three distinct lineages within the Nodosilineales order. Among the six cyanobacterial strains isolated from the islands of Santo Antão and São Vicente, Cabo Verde (**Figure 11**), Geminocystaceae cyanobacterium LEGE 181210 clustered with *Cyanobacterium* Rippka & Cohen-Bazire, but shared only 93 % 16S rRNA sequence identity with it, a value below the 95 % threshold typically required for assignment at the genus level [115]. This low similarity indicates that LEGE 181210 cannot be confidently placed in *Cyanobacterium* and may represent a distinct genus that warrants further investigation.

Additionally, Leptolyngbyaceae cyanobacterium LEGE 181156 and *Leptothoe* sp. LEGE 181201 grouped within a well-supported *Leptothoe* clade, indicating that they belong to this genus. In contrast, *Salileptolyngbya* spp. LEGE 181209, LEGE 181216 and LEGE 181219, clustered within a well-supported *Salileptolyngbya* clade, also indicating their taxonomical classification (**Figure 11**).

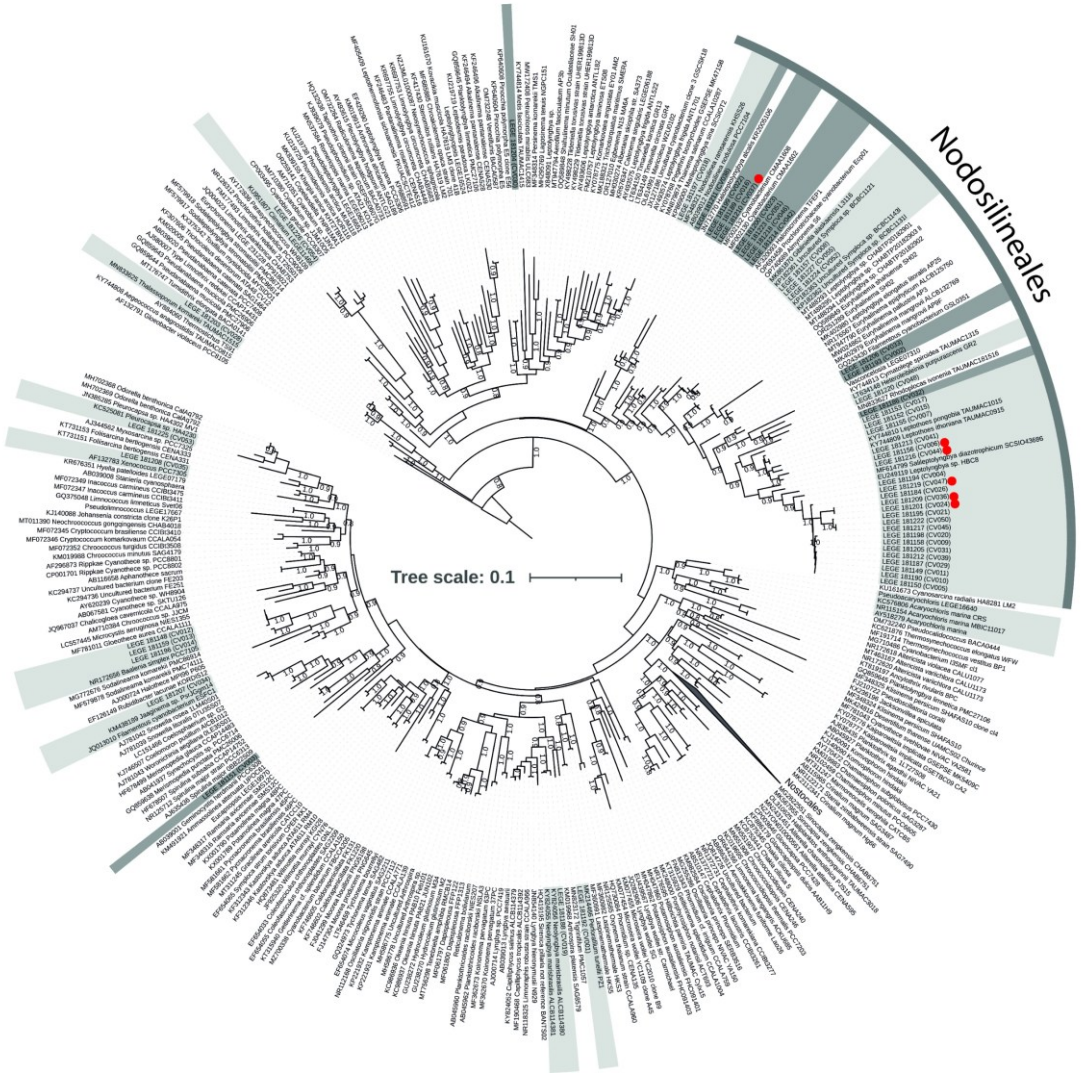


Figure 11. Maximum-Likelihood phylogenetic tree based on 16S rRNA gene sequences of the Cabo Verde isolates and related cyanobacterial taxa. The dark-grey strip indicates the order Nodosilineales. Strains obtained in this study are marked with red dots.

Regarding morphology, all Cabo Verde isolates share key morphological features, in accordance with the Nodosilineales characters. Light microscopy revealed filamentous trichomes with constrictions at cross-walls and surrounded by firm, diffluent sheaths (**Table 3, Figure 12**). Cell dimensions varied among strains, ranging from narrow filaments of approximately 1.7 µm in width (Leptolyngbyaceae cyanobacterium LEGE 181156) to broader trichomes up to 3.8 µm in *Salileptolyngbya* sp. LEGE 181216. Culture colours also differed, from brownish-purple in *Leptothoe* sp. to greenish-cyan and olive green in *Salileptolyngbya* spp., suggesting variability in pigment composition. These morphological traits are consistent with genera previously reported from Cabo Verde marine habitats, particularly *Leptothoe* and *Salileptolyngbya*, both of which have been associated with pigment diversity and antioxidant activity [16], [17]. The morphological

features of the strains are consistent with their phylogenetic placement, corroborating with their taxonomical identification. A summary of morphometric parameters and molecular identities is provided in **Table 3**.

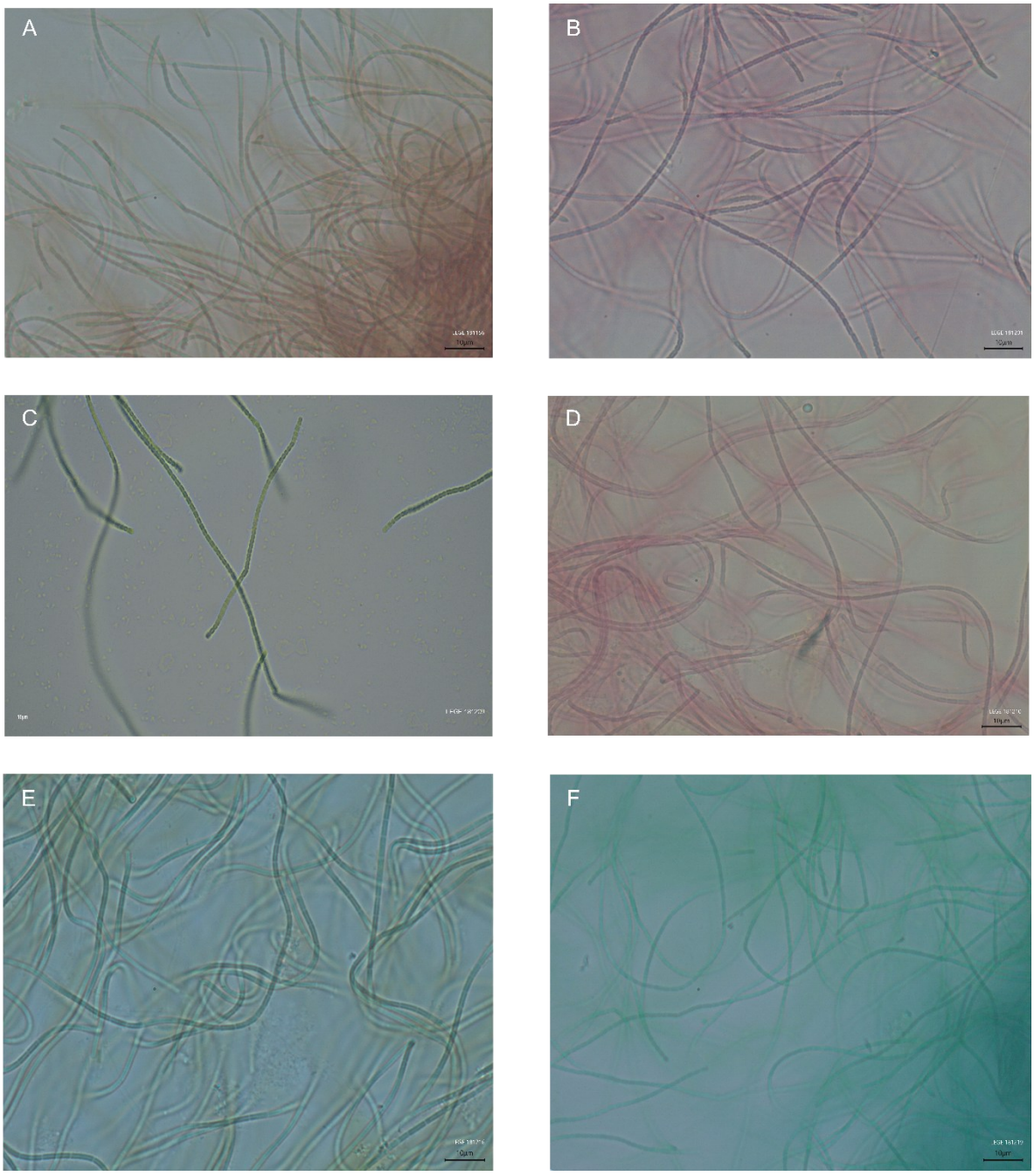


Figure 12. Morphological features of the six cyanobacterial strains isolated from Cabo Verde: (A) Leptolyngbyaceae cyanobacterium LEGE 181156, (B) *Leptothoe* sp. LEGE 181201, (C) *Salileptolyngbya* sp. LEGE 181209, (D) Geminocystaceae cyanobacterium LEGE 181210, (E) *Salileptolyngbya* sp. LEGE 181216 and (F) *Salileptolyngbya* sp. LEGE 181219. Images were captured using a Leica DMLB light microscope equipped with a digital camera.

Table 3. Morphological and molecular summary of the six cyanobacterial strains isolated from Cabo Verde.

Strains	**LEGE code**	**Location / Sampling site**	**Habitat**	**Morphological type**	**Cell shape**	**Cell dimensions (µm)**	**Genus**	**16S rRNA % identity**	**Closest reference strains**
Leptolyngbyaceae cyanobacterium	LEGE 181156	Ponta do Sol (Sto. Antão Island), Cabo Verde	Intertidal rocks	Filamentous	Isodiametric or longer than wide	1.72 ± 0.30 × 1.31 ± 0.06	*Leptothoe*	98	*Leptothoe sithoniana* TAUMAC0915 (KY744809)
Leptothoe sp.	LEGE 181201	Ponta do Sol (Sto. Antão), Cabo Verde	Pier wall	Filamentous	Isodiametric or longer than wide	2.14 ± 0.39 × 1.51 ± 0.06	*Leptothoe*	96.7	*Leptothoe sithoniana* TAUMAC0915 (KY744809)
Salileptolyngbya sp.	LEGE 181209	Ponta do Sol (Sto. Antão), Cabo Verde	Pier wall	Filamentous	Isodiametric or longer than wide	1.86 ± 0.44 × 1.50 ± 0.12	*Salileptolyngbya*	96.7	*Salileptolyngbya diazotrophicum* SCSIO43686 (MF614799)
Geminocystaceae cyanobacterium	LEGE 181210	Praia da Laginha (S. Vicente Island), Cabo Verde	Subtidal	Filamentous	Longer than wide, with rounded ends	2.9 ± 0.78 × 1.34 ± 0.10	Possible new genus	93.1	*Cyanobacterium* CMAA 1602
Salileptolyngbya sp.	LEGE 181216	Baía das Gatas (S. Vicente Island), Cabo Verde	Rocks, next to pier	Filamentous	Isodiametric or longer than wide	3.85 ± 0.58 × 1.58 ± 0.08	*Salileptolyngbya*	95.7	*Salileptolyngbya diazotrophicum* SCSIO43686 (MF614799)
Salileptolyngbya sp.	LEGE 181219	Salamansa (S. Vicente Island), Cabo Verde	Rocks	Filamentous	Longer than wide	2.20 ± 0.51 × 1.12 ± 0.06	*Salileptolyngbya*	96	*Salileptolyngbya diazotrophicum* SCSIO43686 (MF614799)

Among the studied strains, within the *Salileptolyngbya* cluster, the strain LEGE 181209 was more deeply studied using polyphasic approach [115]. This strain is morphologically very similar to the other Cabo Verde *Salileptolyngbya* isolates under light microscopy: trichomes with non-attenuated ends, clear constrictions at cross-walls, homogeneous cell content and comparable cell dimensions. However, SEM revealed a diagnostic ultrastructural feature in LEGE 181209 (conspicuous internal pseudovacuoles) not observed in the other *Salileptolyngbya* already known species: *S. diazotrophicum* and *S. insularis* (**Figure 13, Table 4**).

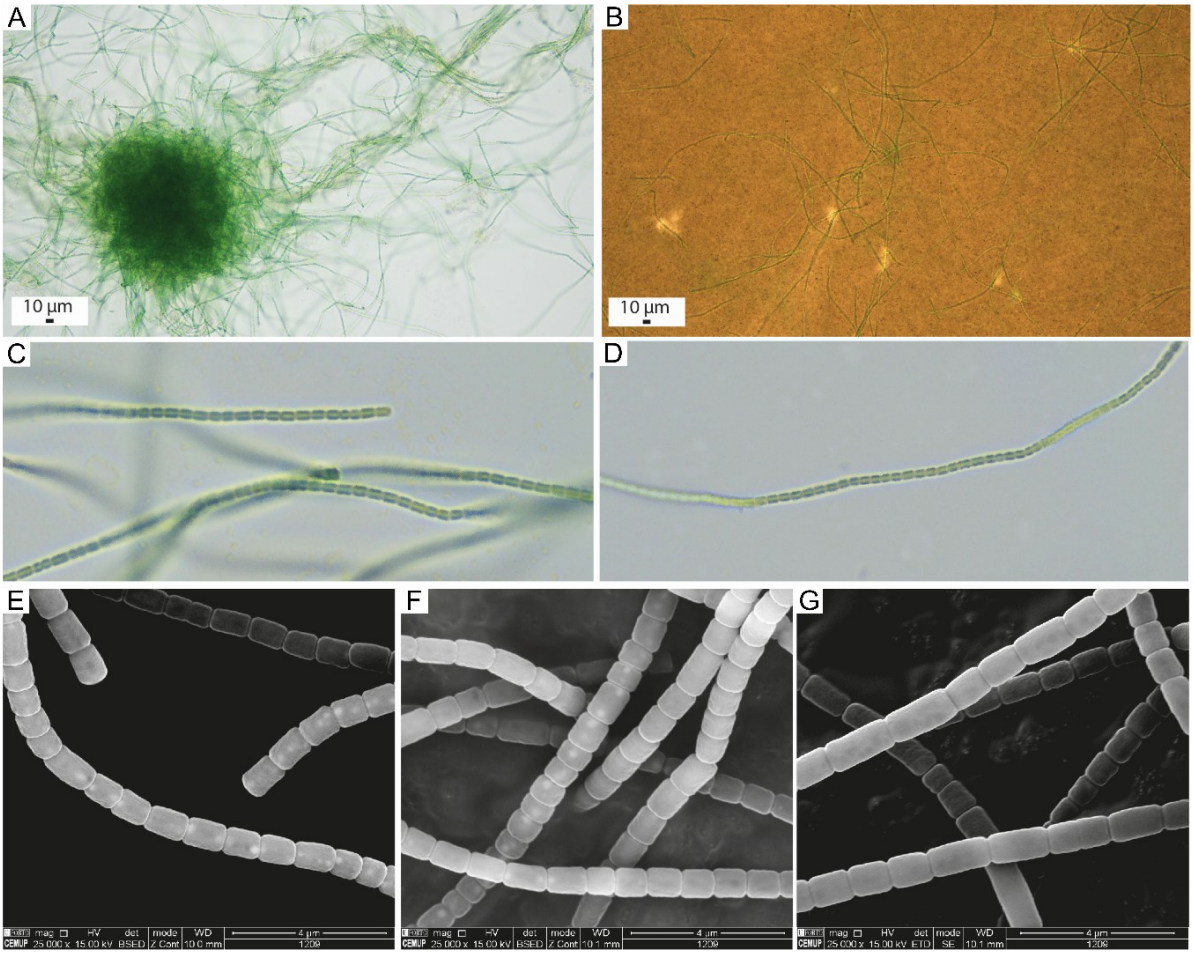


Figure 13. Light and scanning electron micrographs of *Salileptolyngbya* sp. LEGE 181209. (A) Light microscopy showing a dense aggregate of entangled filaments in liquid culture (10 µm). (B) Slide preparation with China ink, showing individual dispersed filaments (10 µm). (C,D) Light-microscopy details of trichomes displaying clear cross-wall constrictions and homogeneous cell content (10 µm). (E,F) Scanning electron micrographs of trichomes with firm sheaths; bright spherical inclusions (white spheres) correspond to internal pseudovacuoles (4 µm). (G) Scanning electron micrograph of trichomes without visible pseudovacuoles (4 µm).

Table 4. Morphological comparisons of *Salileptolyngbya* species.

	S. diazotrophicum [116]	***S. insularis*** [117]	***Salileptolyngbya*** **sp. LEGE 181209 (this study)**
Trichomes	Not attenuated at the ends. Markedly constricted	Not attenuated at the ends. Constricted.	Not attenuated. Constricted
Mucilaginous envelope	Sheaths firm, thin	Absent	Absent
Cells shape	Longer than wide	2.8x longer than wide. Translucent septa between cells.	Isodiametric longer or shorter than wide.
Cells measurements	1.5-2.4 µm long x 0.9-1.5 µm wide.	1.7–3.1 µm long x 0.6–1.0 µm wide	
Cell content	Homogenous. Gas vesicles absent.	Homogenous. Gas vesicles absent.	Pseudovacuoles visible only under SEM. Gas vesicles absent
Habitat	Marine, planktonic	Marine, benthic, epipsamic.	Marine, growing of rocks of a Pier wall.

Beyond this morphological difference, molecular data show clear divergence: LEGE 181209 forms a separate branch within the *Salileptolyngbya* clade and shares < 98 % 16S rRNA sequence identity with its nearest neighbours (*S. insularis* and *S. diazotrophicum*), below the ≥ 98.8 % threshold for species delimitation [118]. 16S-23S ITS analysis further supports this separation, with a 9.81 % sequence difference and distinct secondary-structure patterns in the D1–D1′, Box B and V3 domains (**Figure 14**), far exceeding the ≤ 3 % intraspecific cut-off. Together with the pseudovacuoles visible only by SEM, these molecular and ultrastructural features reinforce the recognition of LEGE 181209 as a candidate novel species, with a formal description in preparation.

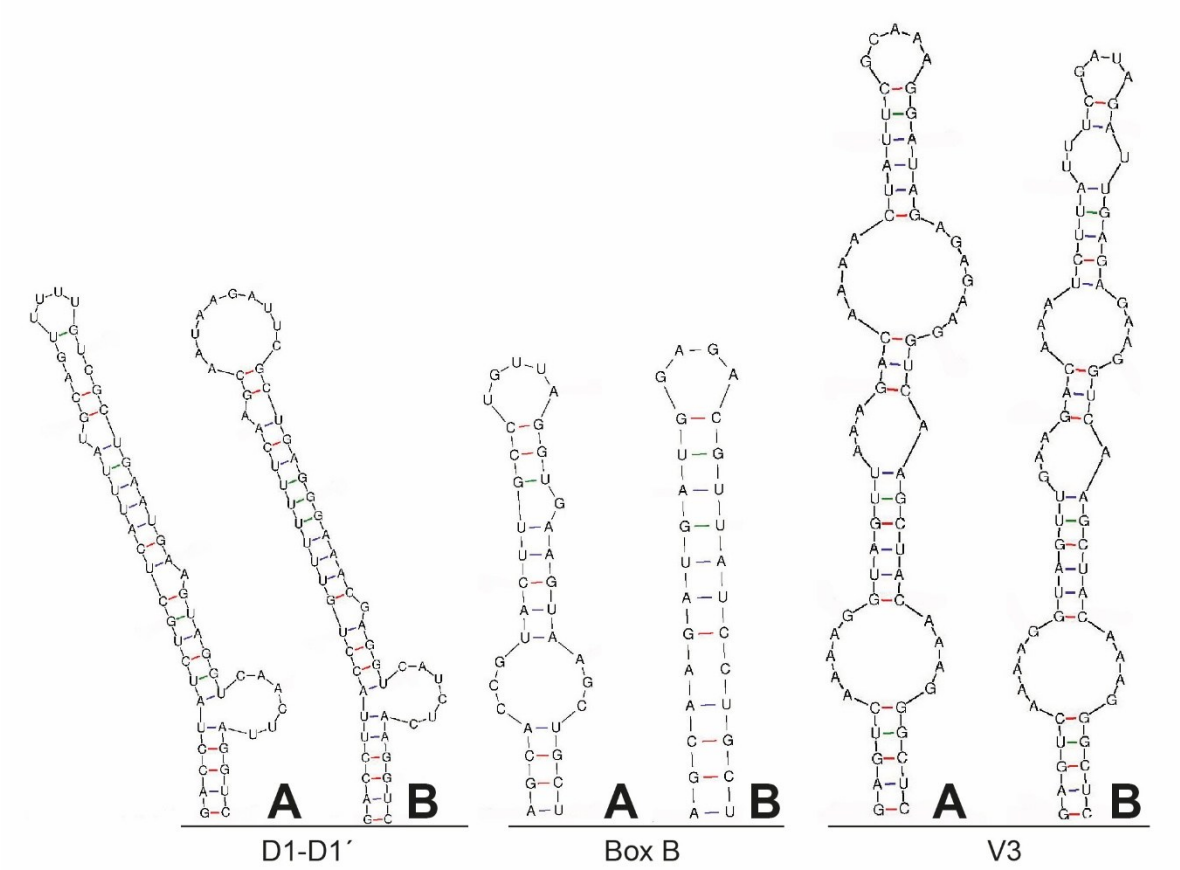


Figure 14. Predicted secondary structures of the 16S–23S ITS regions (D1–D1′, Box B and V3 domains) of (A) *Salileptolyngbya* sp. LEGE 181209 compared with (B) *S. diazotrophicum*, showing clear structural differences supporting species-level separation.

Toxin analysis

PCR assays targeting microcystin (mcyA) and anatoxin (anaC) biosynthetic genes were negative for all isolates (**Figure 15**), demonstrating the absence of these cyanotoxin pathways and supporting their potential for safe biotechnological exploitation.

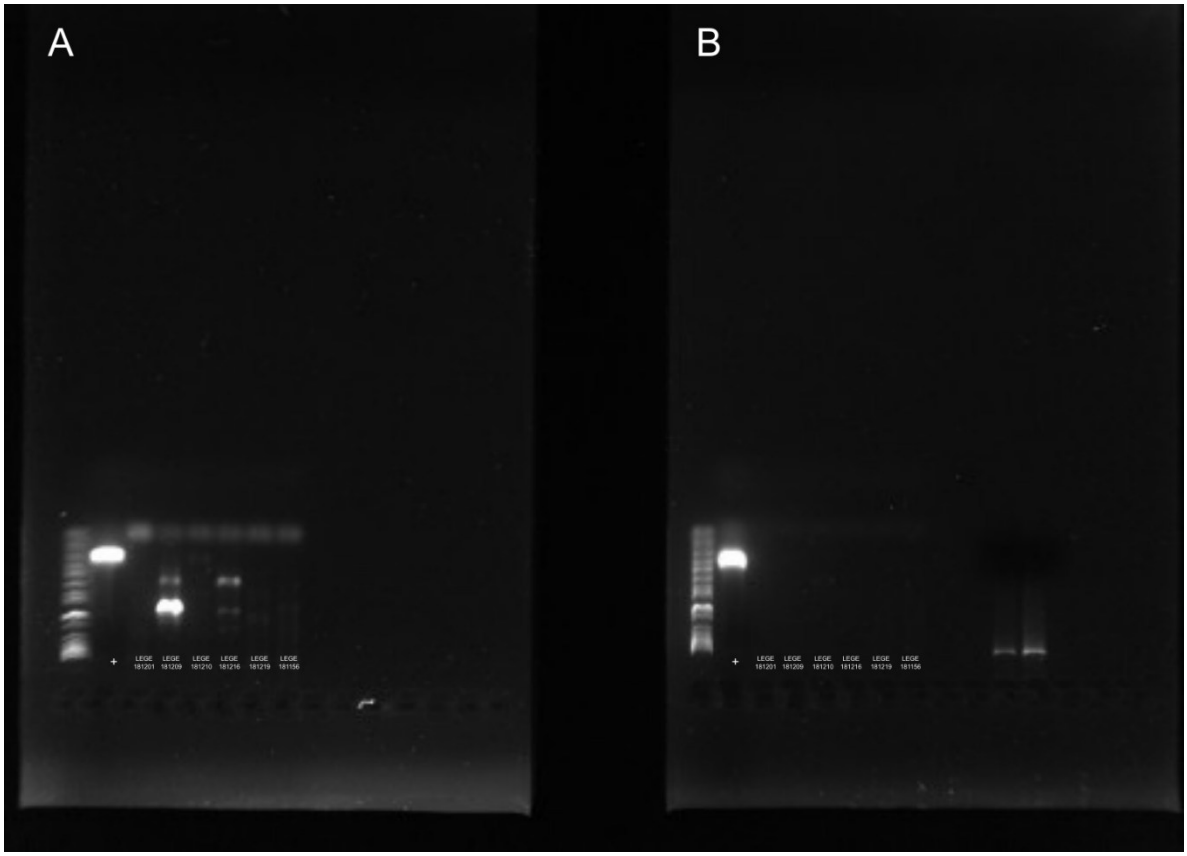


Figure 15. PCR gels showing absence of mcyA (A) and anaC (B) amplification. Positive control (+); *Leptothoe* sp. LEGE 181201; *Salileptolyngbya* sp. LEGE 181209; Geminocystaceae cyanobacterium LEGE 181210; *Salileptolyngbya* sp. LEGE 181216; *Salileptolyngbya* sp. LEGE 181219; Leptolyngbyaceae cyanobacterium LEGE 181156.

4.2. Cytotoxicity of Cyanobacteria extracts

The evaluation of cytotoxicity is a crucial step in characterizing natural extracts, as it ensures the absence of toxic compounds that could compromise applications in health-related fields. Cytotoxicity assays provide insights into the safety of bioactive extracts, reduce the need for animal testing, support sustainable use, and validate their potential for pharmaceutical, cosmetic, or nutraceutical purposes. Human keratinocytes (HaCAT) are particularly relevant for predicting compatibility with the skin barrier, making them appropriate models for dermatological/cosmetic applications [12]. In this study, the cytotoxicity of acetone and aqueous extracts was assessed in HaCAT cells after 24 h and 48 h of exposure (**Figures 16–17**).

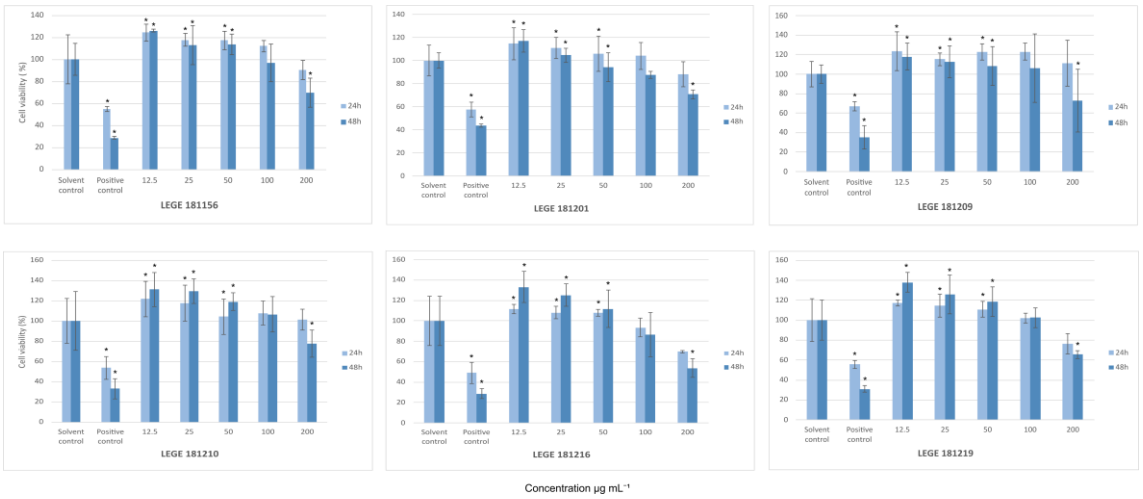


Figure 16. Viability of keratinocytes (HaCAT) after 24 h and 48 h of incubation with cyanobacteria acetonic extracts at concentrations ranging from 12.5-200 µg mL^{-1}. Results are expressed as % of MTT reduction relative to the untreated control. DMSO (20%) was used as the positive control for cytotoxicity. Results are presented as mean ± SD of at least three independent experiments, performed in quadruplicate. Statistical differences are indicated at *p<0.05 (non-parametric bootstrap resampling, 1000 iterations).

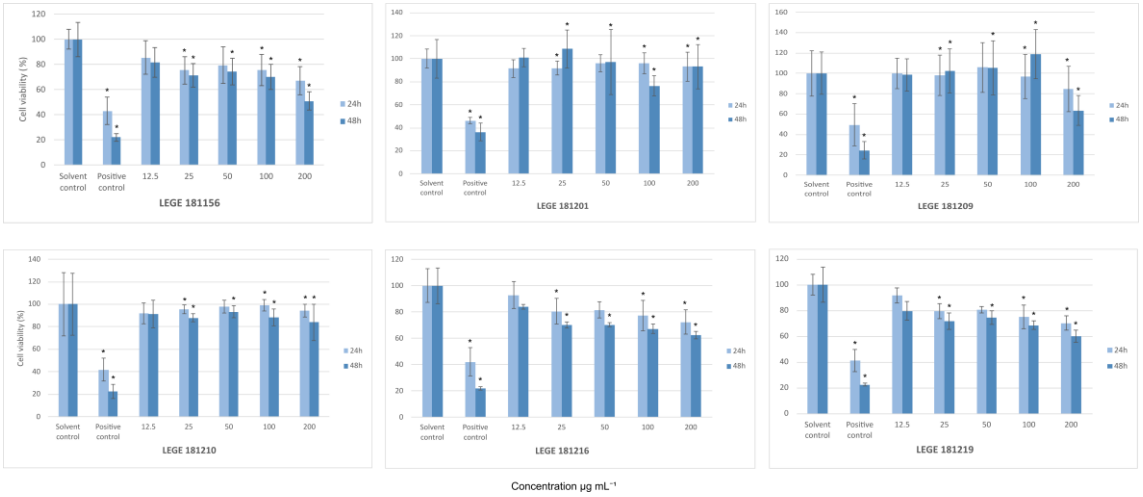


Figure 17. Viability of keratinocytes (HaCAT) after 24 h and 48 h of incubation with cyanobacteria aqueous extracts at concentrations ranging from 12.5-200 µg mL^{-1}. Results are expressed as % of MTT reduction relative to the untreated control. DMSO (20%) was used as the positive control for cytotoxicity. Results are presented as mean ± SD of at least three independent experiments, performed in quadruplicate. Statistical differences are indicated at *p<0.05 (non-parametric bootstrap resampling, 1000 iterations).

For acetone extracts, a significant reduction in cells viability was detected for all the extracts, at highest concentration tested (200 µg mL^{-1}), but only for an incubation period of 48h (p>0.05) (**Figure 16**). For lower concentrations (12.5 – 50 µg mL^{-1}), an increase in cells viability was observed (p<0.05), which could be correlated with the stimulation of cells proliferation by the extracts. However, accounting the high standard deviations inherent to the assay, and considering that there is a tendency for the reduction of cells

viability with increasing extracts concentration, this assumption would need further analysis to be confirmed.

A comparable profile was observed for aqueous extracts, where most concentrations and strains did not induce significant decrease in cells viability (p>0.05) (**Figure 17**). Significant reductions concentrated in Leptolyngbyaceae cyanobacterium LEGE 181156, *Salileptolyngbya* sp. LEGE 181216 and *Salileptolyngbya* sp. LEGE 181219 at 100–200 µg mL^{-1} (more evident at 48 h; p<0.05), with occasional significance already at 50 µg mL^{-1} after 48 h (p<0.05). In contrast, *Leptothoe* sp. LEGE 181201, *Salileptolyngbya* sp. LEGE 181209 and Geminocystaceae cyanobacterium LEGE 181210 maintained viabilities comparable to control across most of the range (p>0.05), showing only occasional deviations without a clear dose-response trend (p<0.05).

Overall, both acetonic and aqueous extracts exhibited low or absent cytotoxicity in HaCAT cells, consistent with previous Cabo Verde studies, where extracts rarely induced marked cytotoxic effects in mammalian cell lines [12], [15]. Notably, the present results are in line with those reported for strains of the same genera in earlier studies. *Salileptolyngbya* strains described by Morone et al. [12] maintained cell viabilities above 80–90% with no significant cytotoxicity, a profile similarly observed for *Salileptolyngbya* sp. LEGE 181209, LEGE 181216, and LEGE 181219 in this study. Likewise, *Leptothoe* sp. LEGE 181201 exhibited negligible cytotoxicity, consistent with the non-toxic profile reported for other *Leptothoe* strains in the same work. Altogether, these findings reinforce the low cytotoxic potential of these genera and support the suitability of these extracts for subsequent analyses.

4.3. Chemical profile

The chemical profile of the cyanobacterial strains was assessed by sequential extraction with solvents of different polarities, providing an overview of their main bioactive constituents. We first analyzed acetonic extracts (of lower polarity, enriched in carotenoids and other lipophilic compounds) and then aqueous extracts (of higher polarity, predominantly containing phycobiliproteins, chlorophylls, phenolics and sugars).

4.3.1. Acetonic extracts

Carotenoids and Chlorophylls profiling by HPLC-PDA

The analysis of the acetonic extracts of the cyanobacterial strains from Cabo Verde by HPLC-PDA enabled the identification of eleven pigments: nine carotenoids, chlorophyll-*a* and a chlorophyll-*a* derivative. Identified pigments included four xanthophylls (lutein (**1**), zeaxanthin (**4**), myxoxanthophyll (**6**), and β-cryptoxanthin (**8**)), one carotene (β-

carotene (**10**)) and chlorophyll-*a* (**3**). In addition, four unidentified carotenoids (**2**, **7**, **9**, and **11**) were detected, displaying spectral characteristics similar to authentic carotenoid standards but distinct retention times. The same was done for chlorophyll-*a* derivative (**5**). Representative chromatographic profiles are shown in **Figure 18**, while quantitative comparisons are summarized in **Figure 19**.

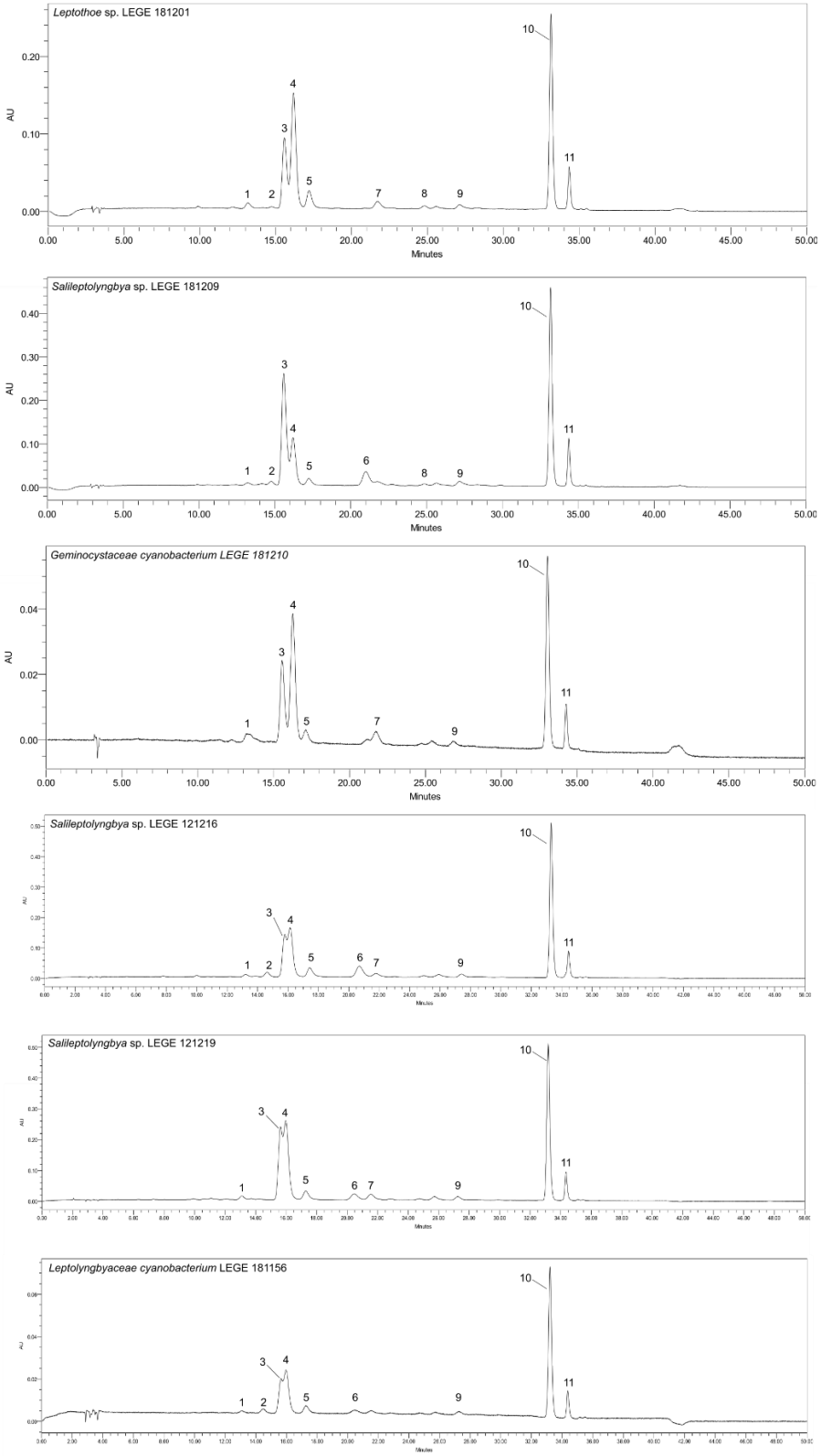


Figure 18. Carotenoid and chlorophylls profiles of the acetonic extracts of the cyanobacteria *Leptolyngbyaceae* cyanobacterium LEGE 181156, *Leptothoe* sp. LEGE 181201, *Salileptolyngbya* sp. LEGE 181209, *Salileptolyngbya* sp. LEGE 181216, *Salileptolyngbya* sp. LEGE 181219 and *Geminocystaceae* cyanobacterium LEGE 181210. HPLC-PDA recorded at 450 nm. Identified pigments: lutein (1), oxygenated derivative of β-carotene (2), chlorophyll-*a* (3), zeaxanthin (4), chlorophyll-*a* derivative (5), myxoxanthophyll (6), oxygenated derivative of β-carotene (7), β-cryptoxanthin (8), β-carotene derivative (9), β-carotene (10), and β-carotene derivative (11).

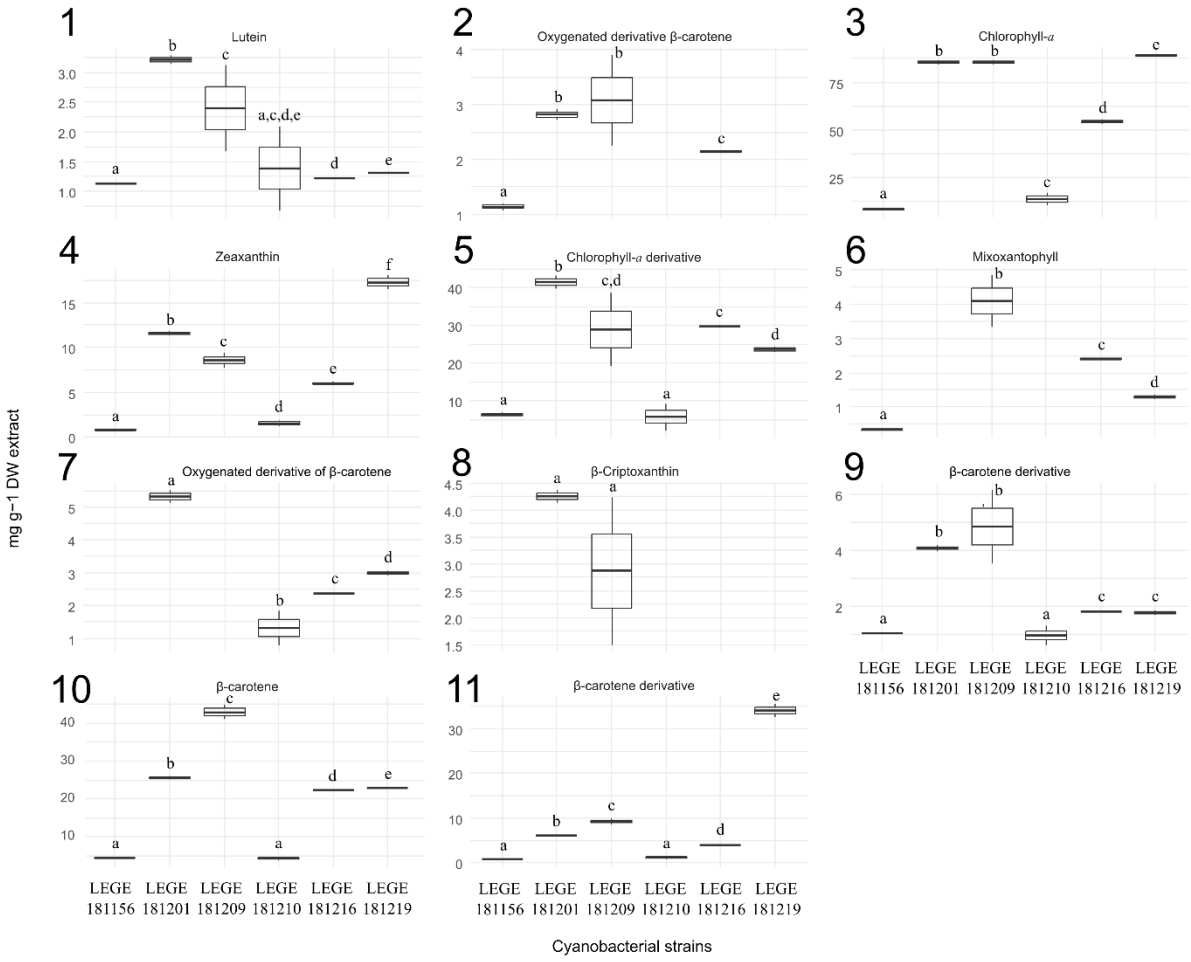


Figure 19. Carotenoid and chlorophylls content (μg mg⁻¹ dry extract) in acetonic extracts, quantified by HPLC-PDA. Different superscript letters denote statistical differences at $p < 0.05$ (non-parametric bootstrap resampling, 1000 iterations).

Although many tropical cyanobacteria are carotenoid-rich, in our strains, chlorophylls prevailed in total content. Total chlorophylls ranged from 14.80 ± 1.36 to 127.09 ± 31.21 μg mg⁻¹ dry extract, with the highest value found in *Leptothoe* sp. LEGE 181201, followed by *Salileptolyngbya* sp. LEGE 181209 (p<0.05). In contrast, total carotenoids ranged from 9.03 ± 1.06 to 80.81 ± 13.09 μg mg⁻¹ dry extract, with *Salileptolyngbya* sp. LEGE 181219 displaying the highest levels, followed by *Salileptolyngbya* sp. LEGE 181209 (p<0.05). Leptolyngbyaceae cyanobacterium LEGE 181156 showed the lowest carotenoid and chlorophylls content, followed by Geminocystaceae cyanobacterium LEGE 181210.

For individual compounds, lutein (**1**) occurred in all acetone extracts (1.13 ± 0.01 to 3.21 ± 0.11 μg mg⁻¹), highest in *Leptothoe* sp. LEGE 181201, then *Salileptolyngbya* sp. LEGE 181209 (2.39 ± 1.03 μg mg⁻¹) (p<0.05). Zeaxanthin (**4**) was among the most abundant

xanthophylls (0.82 ± 0.05 to 17.26 ± 1.10 µg mg⁻¹), maximum in *Salileptolyngbya* sp. LEGE 181219, followed by *Leptothoe* sp. LEGE 181201 (11.56 ± 0.39 µg mg⁻¹) (p<0.05). Myxoxanthophyll (**6**) appeared in four of six strains (0.35 ± 0.03 to 4.09 ± 1.06 µg mg⁻¹), highest in *Salileptolyngbya* sp. LEGE 181209 (p<0.05). β-Cryptoxanthin (**8**) was detected only in *Leptothoe* sp. LEGE 181201 and *Salileptolyngbya* sp. LEGE 181209 (4.26 ± 0.07 and 2.87 ± 1.93 µg mg⁻¹). As expected, β-carotene (**10**) dominated carotenoids (3.50 ± 0.54 to 42.08 ± 2.64 µg mg⁻¹), highest in *Salileptolyngbya* sp. LEGE 181209, then *Leptothoe* sp. LEGE 181201 and *Salileptolyngbya* sp. LEGE 181219 (24.76 ± 0.57 and 22.19 ± 0.01 µg mg⁻¹) (p<0.05). Regarding chlorophylls, chlorophyll-*a* (**3**) ranged from 8.36 ± 0.37 to 88.93 ± 0.72 µg mg⁻¹, being highest in *Salileptolyngbya* sp. LEGE 181219, followed by *Salileptolyngbya* sp. LEGE 181209 (85.61 ± 1.70 µg mg⁻¹) (p<0.05). Its derivative (**5**) was present in all strains at lower levels (6.44 ± 0.61 to 41.48 ± 2.38 µg mg⁻¹), reaching its maximum in *Leptothoe* sp. LEGE 181201.

Compared with other regions, distinct patterns emerged. In Antarctic cyanobacteria, as *Nodosilinea antarctica* LEGE 13457, chlorophylls prevail over carotenoids (417.57 µg mg⁻¹) [32]. Although our Cabo Verde strains showed relatively high chlorophylls content versus earlier Cabo Verde reports (27.72–66.86 µg mg⁻¹) [15], carotenoids remained highly represented, particularly β-carotene and zeaxanthin. Carotenoids here exceeded those of *N. antarctica* LEGE 13457 (lutein 0.58, zeaxanthin 0.625, β-carotene 27.70 µg mg⁻¹) [32]. Morone et al. [15] also reported that Cabo Verde isolates are enriched in these two pigments, with concentrations in the same order of magnitude as those observed herein, although in their study maximum carotenoid levels reached higher values (70.47 to 186.71 µg mg⁻¹). While β-cryptoxanthin was absent in their reports, we detected it in two isolates, reinforcing species-specific pigment variability within the same geographic origin.

Altogether, acetonic extracts were dominated in total by chlorophylls, while carotenoids (β-carotene and zeaxanthin) also reached high levels. This reflects taxonomic identity and environmental adaptation, highlighting the potential of Cabo Verde cyanobacteria as valuable sources of bioactive pigments with photoprotective, antioxidant, and nutraceutical applications.

4.3.2. Aqueous extracts

Phycobiliproteins and Chlorophylls

PBPs, as water-soluble molecules, were quantified spectrophotometrically only in aqueous extracts. All three main components were detected: phycocyanin (PC),

phycoerythrin (PE) and allophycocyanin (APC) (**Figure 20**). PC, responsible for the characteristic blue coloration, was the most abundant, followed by PE, which contributes to reddish tones, whereas APC, associated with a bluish-green color, was comparatively lower. This distribution was also reflected in the coloration of the aqueous extracts as commonly reported [119].

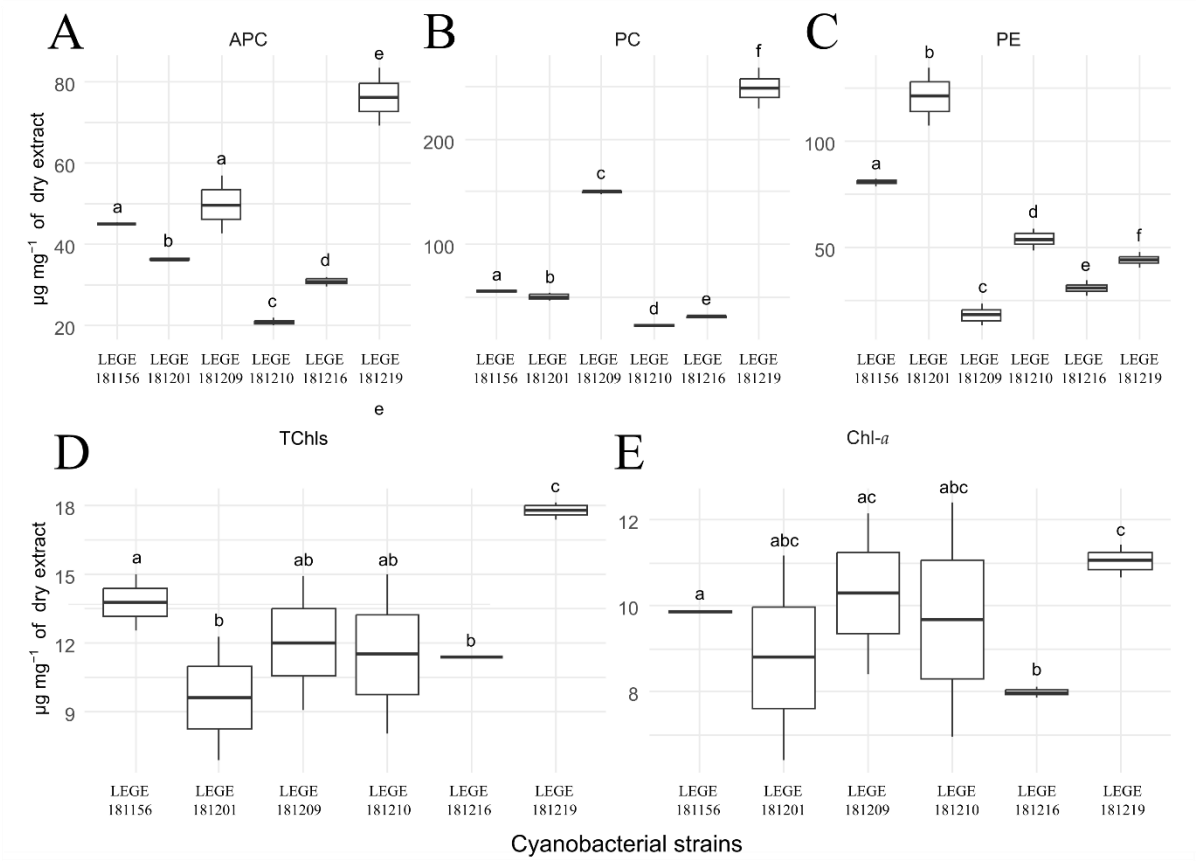


Figure 20. Phycobiliproteins (A–C) and chlorophylls (D–E) in aqueous extracts (µg mg⁻¹ dry extract). Different superscript letters indicate significant statistical differences at $p<0.05$ (non-parametric bootstrap test). APC, allophycocyanin; PC, phycocyanin; PE, phycoerythrin; TChls, total chlorophylls; Chl-*a*, chlorophyll-*a*.

PC ranged from 23.28 ± 0.63 µg mg^{-1} dry extract (Geminocystaceae cyanobacterium LEGE 181210) to 248.06 ± 26.52 µg mg^{-1} (*Salileptolyngbya* sp. LEGE 181219). Intermediate values were observed for *Salileptolyngbya* sp. LEGE 181209 (149.83 ± 2.92 µg mg^{-1}), Leptolyngbyaceae cyanobacterium LEGE 181156 (55.41 ± 0.39 µg mg^{-1}), *Leptothoe* sp. LEGE 181201 (50.74 ± 5.60 µg mg^{-1}) and *Salileptolyngbya* sp. LEGE 181216 (31.57 ± 0.22 µg mg^{-1}) ($p<0.05$). PE was the second most abundant pigment, presenting the highest values in *Leptothoe* sp. LEGE 181201 (121.08 ± 18.85 µg mg^{-1}) and the lowest in *Salileptolyngbya* sp. LEGE 181209 (18.25 ± 7.33 µg mg^{-1}). The remaining strains showed intermediate PE amounts (80.89 ± 2.58 down to 30.94 ± 4.92

μg mg^{-1}) (p<0.05). APC ranged from 20.95 ± 1.39 μg mg^{-1} (Geminocystaceae LEGE 181210) to 76.39 ± 9.99 μg mg^{-1} (*Salileptolyngbya* sp. LEGE 181219).

The predominance of PC, followed by PE, aligns with canonical organization of cyanobacterial phycobilisomes, where PC is the major component of the rods and transfers excitation energy to the APC core [119]. Similar pigment distributions have been consistently reported in other cyanobacteria [15], [40], [41]. The variability observed among strains in this study reflects phylogeny and cultivation conditions (light regime, nutrients, salinity, temperature), with higher temperatures often favoring biomass and PC productivity [40]. The highest PC here (*Salileptolyngbya* sp. LEGE 181219; 248.06 μg mg^{-1}) is close to values reported for *Salileptolyngbya* strains (≈222–221 μg mg^{-1}) [12], supporting its potential as a high-performing PC producer. PE was markedly higher in *Leptothoe* sp. LEGE 181201 (121.08 μg mg^{-1}), consistent with *Leptothoe* as an efficient PE producer in Cabo Verde (≈159 μg mg^{-1}) [12], and in other geographic regions (≈78 μg mg^{-1}) [40]. Other studies corroborate these strain-specific differences. Silva et al. [41], reported that *Tolypothrix* sp. exhibited particularly high PE levels, consistent with observations in other *Tolypothrix* species. Similarly, Soule and coworkers [120], demonstrated that *Nostoc punctiforme* accumulates predominantly PC, followed by PE and APC, a profile comparable to the one observed in the present work. Although in some cyanobacteria APC levels can surpass those of PE, this was not the case in our study, where PE consistently exceeded APC. The relatively high standard deviations observed for PE may be explained by its greater instability compared with PC and APC, as phycoerythrin is prone to degradation during extraction and storage [121], [122].

From a biotechnological perspective, high PC levels in *Salileptolyngbya* strains (LEGE 181219 and LEGE 181209) support their use as natural blue pigments in food and cosmetic industries [59]. Strong PE accumulation in *Leptothoe* sp. LEGE 181201 highlights its use as a natural red dye and fluorescent probe in biomedical applications. Although APC was less abundant, it was consistent across strains and remains valuable as a fluorescent tag in flow cytometry and diagnostic applications [123].

In addition to PBPs, chlorophyll-*a* and total chlorophylls (TChls) were also quantified in aqueous extracts (Figure 15). For Chl-*a*, the highest content was found in *Salileptolyngbya* sp. LEGE 181219 (11.05 ± 0.53 μg mg^{-1}), not significantly different from *Salileptolyngbya* sp. LEGE 181209 (10.29 ± 2.66 μg mg^{-1}), Leptolyngbyaceae LEGE 181156 (9.87 ± 0.00 μg mg^{-1}), Geminocystaceae LEGE 181210 (9.69 ± 3.87 μg mg^{-1}), or *Leptothoe* sp. LEGE 181201 (8.80 ± 3.35 μg mg^{-1}) (p>0.05). The lowest content was

observed in *Salileptolyngbya* sp. LEGE 181216 (8.00 ± 0.17 µg mg^{-1}), significantly different from LEGE 181219 and LEGE 181209 ($p<0.05$), but not from the others ($p>0.05$). For TChls, the highest level was again in *Salileptolyngbya* sp. LEGE 181219 (17.80 ± 0.54 µg mg^{-1}). Slightly lower values occurred in Leptolyngbyaceae LEGE 181156 (13.78 ± 1.72 µg mg^{-1}), *Salileptolyngbya* sp. LEGE 181209 (12.03 ± 4.16 µg mg^{-1}) and Geminocystaceae LEGE 181210 (11.52 ± 0.00 µg mg^{-1}) ($p>0.05$). The lowest TChls were found in *Salileptolyngbya* sp. LEGE 181216 (11.38 ± 0.00 µg mg^{-1}) and *Leptothoe* sp. LEGE 181201 (9.61 ± 3.81 µg mg^{-1}), which differed from LEGE 181219 ($p<0.05$), but not from the other intermediate producers ($p>0.05$). Generally, chlorophylls were lower than PBPs, reflecting functional complementarity: PBPs expand absorption into spectral regions less efficiently captured by chlorophylls [123].

Total Phenols

Phenolic compounds are chemically diverse and associated with antioxidant, anti-inflammatory, antimicrobial, and potential anticancer activities [124]. In cyanobacteria, they contribute to oxidative stress defense and ecological interactions, while also being valued for biotechnological applications [125]. Total phenolic content (TPC) in aqueous extracts was determined by the Folin–Ciocalteu assay and expressed as µg GAE mg^{-1} dry extract (**Figure 21-A**). This colorimetric method is based on the reduction of the Folin reagent, resulting in the formation of a blue chromophore measurable at 725 nm. Although it is not entirely specific to phenolics and may also react with other reducing agents, it remains the standard method for comparative estimations of phenolic content and for inferring the antioxidant potential of extracts [126].

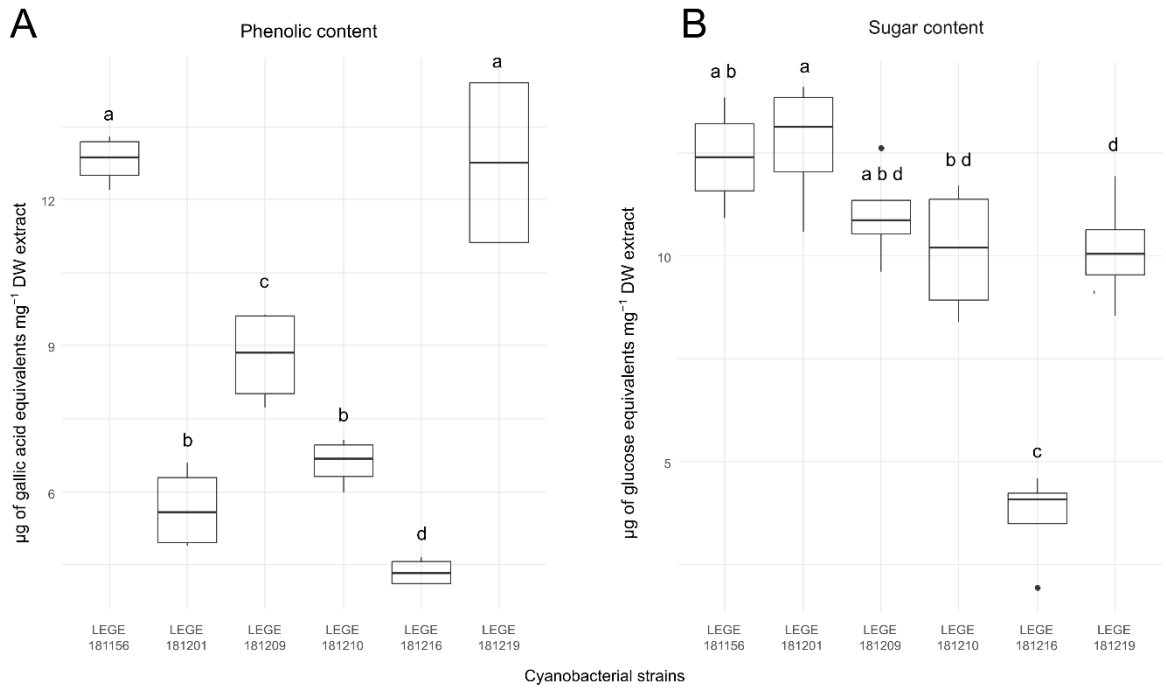


Figure 21. Total phenolics-A (µg gallic acid equivalents (GAE) mg^{-1} dry extract) and total sugars-B (µg glucose equivalents mg^{-1} dry extract) contents in cyanobacteria aqueous extracts. Different superscript letters indicate significant statistical differences at $p<0.05$ (non-parametric bootstrap test).

TPC varied from 4.35 ± 0.34 to 12.81 ± 0.57 µg GAE mg^{-1}. The highest levels occurred in Leptolyngbyaceae LEGE 181156 (12.81 ± 0.57 µg GAE mg^{-1}) and *Salileptolyngbya* sp. LEGE 181219 (12.77 ± 2.32 µg GAE mg^{-1}) ($p>0.05$ between them). *Salileptolyngbya* sp. LEGE 181209 showed intermediate TPC (8.77 ± 1.20 µg GAE mg^{-1}), while Geminocystaceae LEGE 181210 (6.61 ± 0.56 µg GAE mg^{-1}) and *Leptothoe* sp. LEGE 181201 (5.67 ± 1.03 µg GAE mg^{-1}) were lower. The strain with the lowest values was *Salileptolyngbya* sp. LEGE 181216 (4.35 ± 0.34 µg GAE mg^{-1}). Differences among strains were significant overall ($p<0.05$).

Compared with literature, our TPC (≈4–13 µg GAE mg^{-1}) is lower than other Cabo Verde strains (~12–72 µg GAE mg^{-1}) [15], with *Salileptolyngbya* and *Leptothoe* often among top producers. Variation is consistent with phylogeny, cultivation regime, and extraction solvent; environmental stressors such as elevated temperature can also enhance phenolic accumulation [127].

Biotechnologically, phenolic-rich extracts are attractive as sustainable sources of natural antioxidants for nutraceutical, cosmetic and pharmaceutical applications. In addition to their free-radical scavenging capacity, phenolic compounds can act as preservatives, stabilisers and bioactive ingredients in functional formulations [128]. Despite modest

levels quantified in this study, *Salileptolyngbya* sp. LEGE 181219 and Leptolyngbyaceae cyanobacterium LEGE 181156 emerged as the richest TPC producers, together with their pigment productivity, they are promising candidates for integrated antioxidant exploitation.

Total Sugars

Total sugars were quantified in aqueous extracts by the phenol–sulphuric acid method [110]. This colorimetric assay detects all carbohydrate fractions present in the extracts, revealing considerable variability among strains (**Figure 21-B**).

The highest sugar content was observed in *Leptothoe* sp. LEGE 181201 (23.03 ± 1.06 μg mg^{-1}), followed by Leptolyngbyaceae LEGE 181156 (22.96 ± 2.78 μg mg^{-1}) and *Salileptolyngbya* sp. LEGE 181209 (19.71 ± 1.98 μg mg^{-1}). Intermediate values: *Salileptolyngbya* sp. LEGE 181219 (18.68 ± 2.06 μg mg^{-1}) and Geminocystaceae LEGE 181210 (18.04 ± 0.77 μg mg^{-1}). The lowest was *Salileptolyngbya* sp. LEGE 181216 (6.37 ± 1.09 μg mg^{-1}) ($p<0.05$). *Leptothoe* sp. LEGE 181201 exceeded LEGE 181210, LEGE 181216, and LEGE 181219 ($p<0.05$), but did not differ from *Salileptolyngbya* sp. LEGE 181209 or Leptolyngbyaceae LEGE 181156 ($p>0.05$). *Salileptolyngbya* sp. LEGE 181216 presented significantly lower values than all others ($p<0.05$).

When compared with literature values on the same basis, our total sugars content ≈6–23 μg mg^{-1}) was lower than those previously reported for other Cabo Verde strains (≈77–351 μg mg^{-1} dry extract) [12]. Among them, *Neolyngbya* sp. LEGE 181188 (350.66 μg mg^{-1}), *Baaleninema* sp. LEGE 181148 (300.24 μg mg^{-1}) and *Salileptolyngbya* sp. LEGE 181187 (295.75 μg mg^{-1}) stood out as the top producers, with no significant differences among them. Interestingly, these values are comparable to those reported in the literature for *Nostoc muscorum* (≈320 μg mg^{-1} dry extract) [129], a species recognized as a high carbohydrate producer. According to the authors, no other cyanobacteria analyzed so far, including *Spirulina* species often cited for their nutritional and biochemical potential, exceeded the levels reported for Cabo Verde isolates.

In cyanobacteria, carbohydrates fulfil dual roles: they act as intracellular energy reserves, mainly in the form of glycogen and sucrose, and are also secreted as extracellular polysaccharides (EPS), which enhance tolerance to environmental stress and mediate ecological interactions such as adhesion and biofilm development [130]. This metabolic flexibility reflects the strong influence of strain-specific traits and cultivation conditions on sugar accumulation patterns [131]. Even with modest sugars, these isolates remain valuable given EPS applications (stabilizers, thickeners, bioactives) and potential as

feedstocks for biofuels/bioplastics [132]. In this sense, even modest in sugar accumulation, when combined with high pigments production, reinforces the biotechnological value of these strains for integrated valorization strategies [133], [134].

4.3.3. Chemotaxonomy and chemical characterization

Principal component analysis (PCA) and hierarchical cluster analysis (HCA) were carried out to explore the relationships among the studied cyanobacterial strains. For carotenoids and chlorophylls detected in acetonic extracts by HPLC, the first two components explained 78.9% of the total variance (PC1: 57.6%; PC2: 21.3%). PCA revealed a clear separation of the strains (**Figure 22**): LEGE 181219 stood apart due to higher levels of β-carotene derivatives and zeaxanthin, while LEGE 181209 aligned with lutein, β-cryptoxanthin, unidentified carotenoids and oxygenated β-carotene derivatives. LEGE 181201 related most strongly to chlorophyll-*a*, its derivative, and β-carotene. In contrast, LEGE 181156 and LEGE 181210 grouped together on the negative side of PC1, consistent with comparatively lower contributions of the most discriminant pigments, whereas LEGE 181216 occupied an intermediate position, close to the plot centre, indicating a more balanced profile. The HCA (**Figure 23**) supported these patterns, showing that LEGE 181156 clustered first with LEGE 181210, which subsequently grouped with LEGE 181216. This cluster then merged with LEGE 181219, while LEGE 181201 and LEGE 181209 formed a separate subgroup that only joined at the highest linkage distance.

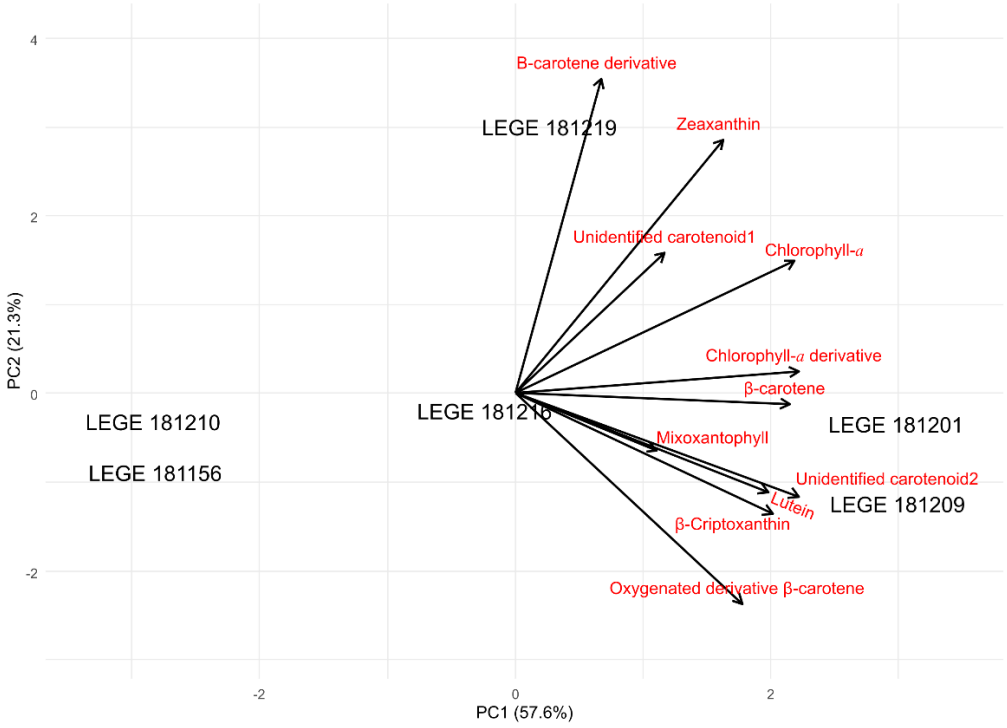


Figure 22. Principal component analysis (PCA) biplot of carotenoids and chlorophylls detected in acetonic extracts. The first two principal components explained 78.9% of the total variance (PC1: 57.6%; PC2: 21.3%). Arrows indicate pigment loadings, and strain codes correspond to cyanobacterial isolates from Cabo Verde.

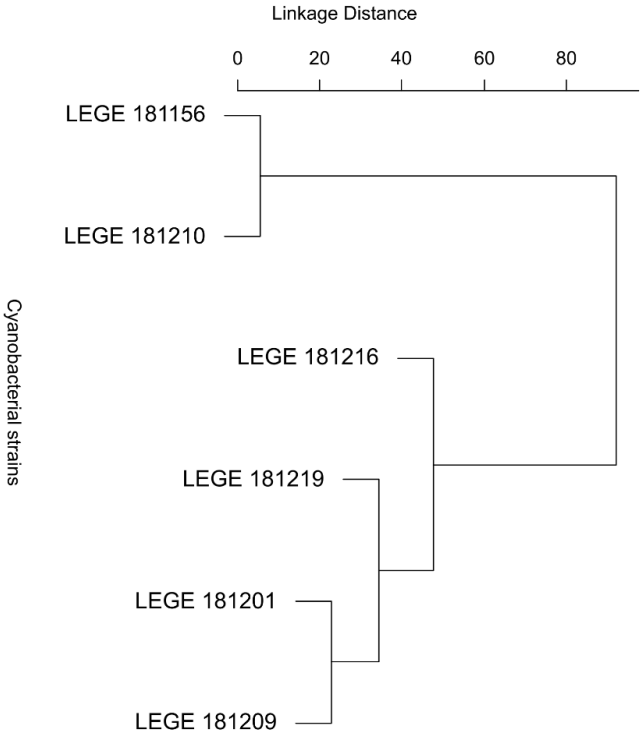


Figure 23. Dendrogram obtained by hierarchical cluster analysis (HCA) based on carotenoid and chlorophylls profile of acetonic extracts from cyanobacterial strains.

Considering the aqueous pigment dataset (phycobiliproteins and chlorophylls), the first two PCs accounted for 89.3% of the variance (PC1: 71.3%; PC2: 18.0%). In the PCA biplot (**Figure 24**), LEGE 181219 projected along the loadings of phycocyanin (PC), chlorophyll-*a*, total chlorophylls and allophycocyanin (APC), whereas LEGE 181201 was driven primarily by phycoerythrin (PE). LEGE 181156, LEGE 181210 and LEGE 181216 remained closer to the origin, reflecting more even pigment proportions. The HCA (**Figure 25**) corroborated these results, initially clustering LEGE 181210 with LEGE 181216, and subsequently joining this pair with the subgroup formed by LEGE 181201 and LEGE 181156. This larger cluster then merged, at a higher linkage distance, with the separate pair LEGE 181209 and LEGE 181219, which were the closest to each other.

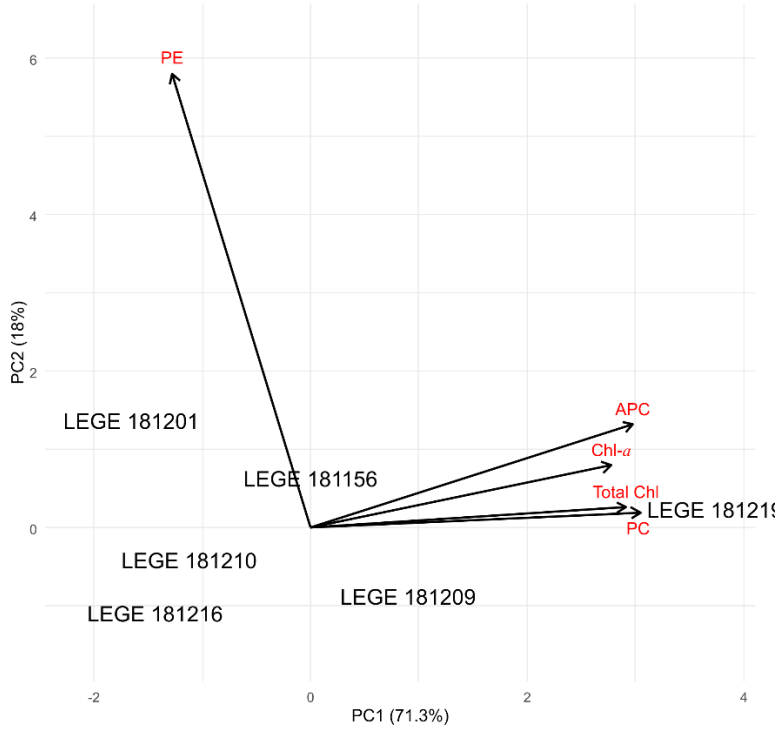


Figure 24. Principal component analysis (PCA) biplot of aqueous pigments (phycobiliproteins and total chlorophylls). The first two principal components explained 89.3% of the total variance (PC1: 71.3%; PC2: 18.0%).

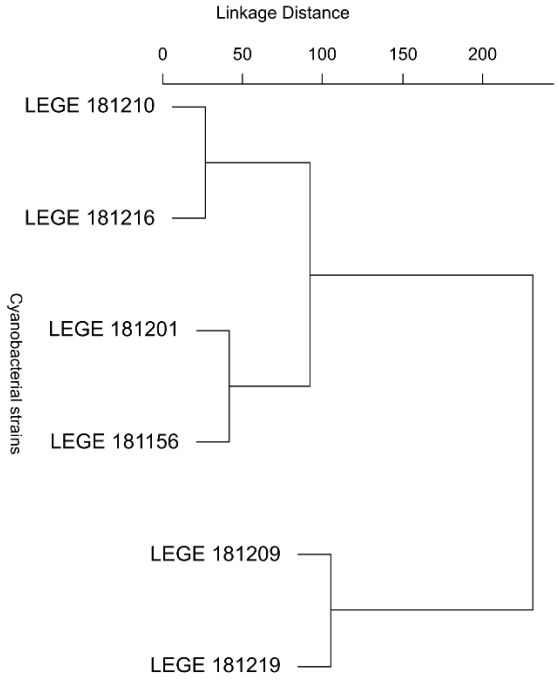


Figure 25. Dendrogram obtained by hierarchical cluster analysis (HCA) based on aqueous pigment composition (phycobiliproteins and total chlorophylls) of cyanobacterial strains.

For the phenolics-and-sugars dataset, the first two PCs explained 100% of the variance (PC1: 74.6%; PC2: 25.4%). Here, PCA (**Figure 26**) separated LEGE 181219 and LEGE 181156 towards higher phenolic content, while LEGE 181201 and LEGE 181210 were positioned by the sugar vector. LEGE 181209 occupied an intermediate space and LEGE 181216 remained set apart, consistent with a distinct composition. The HCA (**Figure 27**) corroborated these tendencies, clustering LEGE 181219 with LEGE 181156, and LEGE 181201 with LEGE 181210 and LEGE 181209 that was more loosely connected. LEGE 181216 emerged once again at the greatest linkage distance, highlighting its distinct chemical profile.

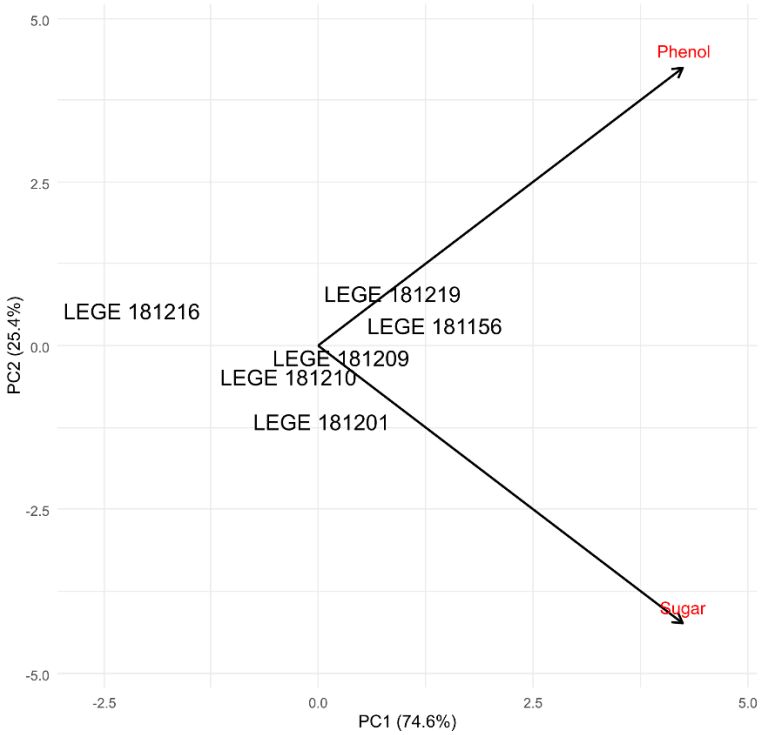


Figure 26. Principal component analysis (PCA) biplot of phenolic compounds and sugars. The first two principal components explained 100% of the variance (PC1: 74.6%; PC2: 25.4%).

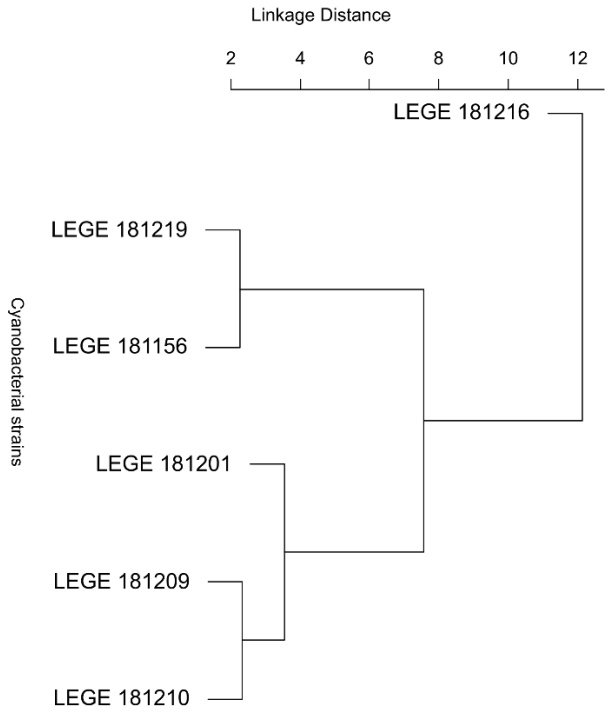


Figure 27. Dendrogram obtained by hierarchical cluster analysis (HCA) based on phenolic and sugar contents of cyanobacterial strains.

Taken together, multivariate analyses consistently show that the strains share the same classes of metabolites but differ in their relative concentrations and proportions, which is sufficient to discriminate them chemotaxonomically. Notably, LEGE 181201–LEGE 181209 behaved as a tight pair in the acetonic dataset, LEGE 181156–LEGE 181210 were consistently paired in the acetonic extract and appeared closely associated also in the aqueous analysis, and LEGE 181216 tended to remain the most distinct when similarity was assessed globally. Although all strains share the same classes of pigments and metabolites, differences in concentrations and relative proportions supported their separation into distinct chemotaxonomic groups, reinforcing the value of pigment and metabolite profiling in discriminating cyanobacterial strains from Cabo Verde.

4.3.4. Nitric Oxide Scavenging

The ability of cyanobacterial extracts to scavenge nitric oxide radicals (•NO) was evaluated using the Griess reaction (**Figure 28**) in both acetonic and aqueous extracts. Sodium nitroprusside (SNP) generates •NO, which, upon reaction with Griess reagent, produces a stable chromophore measurable at 562 nm. The reduction in absorbance relative to the control reflects the scavenging capacity of the extracts. Results were expressed as inhibitory concentration (IC) values, corresponding to the extract concentration (µg mL^{-1} dry extract) required to scavenge •NO.

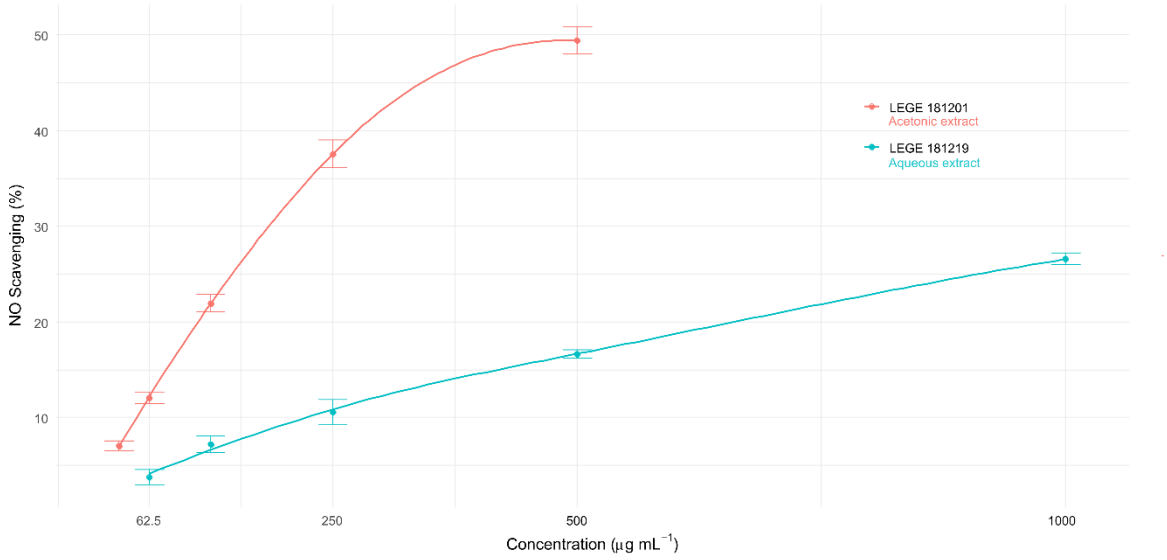


Figure 28. Nitric oxide (•NO) scavenging activity of cyanobacterial extracts. Dose–response curves for the acetonic extract of *Leptothoe* sp. LEGE 181201 (red) and the aqueous extract of *Salileptolyngbya* sp. LEGE 181219 (blue). Results are expressed as mean ± SD of three independent experiments performed in duplicate.

All extracts displayed dose-dependent scavenging profile, with efficiencies differing by solvent. Acetonic extracts were consistently more effective than aqueous ones, since

only acetonic extracts reached IC_{50} values. *Leptothoe* sp. LEGE 181201 was the most effective, achieving IC_{50} = 550 ± 10 µg mL⁻¹. The remaining acetone extracts did not reach IC_{25}, but maximal inhibitions at 1000 µg mL⁻¹ were: *Salileptolyngbya* sp. LEGE 181209 (23 ± 0.7%), *Salileptolyngbya* sp. LEGE 181216 (20 ± 3.0%), Geminocystaceae LEGE 181210 (17.9 ± 5.3%), *Salileptolyngbya* sp. LEGE 181219 (13 ± 1.5%), and Leptolyngbyaceae LEGE 181156 (5.6 ± 0.7%).

For aqueous extracts, none reached IC_{50}. The best performer was *Salileptolyngbya* sp. LEGE 181219, attaining IC_{25} = 1260 ± 280 µg mL⁻¹. Maximal inhibitions at the highest concentration tested (1000 µg mL⁻¹) were: *Salileptolyngbya* sp. LEGE 181209 (24.2 ± 1.4%), Geminocystaceae LEGE 181210 (18.9 ± 0.9%), *Salileptolyngbya* sp. LEGE 181216 (8.5 ± 3.8%), Leptolyngbyaceae LEGE 181156 (6 ± 0.2%), and *Leptothoe* sp. LEGE 181201 (3.5 ± 1.9%).

Compared with the literature, these IC values indicate modest •NO scavenging capacity, particularly for aqueous extracts. Previous works reported stronger activities for cyanobacteria of the same genera. For instance, Morone et al. [15] reported IC_{50} values for acetonic extracts ranging from ≈ 75-266 µg mL⁻¹, with *Leptothoe* sp. LEGE 181156 among the best performers (≈ 95 µg mL⁻¹). Similarly, Rodrigues et al. [40] found that *Leptothoe* sp. LEGE 11479 displayed high efficiency in •NO scavenging with an IC_{50} of 129.47 µg mL⁻¹. In agreement, *Leptothoe* sp. LEGE 181201 was the only acetonic extract here to achieve IC_{25} (120 µg mL⁻¹) and IC_{50} (550 µg mL⁻¹). For aqueous extracts, Morone et al. [12] reported one *Salileptolyngbya* strain reaching IC_{50} (≈ 965 µg mL⁻¹), which is in line with our observation that *Salileptolyngbya* sp. LEGE 181219 was the best aqueous performer (IC_{25}). These patterns emphasize the roles of strain identity, extraction solvent, and cultivation regime [41]. Notably, acetone enriches carotenoids and other lipophilic antioxidants often associated with •NO scavenging.

From a biotechnological perspective, although •NO scavenging was relatively modest overall, the superior performance of acetone extracts underscores the relevance of carotenoid-rich fractions as natural scavengers of reactive nitrogen species. The acetone extract of *Leptothoe* sp. LEGE 181201 showed the most promising activity (IC_{50}), of interest for anti-inflammatory/therapeutic applications. The aqueous extract of *Salileptolyngbya* sp. LEGE 181219 was the strongest within its class, suggesting complementary antioxidant applications.

5. Conclusions

Collectively, our results demonstrate that marine cyanobacteria from Cabo Verde provide a robust basis for biodiversity discovery and pigment centered biotechnology. Within Nodosilineales, 16S rRNA phylogenetics resolved the six isolates and, together with morphology and ultrastructure, refined strain-level distinctions. A central focus of this work is a candidate novel species, provisionally designated *Salileptolyngbya* sp. LEGE 181209, whose distinct ultrastructural trait (conspicuous pseudovacuoles under SEM) and 16S–23S ITS divergence support species-level separation. PCR screening showed no amplification of mcyA or anaC across all strains, reinforcing a safety-forward profile for downstream applications.

Sequential extraction with solvents of different polarities yielded two complementary metabolite fractions. Acetone fractions were enriched in canonical carotenoids (notably β-carotene, zeaxanthin and lutein) and chlorophyll-*a*; aqueous fractions contained abundant phycobiliproteins, predominantly phycocyanin and, in selected strains, phycoerythrin. Across strains, clear profiles emerged: total chlorophylls peaked in *Leptothoe* sp. LEGE 181201 (≈127 μg mg^{-1} dry extract), while total carotenoids were highest in *Salileptolyngbya* sp. LEGE 181219 (≈81 μg mg^{-1}). For individual pigments, zeaxanthin reached its maximum in LEGE 181219 (≈17 μg mg^{-1}) and lutein in LEGE 181201 (≈3.2 μg mg^{-1}). In the aqueous fraction, phycocyanin reached the highest content in *Salileptolyngbya* sp. LEGE 181219 (≈248 μg mg^{-1}), whereas phycoerythrin peaked in *Leptothoe* sp. LEGE 181201 (≈121 μg mg^{-1}). Functionally, acetone and aqueous extracts exhibited low to absent cytotoxicity in HaCAT keratinocytes across 12.5–200 μg mL^{-1} (24–48 h), and nitric oxide scavenging indicated antioxidant potential consistent with pigment signatures. Considering combined performance (high carotenoids, high phycobiliproteins, especially phycocyanin, plus antioxidant readouts and safety), *Salileptolyngbya* sp. LEGE 181219 emerges as the lead, multi-purpose strain, while *Leptothoe* sp. LEGE 181201 stands out as the preferred PE-rich producer. These findings position Cabo Verde cyanobacteria as accessible reservoirs of high-value natural pigments with immediate relevance to blue biotechnology, and, taken together, establish a candidate novel *Salileptolyngbya* species as a focal taxon while identifying *Salileptolyngbya* sp. LEGE 181219 as the most broadly active producer.

6. Future Perspectives

Future work should expand isolations across additional islands and microhabitats in Cabo Verde to broaden taxonomic and ecological coverage. In parallel, a formal description of the candidate *Salileptolyngbya* sp. LEGE 181209 is being prepared as a separate manuscript for publication. On the bioactivity side, further evidence is needed: given that this study employed a single human keratinocyte model, the next phase should include additional cell-based studies and additional models where appropriate, with broader oxidative and inflammatory endpoints (ROS panels, cytokines, COX/LOX and NF-κB/iNOS pathways) and clear dose-response.

On the process side, optimization should focus on increasing the quantity of pigments produced. Practical parameters include adjusting light intensity/spectrum and photoperiod, temperature, salinity and the N:P supply, improving CO_2/aeration, exploring semicontinuous or fed-batch cultivation when useful, and harvesting at the growth phase that maximizes pigment content. After extraction, basic stability tests (heat, pH, light/UV) on crude extracts should guide storage and handling, and routine cyanotoxin screening ought to accompany any scale-up.

Regarding applications, near-term avenues remain clear: PC-rich *Salileptolyngbya* as a vivid, skin-compatible blue; PE-rich *Leptothoe* for red hues and fluorescence-based diagnostics; and carotenoid-enriched extracts as antioxidant co-actives and clean-label food colorants. Given that cyanobacterial pigments and metabolites are already used in cosmetics, foods, and nutraceuticals, a plausible new approach is to evaluate these materials as nutraceutical support in chronic inflammatory contexts, such as endometriosis, framed explicitly as hypothesis-driven research (preclinical models first, with objective oxidative/inflammatory endpoints and pigment bioavailability). This aligns with evidence that endometriosis exhibits elevated nitric oxide and oxidative-stress signatures, and that antioxidant vitamin supplementation can reduce both pelvic pain and inflammation; in parallel, C-phycocyanin from cyanobacteria suppresses LPS-induced NO/iNOS via NF-κB in macrophages [135], [136], [137].

References

[1] J. Komárek and J. R. Johansen, “Coccoid Cyanobacteria,” in *Freshwater Algae of North America*, Elsevier, 2015, pp. 75–133. doi: 10.1016/B978-0-12-385876-4.00003-7.

[2] C. F. Demoulin *et al.*, “Cyanobacteria evolution: Insight from the fossil record,” *Free Radic Biol Med*, vol. 140, pp. 206–223, Aug. 2019, doi: 10.1016/j.freeradbiomed.2019.05.007.

[3] M. Liberton, R. Howard Berg, J. Heuser, R. Roth, and H. B. Pakrasi, “Ultrastructure of the membrane systems in the unicellular cyanobacterium Synechocystis sp. strain PCC 6803,” *Protoplasma*, vol. 227, no. 2–4, p. 129, May 2006, doi: 10.1007/s00709-006-0145-7.

[4] C. W. Mullineaux, “The thylakoid membranes of cyanobacteria: structure, dynamics and function,” *Functional Plant Biology*, vol. 26, no. 7, p. 671, 1999, doi: 10.1071/PP99027.

[5] S. Casella *et al.*, “Dissecting the Native Architecture and Dynamics of Cyanobacterial Photosynthetic Machinery,” *Mol Plant*, vol. 10, no. 11, pp. 1434–1448, Nov. 2017, doi: 10.1016/j.molp.2017.09.019.

[6] B. A. Whitton and M. Potts, Eds., *The Ecology of Cyanobacteria*. Dordrecht: Kluwer Academic Publishers, 2002. doi: 10.1007/0-306-46855-7.

[7] E. Flores and A. Herrero, “Compartmentalized function through cell differentiation in filamentous cyanobacteria,” *Nat Rev Microbiol*, vol. 8, no. 1, pp. 39–50, Jan. 2010, doi: 10.1038/nrmicro2242.

[8] K. J. , M. J. , J. J. R. Komarek J., “Taxonomic classification of cyanoprokaryotes (cyanobacterial genera) 2014, using a polyphasic approach,” *Preslia*, vol. 86, pp. 295–335, 2014.

[9] N.-S. Lau, M. Matsui, and A. A.-A. Abdullah, “Cyanobacteria: Photoautotrophic Microbial Factories for the Sustainable Synthesis of Industrial Products,” *Biomed Res Int*, vol. 2015, pp. 1–9, 2015, doi: 10.1155/2015/754934.

[10] L. A. Gaysina, A. Saraf, and P. Singh, “Cyanobacteria in Diverse Habitats,” in *Cyanobacteria*, Elsevier, 2019, pp. 1–28. doi: 10.1016/B978-0-12-814667-5.00001-5.

[11] M. Mehdizadeh Allaf and H. Peerhossaini, “Cyanobacteria: Model Microorganisms and Beyond,” *Microorganisms*, vol. 10, no. 4, p. 696, Mar. 2022, doi: 10.3390/microorganisms10040696.

[12] J. Morone, G. S. Hentschke, I. B. Oliveira, V. Vasconcelos, R. Martins, and G. Lopes, “Secondary metabolites of cyanobacteria from Cape Verde Archipelago act as NO donors with potential application in dermatology and cosmetics,” *Algal Res*, vol. 86, p. 103952, Mar. 2025, doi: 10.1016/j.algal.2025.103952.

[13] J. A. Brito, “Blue Economy: Potential of Sustainable Fisheries Growth in Cape Verde Economy,” Iceland, 2022.

[14] J. A. F. Brito, T. V. Nguyen, and D. M. Kristófersson, “Evaluating the sustainability and potential of the Blue Economy: A bioeconomic and input–output analysis of the fisheries sector in Cape Verde,” *Ocean Coast Manag*, vol. 250, p. 107042, Apr. 2024, doi: 10.1016/j.ocecoaman.2024.107042.

[15] J. Morone *et al.*, “Carotenoids from cyanobacteria modulate iNOS and inhibit the production of inflammatory mediators: Promising agents for the treatment of inflammatory conditions,” *Algal Res*, vol. 83, p. 103729, Oct. 2024, doi: 10.1016/j.algal.2024.103729.

[16] J. Morone, G. Lopes, J. Morais, J. Neves, V. Vasconcelos, and R. Martins, “Cosmetic Application of Cyanobacteria Extracts with a Sustainable Vision to Skincare: Role in the Antioxidant and Antiaging Process,” *Mar Drugs*, vol. 20, no. 12, p. 761, Dec. 2022, doi: 10.3390/md20120761.

[17] J. Morais *et al.*, “Diversity of Cyanobacterial Genera Present in Cabo Verde Marine Environments and the Description of Gibliniella gelatinosa sp. nov,” *Plants*, vol. 14, no. 3, p. 299, Jan. 2025, doi: 10.3390/plants14030299.

[18] J. Komárek, “A polyphasic approach for the taxonomy of cyanobacteria: principles and applications,” *Eur J Phycol*, vol. 51, no. 3, pp. 346–353, Jul. 2016, doi: 10.1080/09670262.2016.1163738.

[19] J. Dyble, H. W. Paerl, and B. A. Neilan, “Genetic Characterization of *Cylindrospermopsis raciborskii* (Cyanobacteria) Isolates from Diverse Geographic Origins Based on *nifH* and *cpcBA* -IGS Nucleotide Sequence Analysis,” *Appl Environ Microbiol*, vol. 68, no. 5, pp. 2567–2571, May 2002, doi: 10.1128/AEM.68.5.2567-2571.2002.

[20] S. N. Bagchi and P. Singh, “Importance of Cyanobacterial Taxonomy in Biotechnological Applications,” in *Microbial Diversity in Ecosystem Sustainability and Biotechnological Applications*, Singapore: Springer Singapore, 2019, pp. 387–414. doi: 10.1007/978-981-13-8315-1_13.

[21] Y. García-Cazorla and V. Vasconcelos, “Emergent marine toxins risk assessment using molecular and chemical approaches,” *EFSA Journal*, vol. 20, May 2022, doi: 10.2903/j.efsa.2022.e200422.

[22] S. M. V. V. Lopes G, *The Pharmacological Potential of Cyanobacteria*. Elsevier, 2022. doi: 10.1016/C2019-0-01449-5.

[23] A. C. Jones, L. Gu, C. M. Sorrels, D. H. Sherman, and W. H. Gerwick, “New tricks from ancient algae: natural products biosynthesis in marine cyanobacteria,” *Curr Opin Chem Biol*, vol. 13, no. 2, pp. 216–223, Apr. 2009, doi: 10.1016/j.cbpa.2009.02.019.

[24] A. M. Burja, B. Banaigs, E. Abou-Mansour, J. Grant Burgess, and P. C. Wright, “Marine cyanobacteria—a prolific source of natural products,” *Tetrahedron*, vol. 57, no. 46, pp. 9347–9377, Nov. 2001, doi: 10.1016/S0040-4020(01)00931-0.

[25] M. Welker and H. Von Döhren, “Cyanobacterial peptides — Nature’s own combinatorial biosynthesis,” *FEMS Microbiol Rev*, vol. 30, no. 4, pp. 530–563, Jul. 2006, doi: 10.1111/j.1574-6976.2006.00022.x.

[26] E. Dittmann, M. Gugger, K. Sivonen, and D. P. Fewer, “Natural Product Biosynthetic Diversity and Comparative Genomics of the Cyanobacteria,” *Trends Microbiol*, vol. 23, no. 10, pp. 642–652, Oct. 2015, doi: 10.1016/j.tim.2015.07.008.

[27] X. Gao, X. Jing, X. Liu, and P. Lindblad, “Biotechnological Production of the Sunscreen Pigment Scytonemin in Cyanobacteria: Progress and Strategy,” *Mar Drugs*, vol. 19, no. 3, p. 129, Feb. 2021, doi: 10.3390/md19030129.

[28] Q. Gao and F. Garcia-Pichel, “An ATP-Grasp Ligase Involved in the Last Biosynthetic Step of the Iminomycosporine Shinorine in Nostoc punctiforme ATCC 29133,” *J Bacteriol*, vol. 193, no. 21, pp. 5923–5928, Nov. 2011, doi: 10.1128/JB.05730-11.

[29] J. Vega, J. Bonomi-Barufi, J. L. Gómez-Pinchetti, and F. L. Figueroa, “Cyanobacteria and Red Macroalgae as Potential Sources of Antioxidants and UV

Radiation-Absorbing Compounds for Cosmeceutical Applications," *Mar Drugs*, vol. 18, no. 12, p. 659, Dec. 2020, doi: 10.3390/md18120659.

[30] D. K. Saini, S. Pabbi, and P. Shukla, "Cyanobacterial pigments: Perspectives and biotechnological approaches," *Food and Chemical Toxicology*, vol. 120, pp. 616–624, Oct. 2018, doi: 10.1016/j.fct.2018.08.002.

[31] R. M. T. D. Perera, K. H. I. N. M. Herath, K. K. A. Sanjeewa, and T. U. Jayawardena, "Recent Reports on Bioactive Compounds from Marine Cyanobacteria in Relation to Human Health Applications," *Life*, vol. 13, no. 6, p. 1411, Jun. 2023, doi: 10.3390/life13061411.

[32] G. Lopes, D. Clarinha, and V. Vasconcelos, "Carotenoids from Cyanobacteria: A Biotechnological Approach for the Topical Treatment of Psoriasis," *Microorganisms*, vol. 8, no. 2, p. 302, Feb. 2020, doi: 10.3390/microorganisms8020302.

[33] A. Mortensen and L. H. Skibsted, "Importance of Carotenoid Structure in Radical-Scavenging Reactions," *J Agric Food Chem*, vol. 45, no. 8, pp. 2970–2977, Aug. 1997, doi: 10.1021/jf970010s.

[34] J. C. Varela, H. Pereira, M. Vila, and R. León, "Production of carotenoids by microalgae: achievements and challenges," *Photosynth Res*, vol. 125, no. 3, pp. 423–436, Sep. 2015, doi: 10.1007/s11120-015-0149-2.

[35] S. Takaichi and M. Mochimaru, "Carotenoids and carotenogenesis in cyanobacteria: unique ketocarotenoids and carotenoid glycosides," *Cellular and Molecular Life Sciences*, vol. 64, no. 19–20, pp. 2607–2619, Oct. 2007, doi: 10.1007/s00018-007-7190-z.

[36] J. Paniagua-Michel, J. Olmos-Soto, and M. A. Ruiz, "Pathways of Carotenoid Biosynthesis in Bacteria and Microalgae," 2012, pp. 1–12. doi: 10.1007/978-1-61779-879-5_1.

[37] Aditi, R. Bhardwaj, A. Yadav, P. Swapnil, and M. Meena, "Characterization of microalgal β-carotene and astaxanthin: exploring their health-promoting properties under the effect of salinity and light intensity," *Biotechnology for Biofuels and Bioproducts*, vol. 18, no. 1, p. 18, Feb. 2025, doi: 10.1186/s13068-025-02612-x.

[38] M. Martínez-García *et al.*, “Antioxidant, Anti-Inflammatory and Anti-Obesity Potential of Extracts Containing Phenols, Chlorophyll and Carotenoids from Mexican Wild Populations of Bacopa monnieri (L.) Wettst,” *Biology (Basel)*, vol. 12, no. 4, p. 620, Apr. 2023, doi: 10.3390/biology12040620.

[39] C. Vílchez, E. Forján, M. Cuaresma, F. Bédmar, I. Garbayo, and J. M. Vega, “Marine Carotenoids: Biological Functions and Commercial Applications,” *Mar Drugs*, vol. 9, no. 3, pp. 319–333, Mar. 2011, doi: 10.3390/md9030319.

[40] L. Rodrigues, J. Morone, G. S. Hentschke, V. Vasconcelos, and G. Lopes, “Anti-Inflammatory Activity of Cyanobacteria Pigment Extracts: Physiological Free Radical Scavenging and Modulation of iNOS and LOX Activity,” *Mar Drugs*, vol. 22, no. 3, Mar. 2024, doi: 10.3390/md22030131.

[41] R. Silva *et al.*, “Pigments profile and antioxidant potential of extremophile cyanobacteria isolated from the Mexican Volcanic Lake Chichonal,” *Algal Res*, vol. 81, Jul. 2024, doi: 10.1016/j.algal.2024.103578.

[42] R. Favas, J. Morone, R. Martins, V. Vasconcelos, and G. Lopes, “Cyanobacteria Secondary Metabolites as Biotechnological Ingredients in Natural Anti-Aging Cosmetics: Potential to Overcome Hyperpigmentation, Loss of Skin Density and UV Radiation-Deleterious Effects,” *Mar Drugs*, vol. 20, no. 3, p. 183, Mar. 2022, doi: 10.3390/md20030183.

[43] J. Morone, G. Lopes, M. Preto, V. Vasconcelos, and R. Martins, “Exploitation of filamentous and picoplanktonic cyanobacteria for cosmetic applications: potential to improve skin structure and preserve dermal matrix components,” *Mar Drugs*, vol. 18, no. 9, Sep. 2020, doi: 10.3390/MD18090486.

[44] K.-H. Zhao *et al.*, “Phycobilin:cystein-84 biliprotein lyase, a near-universal lyase for cysteine-84-binding sites in cyanobacterial phycobiliproteins,” *Proceedings of the National Academy of Sciences*, vol. 104, no. 36, pp. 14300–14305, Sep. 2007, doi: 10.1073/pnas.0706209104.

[45] H. Scheer and K. -H. Zhao, “Biliprotein maturation: the chromophore attachment,” *Mol Microbiol*, vol. 68, no. 2, pp. 263–276, Apr. 2008, doi: 10.1111/j.1365-2958.2008.06160.x.

[46] F. Pagels, A. C. Guedes, H. M. Amaro, A. Kijjoa, and V. Vasconcelos, “Phycobiliproteins from cyanobacteria: Chemistry and biotechnological

applications," *Biotechnol Adv*, vol. 37, no. 3, pp. 422–443, May 2019, doi: 10.1016/j.biotechadv.2019.02.010.

[47] X. Li, W. Hou, J. Lei, H. Chen, and Q. Wang, "The Unique Light-Harvesting System of the Algal Phycobilisome: Structure, Assembly Components, and Functions," *Int J Mol Sci*, vol. 24, no. 11, p. 9733, Jun. 2023, doi: 10.3390/ijms24119733.

[48] B. L. Montgomery, "Seeing new light: recent insights into the occurrence and regulation of chromatic acclimation in cyanobacteria," *Curr Opin Plant Biol*, vol. 37, pp. 18–23, Jun. 2017, doi: 10.1016/j.pbi.2017.03.009.

[49] R. George and J. A. John, "Phycoerythrin as a potential natural colourant: A mini review," *Int J Food Sci Technol*, vol. 58, no. 2, pp. 513–519, Feb. 2023, doi: 10.1111/ijfs.16229.

[50] M. Campos Assumpção de Amarante, A. R. Cavalcante Braga, L. Sala, and S. Juliano Kalil, "Colour stability and antioxidant activity of C-phycocyanin-added ice creams after in vitro digestion," *Food Research International*, vol. 137, p. 109602, Nov. 2020, doi: 10.1016/j.foodres.2020.109602.

[51] S. M. Bannu, D. Lomada, S. Gulla, T. Chandrasekhar, P. Reddanna, and M. C. Reddy, "Potential Therapeutic Applications of C-Phycocyanin," *Curr Drug Metab*, vol. 20, no. 12, pp. 967–976, Jan. 2020, doi: 10.2174/1389200220666191127110857.

[52] F. Pagels, A. C. Guedes, A. A. Vicente, and V. Vasconcelos, "Cyanobacteria-Based Bioprocess for Cosmetic Products—Cyanobium sp. as a Novel Source of Bioactive Pigments," *Phycology*, vol. 3, no. 1, pp. 47–64, Jan. 2023, doi: 10.3390/phycology3010004.

[53] R. Ambati, S.-M. Phang, S. Ravi, and R. Aswathanarayana, "Astaxanthin: Sources, Extraction, Stability, Biological Activities and Its Commercial Applications—A Review," *Mar Drugs*, vol. 12, no. 1, pp. 128–152, Jan. 2014, doi: 10.3390/md12010128.

[54] N. I. Krinsky and E. J. Johnson, "Carotenoid actions and their relation to health and disease," *Mol Aspects Med*, vol. 26, no. 6, pp. 459–516, Dec. 2005, doi: 10.1016/j.mam.2005.10.001.

[55] A. RAO and L. RAO, “Carotenoids and human health,” *Pharmacol Res*, vol. 55, no. 3, pp. 207–216, Mar. 2007, doi: 10.1016/j.phrs.2007.01.012.

[56] E. J. Johnson, “Role of lutein and zeaxanthin in visual and cognitive function throughout the lifespan,” *Nutr Rev*, vol. 72, no. 9, pp. 605–612, Sep. 2014, doi: 10.1111/nure.12133.

[57] D. B. Rodriguez-Amaya, *Food Carotenoids*. Wiley, 2015. doi: 10.1002/9781118864364.

[58] J. Grabowski and E. Gantt, “PHOTOPHYSICAL PROPERTIES OF PHYCOBILIPROTEINS FROM PHYCOBILISOMES: FLUORESCENCE LIFETIMES, QUANTUM YIELDS, AND POLARIZATION SPECTRA,” *Photochem Photobiol*, vol. 28, no. 1, pp. 39–45, Jul. 1978, doi: 10.1111/j.1751-1097.1978.tb06927.x.

[59] N. T. Eriksen, “Production of phycocyanin—a pigment with applications in biology, biotechnology, foods and medicine,” *Appl Microbiol Biotechnol*, vol. 80, no. 1, pp. 1–14, Aug. 2008, doi: 10.1007/s00253-008-1542-y.

[60] V. Citi *et al.*, “Nutraceutical Features of the Phycobiliprotein C-Phycocyanin: Evidence from Arthrospira platensis (Spirulina),” *Nutrients*, vol. 16, no. 11, p. 1752, Jun. 2024, doi: 10.3390/nu16111752.

[61] T. ; P. A. ; B. N. Agnhage, *Dyeing of polyester fabric with bio-based madder dye and assessment of environmental impacts using LCA tool*, vol. 23. Slovak University of Technology in Bratislava et al., 2016. [Online]. Available: http://www.ft.tul.cz/mini/Vlakna_a_textil

[62] A. Ahmadi, S. A. A. Anvar, B. Nowruzi, and L. Golestan, “Effect of phycocyanin and phycoerythrin on antioxidant and antimicrobial activity of refrigerated low-fat yogurt and cream cheese,” *Sci Rep*, vol. 14, no. 1, p. 27661, Nov. 2024, doi: 10.1038/s41598-024-79375-2.

[63] N. Wada, T. Sakamoto, and S. Matsugo, “Multiple Roles of Photosynthetic and Sunscreen Pigments in Cyanobacteria Focusing on the Oxidative Stress,” *Metabolites*, vol. 3, no. 2, pp. 463–483, May 2013, doi: 10.3390/metabo3020463.

[64] X. Lin and T. Huang, “Oxidative stress in psoriasis and potential therapeutic use of antioxidants,” *Free Radic Res*, vol. 50, no. 6, pp. 585–595, Jun. 2016, doi: 10.3109/10715762.2016.1162301.

[65] W. Zhang *et al.*, “Spinal AT1R contributes to neuroinflammation and neuropathic pain via NOX2-dependent redox signaling in microglia,” *Free Radic Biol Med*, vol. 227, pp. 143–156, Feb. 2025, doi: 10.1016/j.freeradbiomed.2024.12.004.

[66] P. Pacher, J. S. Beckman, and L. Liaudet, “Nitric Oxide and Peroxynitrite in Health and Disease,” *Physiol Rev*, vol. 87, no. 1, pp. 315–424, Jan. 2007, doi: 10.1152/physrev.00029.2006.

[67] L. HE, S. ESLAMFAM, X. MA, and D. LI, “Autophagy and the nutritional signaling pathway,” *Front Agric Sci Eng*, vol. 3, no. 3, p. 222, 2016, doi: 10.15302/J-FASE-2016106.

[68] J. O. Lundberg and E. Weitzberg, “Nitric oxide signaling in health and disease,” *Cell*, vol. 185, no. 16, pp. 2853–2878, Aug. 2022, doi: 10.1016/j.cell.2022.06.010.

[69] I. Belenichev, O. Popazova, N. Bukhtiyarova, D. Savchenko, V. Oksenych, and O. Kamyshnyi, “Modulating Nitric Oxide: Implications for Cytotoxicity and Cytoprotection,” *Antioxidants*, vol. 13, no. 5, p. 504, Apr. 2024, doi: 10.3390/antiox13050504.

[70] N. J. Alp and K. M. Channon, “Regulation of Endothelial Nitric Oxide Synthase by Tetrahydrobiopterin in Vascular Disease,” *Arterioscler Thromb Vasc Biol*, vol. 24, no. 3, pp. 413–420, Mar. 2004, doi: 10.1161/01.ATV.0000110785.96039.f6.

[71] J. Groves, “Nitric oxide synthase: models and mechanisms,” *Curr Opin Chem Biol*, vol. 4, no. 6, pp. 687–695, Dec. 2000, doi: 10.1016/S1367-5931(00)00146-0.

[72] M. E. Kim and J. S. Lee, “Advances in the Regulation of Inflammatory Mediators in Nitric Oxide Synthase: Implications for Disease Modulation and Therapeutic Approaches,” *Int J Mol Sci*, vol. 26, no. 3, p. 1204, Jan. 2025, doi: 10.3390/ijms26031204.

[73] J. R. Kraehling and W. C. Sessa, “Contemporary Approaches to Modulating the Nitric Oxide–cGMP Pathway in Cardiovascular Disease,” *Circ Res*, vol. 120, no. 7, pp. 1174–1182, Mar. 2017, doi: 10.1161/CIRCRESAHA.117.303776.

[74] Y. Ranneh, F. Ali, A. M. Akim, H. Abd. Hamid, H. Khazaai, and A. Fadel, “Crosstalk between reactive oxygen species and pro-inflammatory markers in developing various chronic diseases: a review,” *Appl Biol Chem*, vol. 60, no. 3, pp. 327–338, Jun. 2017, doi: 10.1007/s13765-017-0285-9.

[75] E. Birben, U. M. Sahiner, C. Sackesen, S. Erzurum, and O. Kalayci, “Oxidative Stress and Antioxidant Defense,” *World Allergy Organization Journal*, vol. 5, no. 1, pp. 9–19, 2012, doi: 10.1097/WOX.0b013e3182439613.

[76] O. M. Ighodaro and O. A. Akinloye, “First line defence antioxidants-superoxide dismutase (SOD), catalase (CAT) and glutathione peroxidase (GPX): Their fundamental role in the entire antioxidant defence grid,” *Alexandria Journal of Medicine*, vol. 54, no. 4, pp. 287–293, Dec. 2018, doi: 10.1016/j.ajme.2017.09.001.

[77] W. Miao, R. Huang, X. Huang, F. Gao, X. Leng, and Q. Li, “Physicochemical Properties and In Vivo Hepatoprotective Effect of Polysaccharides from Grape Pomace,” *Antioxidants*, vol. 12, no. 2, p. 394, Feb. 2023, doi: 10.3390/antiox12020394.

[78] A. M. Pisoschi and A. Pop, “The role of antioxidants in the chemistry of oxidative stress: A review,” *Eur J Med Chem*, vol. 97, pp. 55–74, Jun. 2015, doi: 10.1016/j.ejmech.2015.04.040.

[79] K. Jomova, S. Y. Alomar, S. H. Alwasel, E. Nepovimova, K. Kuca, and M. Valko, “Several lines of antioxidant defense against oxidative stress: antioxidant enzymes, nanomaterials with multiple enzyme-mimicking activities, and low-molecular-weight antioxidants,” *Arch Toxicol*, vol. 98, no. 5, pp. 1323–1367, May 2024, doi: 10.1007/s00204-024-03696-4.

[80] S. Singh, B. N. Kate, and U. C. Banerjee, “Bioactive Compounds from Cyanobacteria and Microalgae: An Overview,” *Crit Rev Biotechnol*, vol. 25, no. 3, pp. 73–95, Jan. 2005, doi: 10.1080/07388550500248498.

[81] Q. Wu, L. Liu, A. Miron, B. Klímová, D. Wan, and K. Kuča, “The antioxidant, immunomodulatory, and anti-inflammatory activities of Spirulina: an overview,” *Arch Toxicol*, vol. 90, no. 8, pp. 1817–1840, Aug. 2016, doi: 10.1007/s00204-016-1744-5.

[82] A. K. Koyande, K. W. Chew, K. Rambabu, Y. Tao, D.-T. Chu, and P.-L. Show, “Microalgae: A potential alternative to health supplementation for humans,” *Food Science and Human Wellness*, vol. 8, no. 1, pp. 16–24, Mar. 2019, doi: 10.1016/j.fshw.2019.03.001.

[83] L. WANG, B. PAN, J. SHENG, J. XU, and Q. HU, “Antioxidant activity of Spirulina platensis extracts by supercritical carbon dioxide extraction,” *Food Chem*, vol. 105, no. 1, pp. 36–41, 2007, doi: 10.1016/j.foodchem.2007.03.054.

[84] F. K. E. B. and G. S. E.-B. Hanaa H. Abd El-Baky, “Production of phenolic compounds from Spirulina maxima microalgae and its protective effects in vitro toward hepatotoxicity model,” vol. 3, 2009.

[85] H. Safafar, J. Van Wagenen, P. Møller, and C. Jacobsen, “Carotenoids, Phenolic Compounds and Tocopherols Contribute to the Antioxidative Properties of Some Microalgae Species Grown on Industrial Wastewater,” *Mar Drugs*, vol. 13, no. 12, pp. 7339–7356, Dec. 2015, doi: 10.3390/md13127069.

[86] R. M. M. Abed, S. Dobretsov, and K. Sudesh, “Applications of cyanobacteria in biotechnology,” *J Appl Microbiol*, vol. 106, no. 1, pp. 1–12, Jan. 2009, doi: 10.1111/j.1365-2672.2008.03918.x.

[87] I. Colombo *et al.*, “HaCaT Cells as a Reliable In Vitro Differentiation Model to Dissect the Inflammatory/Repair Response of Human Keratinocytes,” *Mediators Inflamm*, vol. 2017, pp. 1–12, 2017, doi: 10.1155/2017/7435621.

[88] Z. Wang *et al.*, “Moisturizing and Antioxidant Effects of Artemisia argyi Essence Liquid in HaCaT Keratinocytes,” *Int J Mol Sci*, vol. 24, no. 7, p. 6809, Apr. 2023, doi: 10.3390/ijms24076809.

[89] J. Kotai, “Instructions for Preparation of Modified Nutrient Solution Z8 for Algae,” Oslo, 1972.

[90] J. B. Waterbury, “The Cyanobacteria—Isolation, Purification and Identification,” in *The Prokaryotes*, New York, NY: Springer US, 2006, pp. 1053–1073. doi: 10.1007/0-387-30744-3_38.

[91] R. Rippka, “[1] Isolation and purification of cyanobacteria,” 1988, pp. 3–27. doi: 10.1016/0076-6879(88)67004-2.

[92] B. A. Neilan *et al.*, “rRNA Sequences and Evolutionary Relationships among Toxic and Nontoxic Cyanobacteria of the Genus Microcystis,” *Int J Syst Bacteriol*, vol. 47, no. 3, pp. 693–697, Jul. 1997, doi: 10.1099/00207713-47-3-693.

[93] A. Taton, S. Grubisic, E. Brambilla, R. De Wit, and A. Wilmotte, “Cyanobacterial Diversity in Natural and Artificial Microbial Mats of Lake Fryxell (McMurdo Dry Valleys, Antarctica): a Morphological and Molecular Approach,” *Appl Environ*

Microbiol, vol. 69, no. 9, pp. 5157–5169, Sep. 2003, doi: 10.1128/AEM.69.9.5157-5169.2003.

[94] L. Benredjem, J. Morais, G. S. Hentschke, A. Abdi, H. Berredjem, and V. Vasconcelos, "First Polyphasic Study of Cheffia Reservoir (Algeria) Cyanobacteria Isolates Reveals Toxic Picocyanobacteria Genotype," *Microorganisms*, vol. 11, no. 11, p. 2664, Oct. 2023, doi: 10.3390/microorganisms11112664.

[95] A. Katana, J. Kwiatowski, K. Spalik, B. Zakryś, E. Szalacha, and H. Szymańska, "PHYLOGENETIC POSITION OF *KOLIELLA* (CHLOROPHYTA) AS INFERRED FROM NUCLEAR AND CHLOROPLAST SMALL SUBUNIT rDNA," *J Phycol*, vol. 37, no. 3, pp. 443–451, Jun. 2001, doi: 10.1046/j.1529-8817.2001.037003443.x.

[96] F. L. de Oliveira, G. S. Hentschke, J. Morais, R. Silva, P. Cruz, and V. M. Vasconcelos, "Exploring the cyanobacterial diversity in Portugal: Description of four new genera from <scp>LEGE</scp> - <scp>CC</scp> using the polyphasic approach," *J Phycol*, vol. 60, no. 5, pp. 1285–1304, Oct. 2024, doi: 10.1111/jpy.13502.

[97] K. Katoh, "MAFFT: a novel method for rapid multiple sequence alignment based on fast Fourier transform," *Nucleic Acids Res*, vol. 30, no. 14, pp. 3059–3066, Jul. 2002, doi: 10.1093/nar/gkf436.

[98] M. N. Price, P. S. Dehal, and A. P. Arkin, "FastTree: Computing Large Minimum Evolution Trees with Profiles instead of a Distance Matrix," *Mol Biol Evol*, vol. 26, no. 7, pp. 1641–1650, Jul. 2009, doi: 10.1093/molbev/msp077.

[99] I. Letunic and P. Bork, "Interactive Tree Of Life (iTOL) v5: an online tool for phylogenetic tree display and annotation," *Nucleic Acids Res*, vol. 49, no. W1, pp. W293–W296, Jul. 2021, doi: 10.1093/nar/gkab301.

[100] M. Zuker, "Mfold web server for nucleic acid folding and hybridization prediction," *Nucleic Acids Res*, vol. 31, no. 13, pp. 3406–3415, Jul. 2003, doi: 10.1093/nar/gkg595.

[101] A. Lukešová, J. R. Johansen, M. P. Martin, and D. A. Casamatta, "*Aulosira bohemensis* sp. nov.: further phylogenetic uncertainty at the base of the Nostocales (Cyanobacteria)," *Phycologia*, vol. 48, no. 2, pp. 118–129, Mar. 2009, doi: 10.2216/08-56.1.

[102] M. Hernández Mariné, “Microscopy methods applied to research on cyanobacteria,” *Limnetica*, vol. 23, no. 1, pp. 179–186, Jun. 2004, doi: 10.23818/limn.23.16.

[103] Â. Brito *et al.*, “Description of new genera and species of marine cyanobacteria from the Portuguese Atlantic coast,” *Mol Phylogenet Evol*, vol. 111, pp. 18–34, Jun. 2017, doi: 10.1016/j.ympev.2017.03.006.

[104] J. Morone, G. Lopes, J. Morais, J. Neves, V. Vasconcelos, and R. Martins, “Cosmetic Application of Cyanobacteria Extracts with a Sustainable Vision to Skincare: Role in the Antioxidant and Antiaging Process,” *Mar Drugs*, vol. 20, no. 12, p. 761, Dec. 2022, doi: 10.3390/md20120761.

[105] A. Bennett and L. Bogorad, “COMPLEMENTARY CHROMATIC ADAPTATION IN A FILAMENTOUS BLUE-GREEN ALGA,” *J Cell Biol*, vol. 58, no. 2, pp. 419–435, Aug. 1973, doi: 10.1083/jcb.58.2.419.

[106] F. Pagels *et al.*, “Bioactive potential of Cyanobium sp. pigment-rich extracts,” *J Appl Phycol*, vol. 32, no. 5, pp. 3031–3040, Oct. 2020, doi: 10.1007/s10811-020-02213-1.

[107] M. F. Barroso *et al.*, “Total antioxidant capacity of plant infusions: Assessment using electrochemical DNA-based biosensor and spectrophotometric methods,” *Food Control*, vol. 68, pp. 153–161, Oct. 2016, doi: 10.1016/j.foodcont.2016.03.029.

[108] N. B. Rizvi *et al.*, “Effect of the Media in the Folin-Ciocalteu Assay for the Analysis of the Total Phenolic Content of Olive Products,” *Food Anal Methods*, vol. 16, no. 11–12, pp. 1627–1634, Dec. 2023, doi: 10.1007/s12161-023-02527-z.

[109] V. L. Singleton, R. Orthofer, and R. M. Lamuela-Raventós, “[14] Analysis of total phenols and other oxidation substrates and antioxidants by means of folin-ciocalteu reagent,” 1999, pp. 152–178. doi: 10.1016/S0076-6879(99)99017-1.

[110] T. Masuko, A. Minami, N. Iwasaki, T. Majima, S.-I. Nishimura, and Y. C. Lee, “Carbohydrate analysis by a phenol–sulfuric acid method in microplate format,” *Anal Biochem*, vol. 339, no. 1, pp. 69–72, Apr. 2005, doi: 10.1016/j.ab.2004.12.001.

[111] Michel. DuBois, K. A. Gilles, J. K. Hamilton, P. A. Rebers, and Fred. Smith, "Colorimetric Method for Determination of Sugars and Related Substances," *Anal Chem*, vol. 28, no. 3, pp. 350–356, Mar. 1956, doi: 10.1021/ac60111a017.

[112] G. Lopes *et al.*, "Can Phlorotannins Purified Extracts Constitute a Novel Pharmacological Alternative for Microbial Infections with Associated Inflammatory Conditions?," *PLoS One*, vol. 7, no. 2, p. e31145, Feb. 2012, doi: 10.1371/journal.pone.0031145.

[113] Francis M. Awah and Andrew W. Verla, "Antioxidant activity, nitric oxide scavenging activity and phenolic contents of Ocimum gratissimum leaf extract," *Journal of Medicinal Plants Research*, vol. 4, no. 24, pp. 2479–2487, Dec. 2010, doi: 10.5897/JMPR10.407.

[114] R Core Team, "R: A Language and Environment for Statistical Computing," Vienna, Austria, 2019.

[115] J. Komárek, "Review of the cyanobacterial genera implying planktic species after recent taxonomic revisions according to polyphasic methods: state as of 2014," *Hydrobiologia*, vol. 764, no. 1, pp. 259–270, Jan. 2016, doi: 10.1007/s10750-015-2242-0.

[116] W.-G. ZHOU *et al.*, "Marileptolyngbya sina gen. nov., sp. nov. and Salileptolyngbya diazotrophicum gen. nov., sp. nov. (Synechococcales, Cyanobacteria), species of cyanobacteria isolated from a marine ecosystem," *Phytotaxa*, vol. 383, no. 1, p. 75, Dec. 2018, doi: 10.11646/phytotaxa.383.1.4.

[117] V. Loureiro de Araújo, M. Ferreira dos Santos, A. Selbach Schnadelbach, J. M. de Castro Nunes, and T. Aguiar Caires, "New genera of thin homocyted cyanobacteria from Brazilian tropical and subtropical marine islands," *Eur J Phycol*, vol. 58, no. 4, pp. 457–468, Oct. 2023, doi: 10.1080/09670262.2023.2169768.

[118] P. Yarza *et al.*, "Uniting the classification of cultured and uncultured bacteria and archaea using 16S rRNA gene sequences," *Nat Rev Microbiol*, vol. 12, no. 9, pp. 635–645, Sep. 2014, doi: 10.1038/nrmicro3330.

[119] J. Dagnino-Leone *et al.*, "Phycobiliproteins: Structural aspects, functional characteristics, and biotechnological perspectives," *Comput Struct Biotechnol J*, vol. 20, pp. 1506–1527, 2022, doi: 10.1016/j.csbj.2022.02.016.

[120] T. Soule, V. Stout, W. D. Swingley, J. C. Meeks, and F. Garcia-Pichel, “Molecular Genetics and Genomic Analysis of Scytonemin Biosynthesis in *Nostoc punctiforme* ATCC 29133,” *J Bacteriol*, vol. 189, no. 12, pp. 4465–4472, Jun. 2007, doi: 10.1128/JB.01816-06.

[121] S. Boussiba and A. E. Richmond, “C-phycocyanin as a storage protein in the blue-green alga Spirulina platensis,” *Arch Microbiol*, vol. 125, no. 1–2, pp. 143–147, Mar. 1980, doi: 10.1007/BF00403211.

[122] D. A. (Ed.) Bryant, *The Molecular Biology of Cyanobacteria*. Dordrecht: Springer Netherlands, 1994. doi: 10.1007/978-94-011-0227-8.

[123] J. Kollmen, M. Rech, F. Lorig, S. Di Nonno, J. Stiefelmaier, and D. Strieth, “New easy lab methods for the extraction of phycobiliproteins and pigments from cyanobacteria,” *J Appl Phycol*, vol. 37, no. 2, pp. 713–726, Apr. 2025, doi: 10.1007/s10811-024-03414-8.

[124] M. Pérez, I. Dominguez-López, and R. M. Lamuela-Raventós, “The Chemistry Behind the Folin–Ciocalteu Method for the Estimation of (Poly)phenol Content in Food: Total Phenolic Intake in a Mediterranean Dietary Pattern,” *J Agric Food Chem*, vol. 71, no. 46, pp. 17543–17553, Nov. 2023, doi: 10.1021/acs.jafc.3c04022.

[125] A. Guerreiro, M. A. Andrade, C. Menezes, F. Vilarinho, and E. Dias, “Antioxidant and Cytoprotective Properties of Cyanobacteria: Potential for Biotechnological Applications,” *Toxins (Basel)*, vol. 12, no. 9, p. 548, Aug. 2020, doi: 10.3390/toxins12090548.

[126] R. M. Lamuela-Raventós, “Folin-Ciocalteu method for the measurement of total phenolic content and antioxidant capacity,” in *Measurement of Antioxidant Activity & Capacity*, Chichester, UK: John Wiley & Sons, Ltd, 2017, pp. 107–115. doi: 10.1002/9781119135388.ch6.

[127] L. Trabelsi, A. Mnari, M. M. Abdel-Daim, S. Abid-Essafi, and L. Aleya, “Therapeutic properties in Tunisian hot springs: first evidence of phenolic compounds in the cyanobacterium Leptolyngbya sp. biomass, capsular polysaccharides and releasing polysaccharides,” *BMC Complement Altern Med*, vol. 16, no. 1, p. 515, Dec. 2016, doi: 10.1186/s12906-016-1492-3.

[128] I. de Oliveira, C. Santos-Buelga, Y. Aquino, L. Barros, and S. A. Heleno, “New frontiers in the exploration of phenolic compounds and other bioactives as natural preservatives,” *Food Biosci*, vol. 68, p. 106571, Jun. 2025, doi: 10.1016/j.fbio.2025.106571.

[129] V. K. Patel, S. Sundaram, A. K. Patel, and A. Kalra, “Characterization of Seven Species of Cyanobacteria for High-Quality Biomass Production,” *Arab J Sci Eng*, vol. 43, no. 1, pp. 109–121, Jan. 2018, doi: 10.1007/s13369-017-2666-0.

[130] F. R. Jacinavicius *et al.*, “Different ecophysiological and structural strategies of toxic and non-toxic Microcystis aeruginosa (cyanobacteria) strains assessed under culture conditions,” *Algal Res*, vol. 41, p. 101548, Aug. 2019, doi: 10.1016/j.algal.2019.101548.

[131] L. S. Passos *et al.*, “Content of Lipids, Fatty Acids, Carbohydrates, and Proteins in Continental Cyanobacteria: A Systematic Analysis and Database Application,” *Applied Sciences*, vol. 13, no. 5, p. 3162, Mar. 2023, doi: 10.3390/app13053162.

[132] M. Balat and H. Balat, “Recent trends in global production and utilization of bio-ethanol fuel,” *Appl Energy*, vol. 86, no. 11, pp. 2273–2282, Nov. 2009, doi: 10.1016/j.apenergy.2009.03.015.

[133] L. Grossmann, J. Hinrichs, and J. Weiss, “Cultivation and downstream processing of microalgae and cyanobacteria to generate protein-based technofunctional food ingredients,” *Crit Rev Food Sci Nutr*, vol. 60, no. 17, pp. 2961–2989, Sep. 2020, doi: 10.1080/10408398.2019.1672137.

[134] S. Aikawa *et al.*, “Direct conversion of Spirulina to ethanol without pretreatment or enzymatic hydrolysis processes,” *Energy Environ Sci*, vol. 6, no. 6, p. 1844, 2013, doi: 10.1039/c3ee40305j.

[135] K. Campara, P. Rodrigues, F. T. Viero, B. da Silva, and G. Trevisan, “Nitric oxide as a biomarker for patients with endometriosis: a systematic review and meta-analysis,” *Nitric Oxide*, vol. 158, pp. 106–115, Oct. 2025, doi: 10.1016/j.niox.2025.07.002.

[136] G. Scutiero *et al.*, “Oxidative Stress and Endometriosis: A Systematic Review of the Literature,” *Oxid Med Cell Longev*, vol. 2017, no. 1, Jan. 2017, doi: 10.1155/2017/7265238.

[137] S.-H. Zheng, X.-X. Chen, Y. Chen, Z.-C. Wu, X.-Q. Chen, and X.-L. Li, “Antioxidant vitamins supplementation reduce endometriosis related pelvic pain in humans: a systematic review and meta-analysis,” *Reproductive Biology and Endocrinology*, vol. 21, no. 1, p. 79, Aug. 2023, doi: 10.1186/s12958-023-01126-1.